Republic of Iraq

Ministry of Higher Education and Scientific Research

University of Babylon

College of Engineering

Civil Engineering Department

Performance of Halloysite Nano Clay on Engineering Properties of Concrete

A Thesis

Submitted to the College of Engineering /University of

Babylon in Partial Fulfillment of the Requirements for the Degree of Master in Engineering / Civil Engineering / Construction Materials

By

Noor AL-Huda Hakim Abdul Ameer Essa

Supervised By

Prof. Dr. Abbas Salim AL-Ameeri

Dr. Suhalia G. Mattar

2023 A.D. **1444 A.H.**

بسم الله الرحمن الرحيم

(ولسوف يعطيك ربك فترضى)

صدق الله العلي العظيم

(سورة الضحى : آية ٥)

Examination committee certification

We certify that we have read the thesis entitled "Performance of halloysite nano clay on engineering properties of concrete" and as an examining committee, we examined the student " Noor AL-Huda Hakim Abdul Ameer" in its content and in what is connected with it and that in our opinion it is adequate as a thesis for the degree of Master of Science in Civil Engineering.

Supervised by

Signature:

Name: ***Prof. Dr. Abbas Salim Abbas Al-Ameeri***

Date: / / 2023

Supervised by

Signature S Mattar

Name: ***Dr. Suhaila Mattar***

Date: / / 2023

Member

Signature: H. M. O.

Name: ***Asst. Prof. Dr. Haider M. Owaid Al-Rubaie***

Date: / / 2023

Member

Signature:

Name: ***Asst. Prof. Dr. Nahla Naji Hilal***

Date: 5 / 10 / 2023

Chairman

Signature:

Name : ***Prof. Dr. Ghalib M. Habeeb***

Date: / / 2023

Approval of Head of Civil Engineering Department

Signature:

Name : ***Asst. Prof. Dr. Zaid H. Majeed Al-Hasson***

Date: / / 2023

Approval of Deanery of the College of Engineering

Signature:

Name :***Prof. Dr. Laith Ali Abdul- Rahaim***

Date: / / 2023

Supervisor's certificate

I/We certify that the thesis entitled "**Performance of Halloysite Nano Clay on Engineering Properties of Concrete**" was prepared by "Noor Al-Huda Hakim Abdul Ameer" under our supervision at the Department of Civil Engineering, Faculty of Engineering- University of Babylon as a partial of fulfilment of the requirements for the Degree of Master of Science in Civil Engineering.

Signature:

Prof. Dr. Abbas Salim AL-Ameeri

Date: / / 2023

Signature: S Mattar

Dr. Suhalia Mattar

Date: / / 2023

Dedication

I dedicate this achievement to **my mother and my father,** who with love and effort have accompanied me in this process, without hesitating at any moment of seeing my dreams come true, which are also their dreams.

Noor AL-Huda Hakim

Acknowledgements

At the outset, I thank God and thank him for directing me to this scientific path.

Secondly, all thanks, appreciation and respect to the **(Prof. Dr. Abbas Salim AL-Ameeri)** for my constant support and encouragement and the research evaluation to complete the research requirements

I also thank and appreciate **(Dr. Suhalia G. Mattar)** for her wonderful suggestions, encouragement and guidance during the research

Finally, I extend my sincere thanks to my family and my friend Aliyaa, for their continued support and care

Thanks to all the staff of Civil Engineering Department /College of Engineering /University of Babylon for their appreciable support.

Abstract

There have been many challenges posed by both its durability and CO_2 emissions in concrete production. This study focuses on replacement of nano-calcined halloysite and blast furnace slag (GGBS) with cement and examines its ability to enhance the durability of concrete structures. And it aims to reduce the environmental impact by providing a sustainable and environmentally friendly alternative to the construction industry.

Three concrete mixtures were employed. The first mixture is named (NC) with a design strength of 40 MPa, (cement 370 kg/m^3, sand 706 kg/m^3, gravel 1080 kg/m^3, w/c 0.5, SP 0.5%).Second mixture (HS) with a design strength of 50 MPa, (cement 420 kg/m^3, sand 678.4 kg/m^3, gravel 1080 kg/m^3, w/c 0.45, SP 1%), also the last mixture is (GG) with a design strength of 40 MPa, (cement 277.5 kg/m^3, sand 706 kg/m^3, gravel 1080 kg/m^3, w/c 0.5, SP 0.5% with 25% GGBS was replaced by mass of cement). Also, three mortar mixture were tested, MC, MH were with mix proportion (1:2.75) and w/c=0.5,0.48 receptively and MG was with 1.2.75 C: S and 25% GGBS was replaced by mass of cement.

Fresh and mechanical tests were conducted for the concrete and mortar included (workability, compressive strength, splitting tensile strength, flexural strength, water absorption, porosity, surface absorption, chloride penetration depth, chloride migration, chloride concentration, impress current, drying shrinkage, Schmidt hammer rebound value, and Ultrasound pulse velocity).

The results of this study showed a decrease in the slump of concrete when replacing CHNC was increased compared to the control mixture by (25 and 23.07%) for mixing NC3 and GG 3 for the replacement ratio of 3%. As for the compressive strength began to increase with increasing the replacement ratio for age 7, 28, and 90 days (17.14, 12.86 and 14.26%) for the GG 4.5

mixtures, replacing 4.5% CHNC due to the effectiveness of halloysite in improve the bonding and enhance the transition zone between the cement paste and the aggregate. Also for both the flexural and splitting tensile test there was an increase with an increase in the percentage of CHNC replacement for the three mixtures at 7, 28 and 90 days. As for the durability of concrete, there was a clear improvement in all tests when halloysite was used, as it showed a decrease in water absorption, porosity, and surface absorption when halloysite was replaced for the three mixtures. This is due to halloysite filling the pores and dense the concrete. In addition, the use of granulated blast furnace slag (GGBS) had a good effect in improve the microstructure of concrete. As for the effect of CHNC on the penetration of chlorides, it reduced the penetration of chlorides into concrete, both by 1.5 percent in a small amount, and in a larger amount at 3 and 4.5 percent of CHNC, as the migration coefficient decreased for 4.5% of CHNC (21.21%, 45.30%, and 54.18%) NC 4.5, HS4.5 and GG 4.5. Also the impress current test reduced the penetration of chlorides by (23.38, 34.59, and 36.69%) for the mixtures NC3, HS3 and GG3 compared to the control.

CHNC reduced concrete exposure to drying shrinkage compared to the control mix, where 3% was better at reducing concrete drying shrinkage. At the same time, it showed good behavior when examining concrete with non-destructive tests, as by increasing the replacement rate, the surface hardness and ultrasonic pulse velocity increased.

Table of Contents

List of Tables

List of Figures

List of Abbreviations

Symbol	Description
Å	Angstrom (Basal spacing unit)
AASHTO	American Association of State Highway and Transportation Officials
ACI	American Concrete Institute
ASR	Alkali Silica Reaction
ASTM	American Society for Testing and Materials
BS	British Standard
C_3A	Tricalcium Aluminate
C_4AF	Tetracalcium alumino ferrite
C-A-H	Calcium Aluminate Hydrate
CH	Calcium Hydroxide
CHNC	Calcined Halloysite Nano Clay
CNT	Carbon Nano Tube
CO_2	Carbon dioxide
C-S-H	Calcium Silicate Hydrate
CTCs	Capture Tumor Circulating Cells
d001	Basal spacing in a phyllosilicate
DSC	Differential Scanning Calorimetry
FS	Friedel's salt
GG	Mixture with 40 MPa (Control mixture)+25% GGBS
GG1.5	40MPa+ 1.5% halloysite+25% GGBS
GG3	40MPa+ 3 %halloysite +25%GGBS
GG4.5	40MPa+ 4.5% halloysite+25%GGBS
GGBS	Ground Granulate Blast Furnace Slag
HNTs	Halloysite Nano Tubes
HS	Mixture with 50 MPa (Control mixture)
HS1.5	50MPa+ 1.5 %halloysite
HS3	50MPa+ 3% halloysite
HS4.5	50MPa+ 4.5% halloysite
HSBFC	High Slag Blast Furnace Cement
HVS	High Volume Slag
IQS	Iraqi Standard
NC	Nano clay
NC	Mixture with 40 MPa (Control mixture)
NC1.5	40MPa+ 1.5% halloysite
NC3	40MPa+ 3 %halloysite
NC4.5	40MPa+ 4.5% halloysite
NS	nano-silica
NT	Nord Test

OPC	Ordinary Portland Cement
PBFC	Portland Blast Furnace Slag Cement
RCPT	Rapid Chloride Permeability Test
RH	Relative Humidity
RN	Rebound Number
SEM	Scanning Electron Microscopy
SF	Silica Fume
SP	Superplasticizer
UHPC	Ultra-High-Performance Concrete
UPV	Ultrasonic Pulse Velocity
XRD	X-ray diffraction analysis

Chapter one
Introduction

Chapter one
Introduction

1.1. General Overview

Concrete is a cost-effective and readily available construction material because it has good mechanical properties such as compressive strength, concrete possesses two significant properties that contribute to its structural integrity, its capacity to interconnect building units and its capability to establish bonds with steel reinforcement. These characteristics play a crucial role in enhancing the overall strength of concrete, especially considering its inherently brittle nature. Two of the basic things should be available in structural design of concrete structures are strength and durability, as well as low cost. The production of cement each year is approximately 6 billion cubic meters, which is equivalent to one cubic meter per capita on the ground. Concrete has also become the preferred material for the construction of structures subjected to harsh environmental conditions. Minor advancements in concrete design, production methods, and material performance can yield significant social and economic impacts. **(Kiran et al, 2021)**

The cement production process is accompanied by the emission of greenhouse gases, whether these emissions are indirectly from calcine limestone and clay to produce cement clinker, or directly through the process of burning fuels to generate the heat needed for the cement production process. **(Greenhouse Gas Emissions in the United States, 2006)**. In 2021, the global production of cement reached about 4.4 billion tons, which contributes to 7-8% of carbon dioxide emissions CO_2 **(Statista ,2022)**.

The production capacity of clinker in the world for the year 2021 is estimated at about 3.7 billion metric tons **(Statista ,2022)** and according to **(Hendrik et al ,2011)**, the chemical conversion process of limestone and

other raw materials into clinker, and this emits about 0.51 cubic meters of carbon dioxide and 0.40ton CO_2 from the combustion of fuel.

There were multiple and varied directions to reduce the consumption of cement and fuel one of the innovative techniques was used to reduce the waste sent to the landfill and to use recycled and entered it into concrete to reduce the amount of cement production and fuel used for production and at the same time reduce the accumulated harmful waste **(Baalbaki, 2003)**. The other trend was towards the by-products of materials called pozzolanic materials such as silica fume, fly ash, and ground granulated blast furnace slag (GGBS), limestone which, when used and treated properly, interacts with cement products and forms a strong pozzolanic reaction that results in gelatinous materials that improve and increase the strength and durability of concrete **(Nicoara, etal. 2020)**.

Clay minerals have been a part of society and human existence since the dawn of time **(Rytwo, 2008)**. Clay has several important properties due to its varied mineral composition, such as plasticity and cohesiveness **(Andrade, 2011)**. As a result, it is widely used as a constituent in industrial and commercial applications. Furthermore, clay can be associated with nanotechnology to produce nanoclays, a mineral used in the application of materials.

The utilization of nano-clays in cement-based materials has gained momentum due to their affordability and widespread accessibility compared to other types of nanoparticles. Nano-clays, including organically-modified nano-clays, kaolinite, bentonite, hectorite, montmorillonite, and halloysite (organo-clays), are categorized into different groups based on their chemical composition and morphology, these nano-clays are employed to enhance the

engineering properties and overall performance of cement and concrete. **(Taghiyari, 2011).**

Nanomaterials' prominent chemical and physical properties enable them to play an important role in a variety of applications, such as modifying material structure, improving composite properties, and manufacturing new multifunctional products. One of the studies conducted on the effect of nanoparticles on the performance of concrete, showed an improvement in the properties of concrete **(Jeevanandam et al, 2018)**.

1.2 Research Significance

Concrete is the most commonly used building material in the planet, with a bit higher permeability that allows water and other aggressive elements to enter, resulting in carbonation and chloride ion attack and corrosion problems. As a result, the nanoscale investigation of hydration products (calcium hydroxide, ettringite, monosulfate, unhydrated particles, and air voids) as a method to overcome durability issues is a critical step in concrete sustainability.

The purpose of this research is to achieve a better understanding of the behavior of halloysite nanoclay in concrete and finding the optimum halloysite nanoclay percentage that improve the resistance of concrete to external corroding chloride attack. The experimental programed consider the mechanical properties of concrete, chloride penetration, and visual observation. For each mix, the embodied carbon dioxide was computed, the chloride penetration was measured in order to reduce the steel rebar's corrosion and the cost of repairing structures by lowering the permeability of concrete to reduce chloride entry. The Reduction of the amount of cement in concrete lessened the environmental impact while halloysite, is a natural, sustainable alternative that reduces emissions and cuts fuel cost.

Additional care was taken to ensure that concrete specimens were designed in accordance with the optimized requirements established by previous studies. The experiment was expected to last about 90 days, with data being collected continuously throughout. In addition, any unexpected error or limitation affecting results or shortening the experimental period was highlighted and discussed. If the results were inconclusive, more research was recommended.

1.3 Objectives of Research

Concrete specimens were cast with varying percentages of halloysite nanoclay replacement. The content of halloysite nanoclay in the specimen mixture ranged from 1.5% to 3% to 4.5%. The specimens were cured for 28 days. The cement was replaced by 25% of GGBS in the GG mixture.

- Conducting a slump test on the concrete and the flow table on the mortar.
- The study involved conducting compressive, flexural, and splitting tensile strength tests on concrete mixtures containing (1.5%, 3%, and 4.5%) of halloysite nanoclay. These tests were carried out at the ages of 7, 28, and 90 days for each of the mixtures. The results of these tests were compared with the control mixture
- After processing the samples for 28 days, tests were conducted on water absorption, porosity, and sorptivity at age 7, 28, and 90 days.
- Chloride penetration tests, such as chloride migration (NT-Build 492) and concentration tests with depth, were conducted to quantify the extent of chloride penetration into the concrete. For these tests, the concrete specimens were immersed in a container containing a solution of 5% sodium chloride and 95% water to simulate chloride exposure. Also impress current test was conducted at age of 26 days.

- The change in length was studied for both concrete and mortar and reached 120 days.
- Non-destructive tests such as ultrasonic tests and Schmidt hammer tests were studied according to specifications ASTM and the examination was carried out at the ages of 7, 28 and 90 days.
- The amount of carbon dioxide emissions (CO_2) in concrete mixtures was calculated after replacing them with halloysite and GGBS by using an equation where the amount of carbon dioxide emission for each material is multiplied by the mass of the material.

1.4 Research layout

The thesis is organized in five chapters, each representing a significant stage in the research project. Here's a reformulation summarizing the content of each chapter:

Chapter One: Is an introduction; the problem, study aim and objectives, are presented; and it also lists the layout of this thesis.

Chapter Two: In this chapter, an assessment of the literature as well as a comprehensive explanation of halloysite, its physical and chemical properties, and applications was reviewed. An explanation of how chlorides enter concrete, the mechanism of entry, and the measures of chloride penetration into concrete was also reviewed. In addition, it included a detailed explanation of the GGBS manufacturing process and its properties.

Chapter Three: The materials used in the research (cement, aggregate, SP, Halloysite, and GGBS) and the experimental program were covered. The experimental program included workability, strength tests, sorptivity, water absorption, chloride

migration, impressed current, diffusion coefficient, and non-destructive tests.

Chapter Four: This chapter included laboratory work results, analysis and discussion of the results, and comparison with the previous literatures .

Chapter Five: It included a summary of the research outcomes as well as recommendations for future research.

Chapter Two

Literature Review

Chapter Two
Literature Review

2.1. Introduction

Nanotechnology, viewed as a groundbreaking emerging technology, has captivated manufacturers, particularly in the construction sector. Ready-mixed concrete and concrete products were highlighted among the top 40 industrial sectors anticipated to be influenced by nanotechnology in the next 10 to 15 years **(Ganesh, 2012)**. Despite its potential, the construction industry lagged in adopting nanotechnology, prompting major industrial companies and financiers to invest heavily in research and development. Recognizing this, the European Commission approved funding for the Growth Project NANOCONEX in 2002, aiming to establish a network of excellence in nanotechnology for construction. Cement-based materials, although omnipresent, are poorly understood due to their intricate nature **(Jensen & Hansen, 2001)**. Nanoclay, a nanoparticle, enhances concrete's mechanical properties, representing the interdisciplinary synergy of nanotechnology and concrete knowledge. This interaction has the potential to revolutionize the construction industry by filling concrete pores and forming nano-crystals, significantly improving concrete performance.

This literary review covered the background on halloysite Nano clay, the penetration of chlorides into concrete, previous studies on the effect of adding halloysite to mortar, and previous studies that explained the behavior of concrete containing nano materials against the entry of chlorides.

2.2. Calcined Halloysite Nano Clay

Nanoclays are nanoparticles of silicate with nanopores. The kaolinite group (Kaolin or halloysite), the montmorillonite/smectite group, the illite

group, and the chlorite group are the four major groups of clay (**Gujjari, 2017)**.

Halloysite described by Berthier in 1826 as a member of the kaolin group, specifically a dioctahedral 1:1 clay mineral. Halloysite consists of one-to-one layers with Al^{3+} in octahedral sites and Si^{4+} in tetrahedral sites. The electrically neutral layers are bonded via hydrogen interactions between tetrahedral basal oxygen and adjacent octahedral sheet's hydroxyls as shown in Figure(2-1). The two layer separated by a monolayer of water molecules, so the basal spacing (d001) of hydrated halloysite is 10Å, which is 3Å greater than that of kaolinite. Because the interlayer water is weakly held, halloysite 10Å can easily and irreversibly dehydrate to form halloysite 7Å **(Al-Adwane, etal. ,2023)**.

According to **(Churchman, 2000),** halloysite is commonly found in weathered rocks and soils, resulting from the alteration of various types of igneous and non-igneous rocks. In wet tropical and subtropical regions, halloysite often serves as a significant component in andisols and soils derived from volcanic materials.

Naturally occurring Halloysite appears in varied morphologies, such as platy, spheroidal, and tubular. However, the tubular structure is the dominant morphology of halloysite in nature. Tubules can be long and thin, short and stubby, or they can emerge from other tubes. Tubular halloysite is typically formed from crystalline minerals like feldspar and mica **(Joussein, 2016)**.

Spheroidal halloysite is found in environments like weathered volcanic ash and marine settings, with diameters ranging from 0.05 to 0.5 mm. It forms due to rapid dissolution of volcanic glass, leading to either halloysite-only or allophane followed by halloysite formation, depending on

the dissolution rate and available space If they are physically constrained Spheroidal halloysite will develop **(Cravero & Churchman, 2016)**.

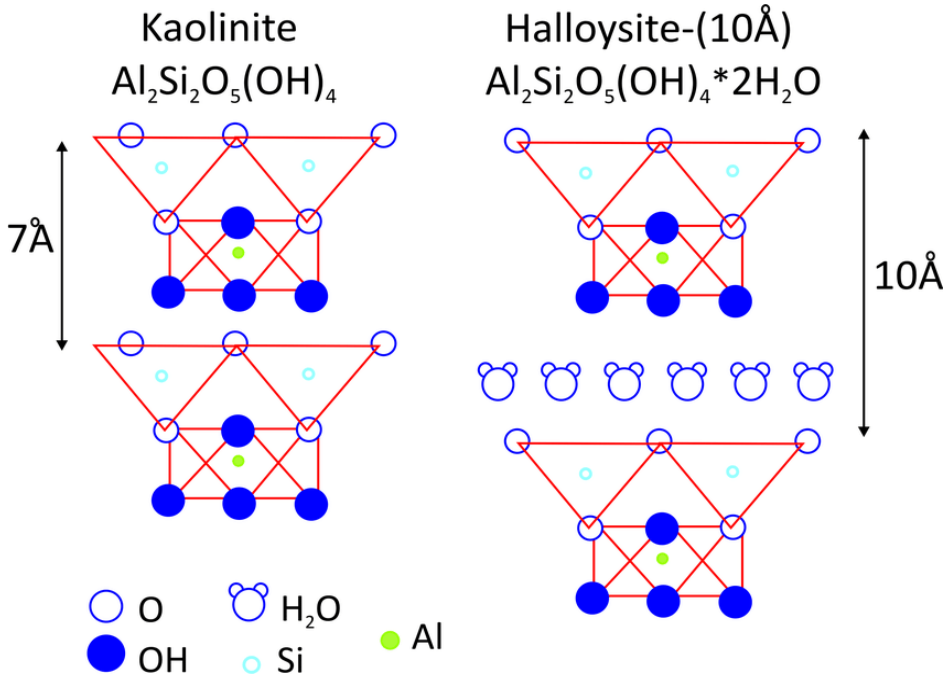

Figure 2-1: structure of kaolinite and halloysite ((Lázaro, 2015)

Halloysite nanoclay is wiely distributed around the world, It is naturally occurring mineral that forms from volcanic deposits, particularly volcanic ash, which undergoes weathering and transforms into rock and soil. In New Zealand, halloysite formation is associated with hydrothermal activity, while in Australia, it is formed through the action of acidic groundwater on fine-grained sediments. These geological processes contribute to the widespread occurrence of halloysite nanoclay in various regions **(Churchman et al., 2012).**

According to **(Yuan ,2015)** the greatest deposite of halloysite found in china, Australia, New Zealand, USA, Brazil, Mexico.

In Iraq, besides kaolinite, the halloysite was found in minor quantities only in the upper mudstone horizon (sublithofacies B3: reddish-brown kaolinitic mudstone, this sublithofacies is common throughout the

Hussainiyat clastics, either overlying sublithofacies (A2: cross-bedded sandstone) with a gradational contact, or overlying (C:ironstone). This mudrock ranges in thickness from 2 to 11 meters) in the Hussainiyat Fe deposit, Wadi Al-Hussainiya, Al-Rutba District, Al Anbar (**Al-Bassam & Tamar-Agha, 1998)** as shown in Figures (2-2) and (2-3).

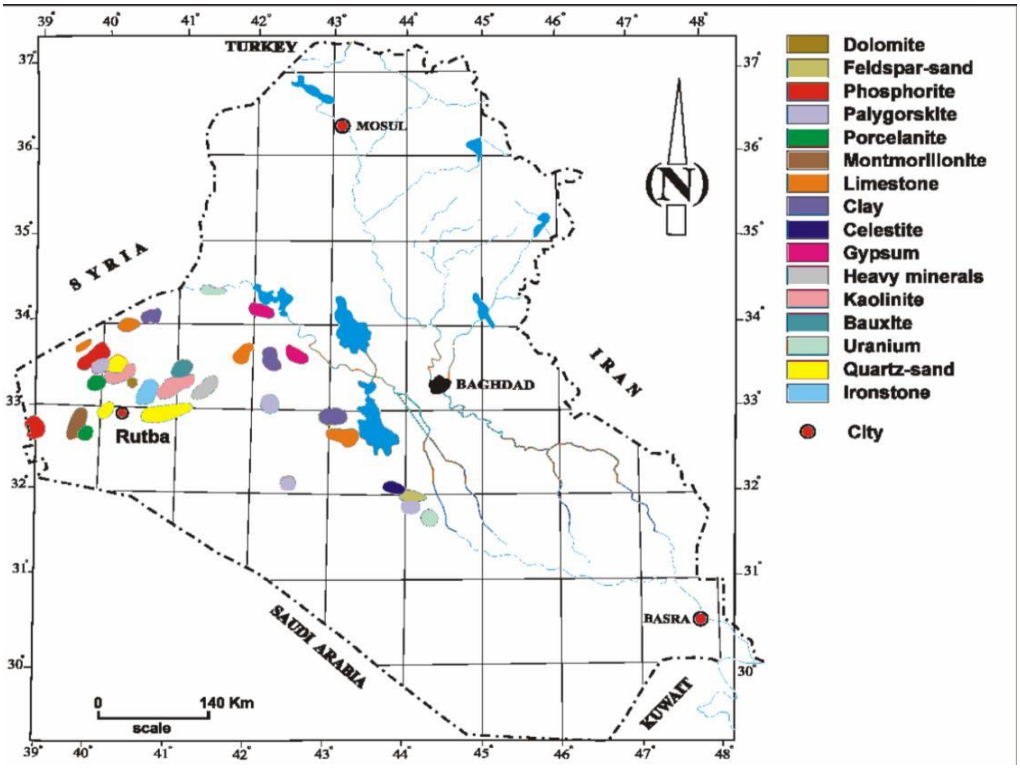

Figure 2-2: Distribution of mineral resources and in the Western Desert (Al-Bassam, 2007)

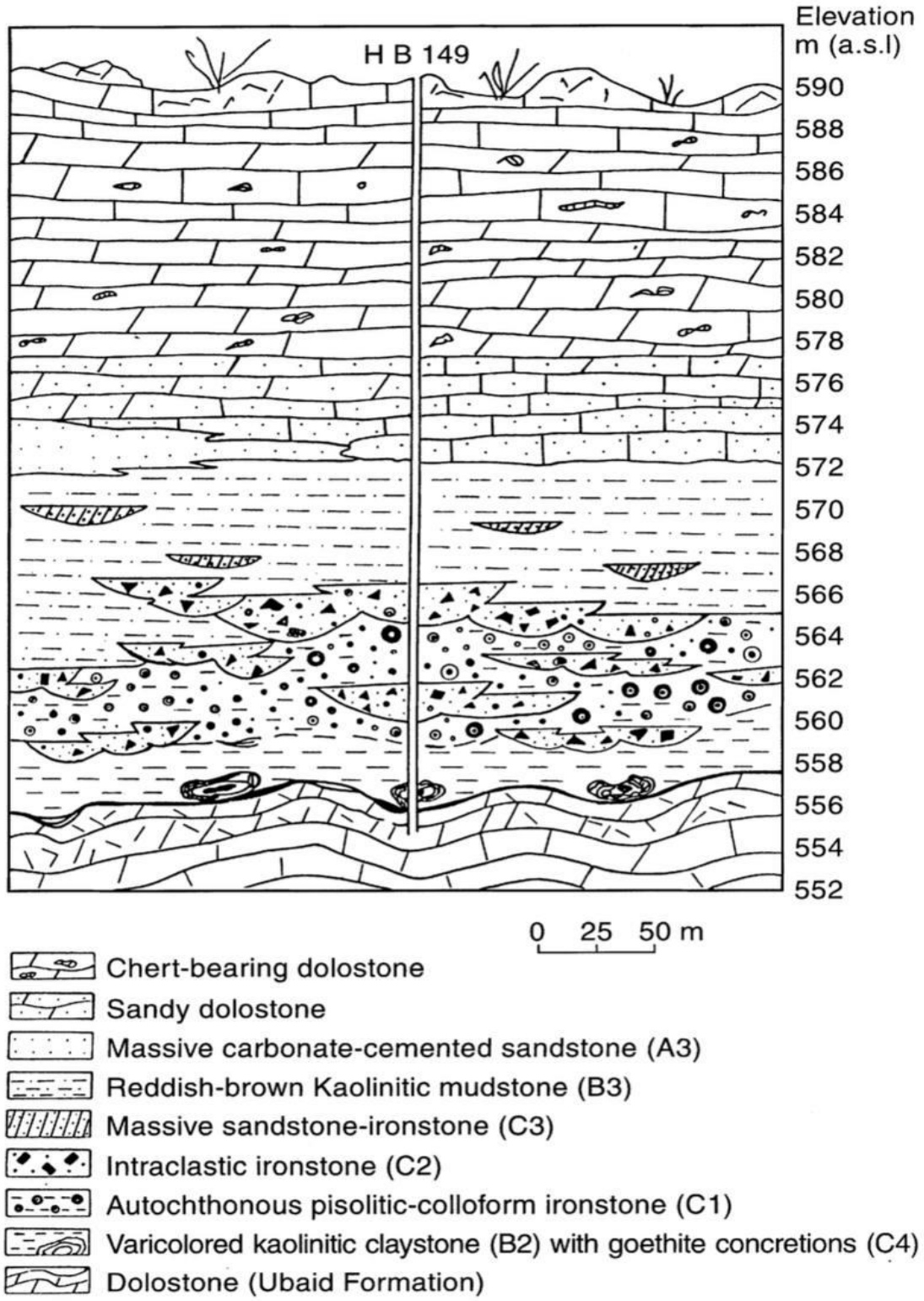

Figure 2-3*:* Geological cross section of the ironstone-bearing sequence in the vicinity of borehole no. HB 149 (Al-Bassam & Tamar-Agha, 1998)

2.3. Physical Properties of Calcine Halloysite Nano Clay

The crystal structure of halloysite is of the phyllosilicate type that contains silicon, aluminum or magnesium, oxygen and hydroxyl (OH). These ions and OH groups are organized into two-dimensional structures called sheets, occurring in two types: tetrahedral sheets and octahedral sheets **(Lázaro, 2015).**

Halloysite may contain impurities in the crystal structure such as Fe^{+3} , Cu ,K et al and this impurity changes the color of white halloysite of high purity, which usually ranges from 90-100% (**DeArmitt,2015**) to impurities of colors such as yellow, reddish brown, gray.

Halloysite has various shapes such as tubular, spherical, platy, and prismatic. The most common and most efficient is the tubular shape. The length of the tube usually ranges from 0.2-40 μm and the outer diameter is 50-70 nm because it contains a cavity, where the inner diameter is 10-20 nm (**Lisuzzo, 2018)**. In addition to this, halloysite has a high surface area estimated at about 64-120 m^2/g.

One of the physical properties of mineral is hardness, which means depending on **U.S. National Park Service** (A mineral's hardness is a measure of its relative resistance to scratching, measured by scratching the mineral against another substance of known hardness on the Mohs Hardness Scale) and its magnitude in Halloysite(1-2) and sometime reach to 2.5 **(DeArmitt, 2015)** .

HNTs have low density (2 - 2.65 g/cm^3) with high porosity and large pore volume (1. 25 ml/g) which makes HNTs hydrophilic and highly absorbent (**Liu, 2020)**. The physical properties of halloysite are shown in Table (2-1).

Table 2-1: physical properties for halloysite nonaclay (Lutyńskiet al. (2019)

Category	Phyllosilicates(Kaolinite-serpentine group)
Color	White; grey, green, blue, yellow, red from included impurities.
Hardness	1 - 2 on Mohs scale
Typical specific surface area	64-120 m^2/g
Pore volume	1. 25 ml/g
Refractive index	1.54
Specific gravity	2.53
External tube diameter	50-70 nm
Inner lumen diameter	10-20 nm
Length	0.2-40μm
Form	Nano Powder
Purity	90-100% (depending on source)
Density	2-2.65 g/cm^3 (Measured) 2.14 g/cm^3 (Calculated)
Luster	Earthy (Dull)
Streak	white
Stability	Stable under recommended storage conditions
Moisture content of adsorbent	8

Bulk density	800-900kg/m^3

2.4. Chemical Composition of Calcine Halloysite Nano Clay

The chemical formula for halloysite is $Al_2(OH)_4Si_2O_5.nH_2O$. When n = 2, the hydrated form of halloysite is referred to as "halloysite-(10Å," with one layer of water molecules present between the multilayers and the "10Å" designation indicating the d001-value of the layers. The dehydrated structure of halloysite (when n = 0) is known as "halloysite-(7Å)" and can be obtained by losing the interlayer water molecules in a mild heating and/or vacuum environment. **(Joussein et al., 2005)**. The common impurities with holloysite minerals are Ti, Ca, Na, K, Fe, Cr, Mg, Ni, Cu and the Molecular Weight = 294.19 gm/mol. The measured modulus is 150 GPa versus the 200-300 GPa calculated value. The tubes can flex nearly 90 degrees without breaking and have a dry crush strength of more than 1500 GPa , more than 250 000 psi, or more than 130 tons per square inch (beyond the limit of the machine used) **(Lu et al., 2011)**. The common chemical compositions of holloysite are listed in Table (2-2 and Figure (2-4).

Table 2-2: Composition of halloysite and chemical properties

https://polymerexpert.biz/blog/162-halloysite-clay-nanotubes

Main element	Mass fraction %	Main oxide	Mass fraction %
Aluminum(Al)	20.90 %	Al_2O_3	30-40 %
Silicon (Si)	21.76 %	SiO_2	40-50 %
Hydrogen(H)	1.56 %	H_2O	(14.3-15.35) *
Oxygen (O)	55.78 %	CaO	0.02-0.77%
Chemical properties of halloysite *			
Loss on Ignition 1000Cº		18%	
pH		4.5-7*	
Flexural modulus tube		130-150 Gpa	
Compressive strength		>1500GN/ m^2	
Specific heat capacity		0.92KJ/Kg.K	
Thermal conductivity		0.092W/K.m	
Thermal diffusivity		5.04*$10^{-4} cm^2$/sec	
Cation exchange capacity		20-60 cmol/kg	
Low electrical conductivity		3.5 x 10^{-5} Scm^{-1}	

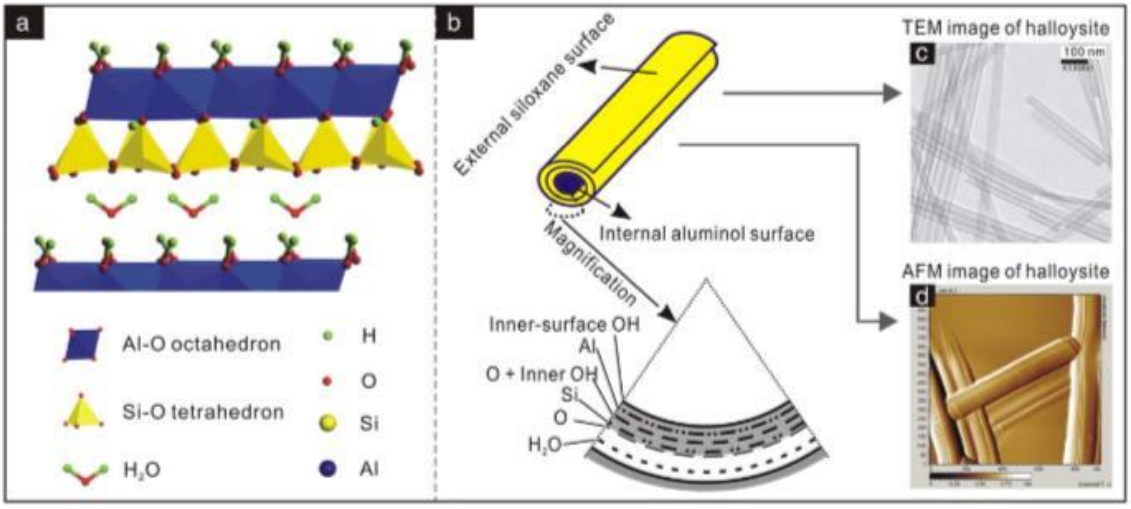

Figure 2-3: Schematic diagram of (a) crystalline structure of Halloysite-(10 Å), (b) structure of Halloysite particle, (c–f) TEM and AFM images of Halloysite. (Yuan, P., et al., 2015)

Nano-clay is primarily composed of silica, making it the most abundant component, followed by alumina, which constitutes over 60% of its total composition. This composition renders nanoclay a significant pozzolanic - material **(Chithra, 2016)**. It possesses the capability to react with calcium hydroxide (CH) created during cement hydration and facilitate the generation of numerous hydrates, such as calcium silicate hydrate (C-S-H) and calcium alumina hydrate (C-A-H) gels. This reactivity contributes to the enhancement of cement-based materials properties (**Papatzani, 2016)**.

On the other hand the chemical composition , varies a little. Halloysite impurities (associated with clay minerals, Fe oxides, or poorly organized minerals, some of which may also be localized within halloysite tubes) are common in halloysitic samples, making determining the chemical composition of the halloysite difficult. Many halloysites contain significant amounts of Fe_2O_3 (up to 12.8 % by mass) and this may be due to the partial isomorphous substitution of Fe^{3+} for Al^{3+} in the octahedral sheet or to physical mixtures with very fine iron oxides (e.g. hematite and goethite) according to chemical analysis **(White and Dixon, 2002)**.

Natural halloysite clay piques the interest of material developers because it is one of the few low-cost nanomaterials available in thousands of tons. According to **(Lvov et al., 2008),** the halloysite is a low-cost material (at about $4 per kg, though the purification process may raise the price of raw ores, which is much less expensive in developed countries), and its global supply exceeds thousands of tons per year, implying that true mass-scale industrial applications are easily achievable as opposed to the gram-scale yielding of Carbon Nano Tube (CNT), which is very expensive ($500 per kg).

2.5. Applications and Uses of Calcine Halloysite Nano Clay

Halloysite is a great industrial and medical importance due to its unique qualities. It has been used in many medical, agricultural, industrial and environmental fields. In the next section, some applications of halloysite will be presented.

2.5.1. Halloysite for Corrosion Prevent

Metal corrosion poses a significant technological challenge, and various methods have been developed to combat it, including cathodic protection, insulating coatings, and corrosion inhibition. Among these methods, an inhibitor enhanced coating has proven to be highly effective. In this approach, halloysite nanotubes are utilized to enable the controlled release of corrosion inhibitors. The inner voids of halloysite nanotubes can be loaded with corrosion inhibitors such as 2-mercaptobenzothiazole or benzotriazole, which are known for their anticorrosive properties. This allows for the gradual release of the inhibitors, providing long-term protection against corrosion for the metal surfaces **(Rawtani and Agrawal, 2012).**

2.5.2. Halloysite for Thermal Resistance (HNT)

The incorporation of HNTs significantly improve the thermal stability and fire retardancy of the nanocomposites. HNTs are typically used in the production of high-quality ceramics and white ware. Halloysite nanotubes affect the fire performance of composites by forming a thermal insulation barrier at their surface during combustion. This created a barrier that either retarded the burning without stopping or, more often than not, doubled the total burning time **(Rawtani and Agrawal, 2012)**.

2.5.3. Halloysite Nanotubes as Filler for Various Nanocomposites

Halloysite nanoparticles are used as an additive to improve the mechanical performance of polymers particularly epoxies, by strengthening and toughening them. Halloysite nanotubes have a larger luminal diameter, they can accommodate different polymer molecules, making polymeric composites possible **(Rawtani and Agrawal, 2012)**.

2.5.4. Halloysite as Sieve for Sequester Pollutants

Halloysite performs as an effective sieve to sequester pollutants released from a variety of sources such as oil spills, power plants, or mining sites. Once captured, the pollutant is immobilized in a solid form where it can be collected and disposed in an eco-friendly manner.

2.5.5. Use of Natural Halloysite Nanotubes Medical Uses

There are many uses of holloysite in medical sector such as:

A. Capture of Flowing Cells Improved

The incorporation of halloysite Natural Tubes (HNT) onto the surface of devices used to capture circulating tumor cells (CTCs) in blood enhances the capture of flowing cells (**Hughes& King , 2010)**.

B. HNTs as Nano reactors or Nano templates

Recently, HNTs have been used as alternative nanoreactors to fabricate nanowires, nanoparticles and for similar purposes (**Suh, et al., 2011).**

C. Clay nanotubes drug delivery systems

Halloysite nanotubes (HNTs) have shown promise in the field of sustained drug delivery systems. When combined with existing pharmaceuticals, HNTs can enhance drug delivery by providing controlled and sustained release of the drug.

2.6. Review of Previous Uses of Halloysite Nanoclay in Concrete

Although nanoclay has been extensively studied for its application in nanocomposite polymers, its effects on cement mortars and concrete have received relatively less attention. A few studies on the addition of halloysite to concrete have been conducted, where **(Razzaghian et al., 2018)** discovered that replacing 3% of the cement by mass with halloysite nanotubes reduces the initial setting time of the mortar by 23% and the slump and flow of the mortar by 45% and 26%, respectively. In addition, adding halloysite nanotubes to cement sand mortar increases the electrical resistance by about 22%. This improves the corrosion resistance of cement sand mortar. Furthermore, water absorption tests show that the porosity of the samples modified with halloysite nanotubes is lower than that of the control samples. The mass replacement 3% of cement mortar containing halloysite nanotubes reduces the rate of water absorption by 20% and the volumetric water absorption by 10%.

Another study conducted by **(Farzadnia et al. ,2013)** discovered that when halloysite nano clay was added to mortars, the flow-ability of the mixes decreased as the dosage of nano clay increased. In samples containing 3%

nano clay, there was a significant decrease in flowability, with a notable 65% reduction compared to the control samples. However, despite the decrease in flowability, the incorporation of nanoclay into mortars resulted in improved compressive strength, with an increase of up to 24% in samples containing 3% nanoclay. Among the samples, those containing 2% nanoclay exhibited the lowest permeability, showing a significant 56% decrease compared to the control samples.

Razzaghian et al.(2021) studied the mortars containing 3 mass% HNTs, slump and flowability were reduced by 31% and 29%, respectively. The incorporation of HNTs into the mortar reduced permeability due to the HNTs improved microstructure and void-filling effect. Loading 3 massd % HNTs into mortar increases electrical resistivity by about 28% and decreases capillary water absorption, water desorption, and helium porosity by up to 25, 15, 22, and 34%, respectively. HNT-containing samples have higher compressive and flexural strengths than control samples, and the higher the dosage of HNT in the sample, the higher compressive and flexural strength of the mortar. For example, adding 3% HNT improves this strength by up to 25% and 20%, respectively, when compared to the control sample at 28 days of curing time. **(Dungca ,2019)** investigated the combined effect of halloysite nanoclay and nano-montmorillonite as partial substitutes with cement. The results showed that the workability of fresh concrete generally decreased when nanoclay was added to the mix, with a maximum loss of 50% in slump observed for a 5% replacement of the nanoclay combination. Furthermore, a 28th-day compressive strength of 44.5 MPa is obtained as the highest among the concrete samples at 3% replacement, demonstrating a 27.4% increase over a control specimen with a strength of 34.95 MPa.

Allalou et al.(2019) was tested a 6% content of calcined Halloysite Nano Clay (CHNC) in cementitious composites, where ordinary Portland cement

clinker was partially substituted by 70% GBFS (Ground Granulated Blast Furnace Slag). The inclusion of CHNC resulted in an increase in the water percentage required for standard consistency due to its high specific surface area. The addition of calcined HNC significantly reduced the initial and final setting time of High Volume Slag (HVS). As the CHNC content increased, the free lime content decreased, attributed to the strong pozzolanic reaction between this nano-clay and lime released during clinker hydration, leading to the formation of more hydrated products, primarily C-S-H (Calcium Silicate Hydrate). The addition of CHNC positively influenced the chemically combined water content, resulting in enhanced early mechanical strengths of HVS cement mortars. When compared to plain HVS cement mortars, the incorporation of 5% CHNC as a partial replacement for HVS cement substantially improved the compressive and flexural strengths by approximately 105%, 73%, and 71% at 2 days, respectively. Additionally, the compressive strength of HVS mortar increased by approximately 29.70% and 36.21% after 7 and 28 days, respectively, with a corresponding increase of approximately 16% and 16.41% in flexural strength at 7 and 28 days.

Many researchers had studied the addition of halloysite to mortar, but limited research had been done regarding the addition of halloysite to concrete. Therefore, this research investigated the effect of adding halloysite in various proportions to concrete.

2.7. Cementitious Materials

Concrete consists of gravel, sand, cement, water and some additives. Gravel occupies a large volume of concrete, cement material is linking the components with each other and giving strength and durability to concrete through pozzolanic reactions with calcium hydroxide(CH) during the process hydrate **(Peter ,2019).**

According to **ACI (Education Bulletin E3-13)**, the cementitious materials are two types; the hydraulic cement, which is represented by ordinary Portland cement and the supplementary cement materials represented by by-products of different industries, it was found that supplementary cement materials have a benefit when adding them to concrete, the supplementary cement materials includes Fly Ash, Silica Fume and Granulated Blast Furnace Slag (GGBS). As mentioned previously, the production of cement requires a large energy, and this process results in the release of a large amount of carbon dioxide (CO_2), so there is an urgent need to reduce cement consumption, therefore cement supplementary materials are introduced to replace part of cement, to reduce CO_2, improve the cohesion and workability and reduces the heat resulting from the reactions of hydration in addition to improving strength and durability of concrete **(Kosmatka, 2002).**

2.7.1. Ground Granulated Blast Furnace Slag (GGBS)

It is a supplementary cementitious materials called Ground Granulated Blast Furnace Slag (GGBS) and it is a by-product of the iron industry. Iron ore, coke and limestone are fed carefully into a pumped pump at a temperature of 1500Cº. It produces iron and residual slag that floats on top of the iron and this slag is in a molten liquid form. It is quickly quenched with water to turn into GGBS in the form of granules resembling coarse sand, then dried and ground into a fine material **(Suresh, 2015)**.

It is first discovered in Germany in 1826. At the present time, the global production of GGBS will reach about 269 million tons between 2020 and 2025. It is distinguished by its white color and contains a high amount of calcium, silica and aluminate, which makes it suitable in the concrete industry and that the chemical composition changes depending on the raw materials for the iron industry **(Aydın & Baradan, 2014)**.

Since the chemical composition of GGBS contains silica, calcium, alumina, magnesia and iron and formed in concentrations greater than 70%, which is in fact what is classified as pozzolanic materials.

It is usually used in the production of ready-mixed concrete. It is also used in the production of Portland blast furnace slag cement (PBFC) and high slag cement(HSBFC), which content GGBS about 30-70% **(Suresh, 2015)**.

2.7.2. The Effect of GGBS on Concrete Properties

The combination of GGBS with Portland cement may change the fresh, mechanical and durability properties of the concrete, which are discussed in the next section.

2.7.2.1. Workability

Many studies have mentioned that adding GGBS to concrete improves its rheological properties. The higher level of replacement, is the greater workability. **(Arivalagan,2014)** mentioned that GGBS increase the workability of concrete and replacing ordinary Portland cement by of GGBS 0,20,30 and 40% % GGBS will increase the workability and the slump was (24,26,27 and 28 cm) respectively. Also **(Soni, 2016)** studied the effect of replacing cement with GGBS on the workability of concrete, where cement is replaced with GGBS (30, 40, and 50%), and found that 30% GGBS decrease the slump to 85mm in comparison with reference mixture that have slump 100 mm, however there was an increase in the value of slump when the replacement of GGBS increased, the slump was (110and 130 mm) for 40 and 50% of GGBS. **(Boukendakdji, 2012)** studied the effect of GGBS on the fresh properties of self-compacting concrete by replacing 25% of the cement with GGBS, which leads to an increase in the flowability by 5%.

But not all studies are consistent in terms of increasing the flowability, as there is research that included that when replacing cement with percentages

of GGB by (20, 40 and 60%), it led to a decrease in its amount of workability (87 ,68 and 48mm) respectively, compared to the original concrete 112mm **(Patra, 2017)**. This is what is observed when conducting the practical side of the existing study, where there is a clear decrease in the slump value of concrete containing GGBS by 25% and halloysite (1.5,3 and 4.5%).

2.7.2.2. Strength

GGBS significantly affects the development of (compressive, flexural and tensile strength). Although this development in gaining resistance in ordinary concrete replaced by different percentages of GGBS such as the replacement ratio of GGBS, water / binders, type of curing, the age of the test and the content of cementitious materials that increase or decrease the strength development **(Suresh,2015)**.

(Ahmad, 2021) mentioned in his study that the compressive, flexural and tensile strength when using 20% of GGBS, the strength will increase, but behind this percentage the strength begins to gradually decline. The reason is classified that when using high doses, it leads to the formation of unreacted silicon oxide in excessive doses, and it quickly reacts to be an alkaline, alkali silica reaction (ASR) that leads to stresses and cracks in the concrete and the consequent decrease in the strength of the concrete. **(Majhi, ,2018)** studied the effect of replacing cement with GGBS in proportions of (20,40 and 60%), as well as replacing natural coarse aggregate with recycled coarse aggregate with replacement ratios of (0,25,50 and 100%). The result show that the compressive, flexural, and splitting tensile strength decreased with the increase in the replacement percentage for each of the GGBS and recycled coarse aggregates, or both.

2.7.2.3. Durability

Reinforced concrete structures can collapse when exposed to aggressive environments such as sulfate and chloride attack, and this depends on many properties includes; the density, permeability and porosity of concrete that allows these aggressive salts to enter the concrete. it has in many researches that adding GGBS to concrete improves its resistance to sulfate and chloride attacks.

GGBS increases the density of concrete so that the concrete becomes stronger and also reduce the permeability of the concrete because GGBS interacts with the cement to be additional product of CSH, which works to fill the voids and bind the concrete components in a better way **(Ahmad, 2022)**.

The replacement equal amounts of GGBS and metakaoline with ratios of 0,10,15 and 20% of the cement has a clear improvement in decreasing the permeability and an increase in the density of concrete with the increase in the quantities of the replacement of GGBS and metakaolin **(Bheel, 2020)**. Also, he mentioned that GGBS worked to reduce the penetration of chlorides into the concrete. There is a close link between the permeability and penetration of chlorides, the higher the permeability and porosity of concrete, the greater the penetration of chlorides, and thus increasing the possibility of corrosion of reinforcing steel and failure of concrete.

2.8. Chloride Penetration of Concrete

Many concrete structures continue to have insufficient corrosion-free service life, particularly when located in marine and coastal areas with high chloride concentration **(Papanikolaouet al., 2019)**.

Consequently, numerous infrastructure elements necessitate repair within a decade of service due to reinforcement corrosion. The deterioration

caused by corrosion is particularly severe in chloride-rich environments (**Koch et al., 2016)**.

According to **(Mir etal. , 2020)**, the service life of concrete structures is divided into two stages as shown in Figure (2-5). The first stage - initiation phase - is related to the penetration of the critical chloride concentration up to the level that has limited impact on reinforcement bar in concrete structures. Whereas, the second stage - propagation phase - is related to the reinforcement corrosion and concrete cover cracking and spalling and is associated with severe damage.

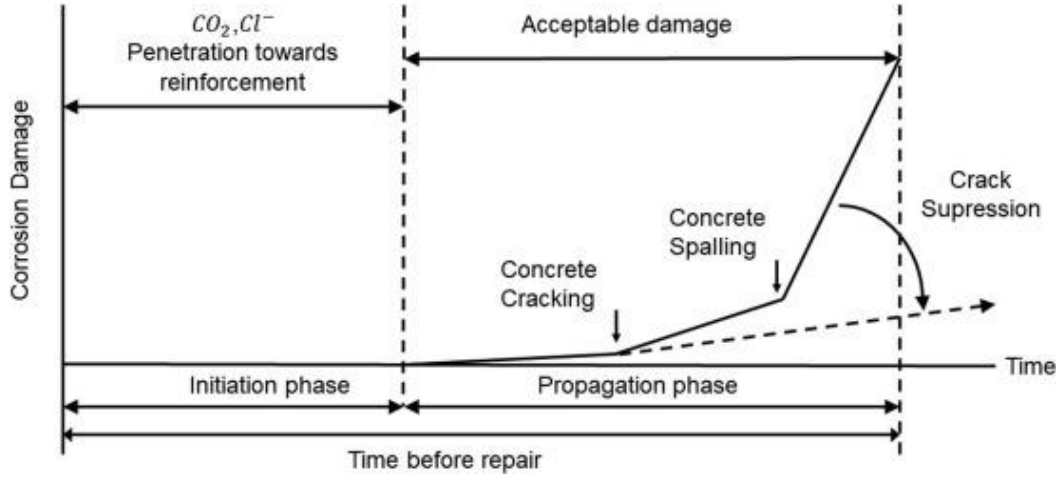

Figure 2-4: Schematic sketch of steel corrosion sequence in concrete (Mir et al. , 2020)

To address the challenges posed by chloride-induced corrosion and other forms of degradation, it is crucial to utilize high-quality concrete that possesses sufficient resistance to chloride penetration. Chloride ingress into concrete can occur only if the concrete pores are completely or partially filled with water. Permeation, capillary suction, and diffusion all contribute are methods to penetration through capillary pores or cracks **(De Weerdt et al, 2023).**

2.8.1. Chloride Ions Sources

Two sources of ions of chloride maybe penetrate to concrete structures, internal and external will be shown in next sections.

2.8.1.1.Internal Source of Chloride Ions

Chloride ions may be found in concrete when they are introduced into the concrete mixture through contaminated aggregate, the use of seawater or brackish water, or the incorporation of admixtures containing chlorides **(Ukpata et al., 2022).**

The British Standard **BS 882: 1992** (withdrawn) limits on the chloride ion content by mass, expressed as a percentage of the mass of the total aggregate, are as follows:

- For prestressed concrete 0.01
- For reinforced concrete made with sulfate –resisting cement 0.03
- For other reinforced concrete 0.05

Also, the **EN BS 197-1:2011** limits the chloride content in cement should be not more than 0.1% and **BS EN 12620:2002+A1:2008** Limits Cl^- content in aggregate should be not more than 0.06%.

Concrete mixture, if the process water contains chlorides, or if the structure is exposed to salt water too early, the salt maybe penetrates deeply into the young concrete because its permeability is high and the shrinkage absorbs water into the young concrete. Salt water penetrates cracks and joints very easily **(Cao et al. ,2022).**

2.8.1.2.External Source of Chloride Ions

Another source of ingress of chloride ions from external sources can be caused by:

A. De-icing Salts

Bridges and road hobbyists exposed to de-icing salts have different conditions. In winter, parts of the primary structure of saturated salt solutions are diluted as quickly as melts ice and snow as shown in Figure (2-6) **(Cao, et al. ,2022)**.

Salt actually lowers the freezing temperature of the water. Instead of freezing at 0 degrees Celsius, salt brings the freezing temperature down to around -17.78 degrees Celsius. The concrete is then penetrated by chloride salt **(Paw, 2022**)

Figure 2-5: De-icing salt of road De-icing of roads. (2023),https://eusalt.com/about-salt/salt-uses/road-safety/

B. Marine Environmental Exposure

The European standard **EN BS 206:2014** provides a classification of exposure classes for concrete based on chloride exposure. These exposure classes are divided into two categories: chlorides from sea water (XS) and chlorides from sources other than sea water (XD).

In the XS category, concrete members are further classified into three exposure classes:

XS1: Concrete in this exposure class is exposed to airborne salts from sea water but does not come into direct contact with sea water. Examples include structures located along the coast beyond the spray zone. XS2:

Concrete in this exposure class refers to marine and coastal structures that are permanently submerged in sea water. Although there may be a significant chloride penetration due to limited oxygen supply, corrosion may not be significant. XS3: Concrete in this exposure class is located in the tidal, splash, and spray zones. Marine and coastal structures that experience these conditions fall under this category.

In the XD category, exposure classes are as follows:

XD1: Concrete in this exposure class is exposed to moderate humidity and comes into contact with airborne chlorides from sources other than sea water. Examples include structures near highways where chlorides are present in the air. XD2: Concrete in this exposure class is in contact with water containing chlorides other than sea water. Structures such as swimming pools or those exposed to chloride-containing industrial waters fall under this category. The concrete in XD2 exposure class is exposed to a cyclically wet and dry environment, and the chlorides are not derived from sea water **(Zych, 2015)**.

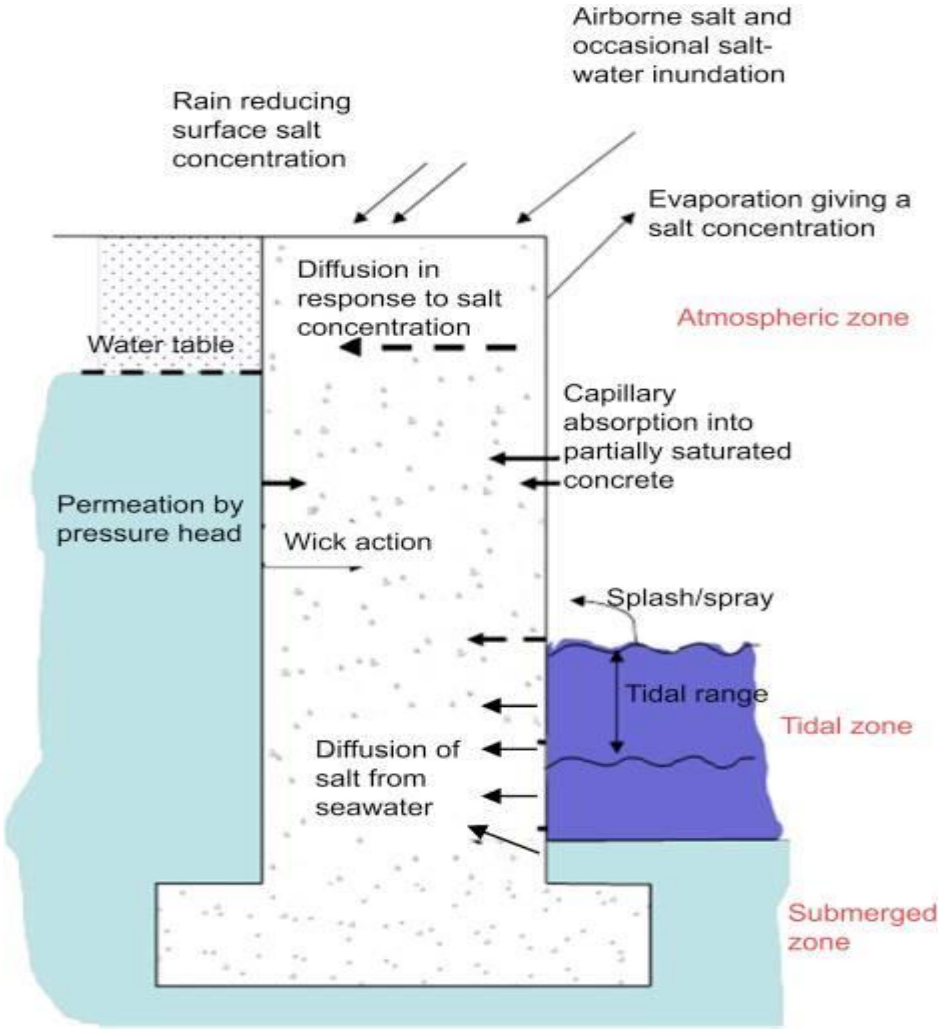

Figure 2-6: Deterioration of concrete in the marine environment (XS) (Santhanam& Otieno, 2016)

2.8.2. Types of Chlorides in Concrete

Chloride ions can chemically or physically bind with hydration products or remain free in the concrete pore solution during diffusion **(Karthick et al., 2016)** to form the aggressive reaction with steel **(Neville, 2011)**. Figure (2-8) illustrates the relationship between concentrations of these forms of chloride ions with depth of concrete

Where some of the chlorides are chemically bound and are found in cement hydration products. Other chlorides are physically bound because they are adsorbed on the surface of the gel pores **(Neville, 2011)**.

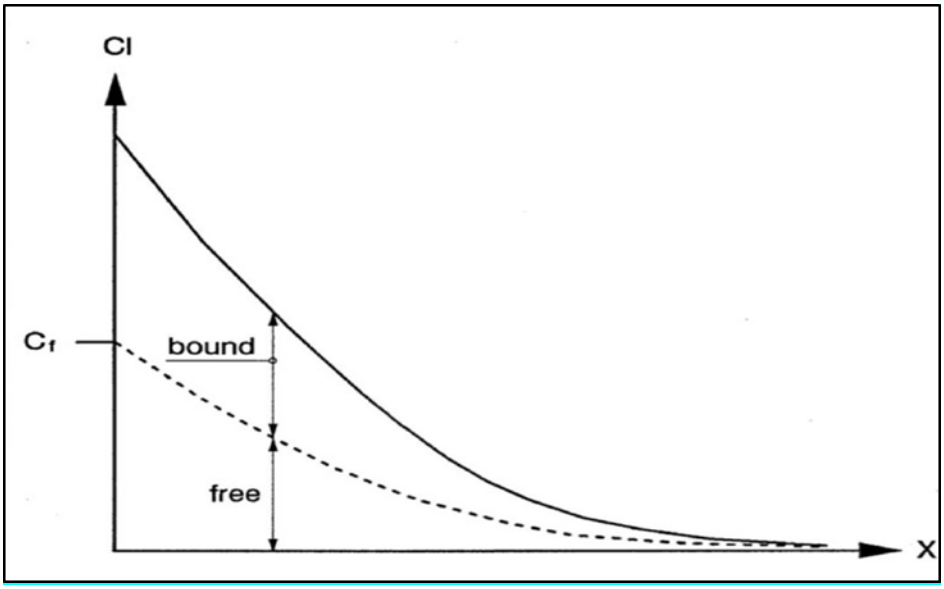

Figure 2-7: Typical profile of free and bound chloride by (Neville, 2011)

2.8.3. Transport mechanisms of Chloride Ions in Concrete

Because of their interactions with concrete constituents or pore water, the movement of gases, liquids, and ions through concrete is important, and it can alter the integrity of concrete directly and indirectly, leading to the deterioration of concrete structures.

Chloride ions diffuse deeper into concrete as a result of the concentration gradient **(Mir et al. , 2020)**. Where, the presence of chloride ions triggers the formation of Friedel's salt (FS)., that reduce the rate of chloride transport **(Han, 2007)**. The resistance of concrete to chloride attack is determined by its capacity to bind chloride ions (chloride transport resistance) and the apparent diffusion coefficient D_a (**Yuan, 2015)**. Various chloride binding mechanisms exist in concrete, including chemical reactions between chloride ions and hydration products such as tricalcium aluminate (C_3A) and tetracalcium alumino ferrite (C_4AF), leading to the formation of Friedel's salt ($3CaO\ Al_2O_3\ CaCl_2\ 10H_2O$). Friedel's salt is known to be stable in alkaline environments; however, its stability decreases at lower pH

values, particularly when concrete undergoes carbonation **(AL-Ameeri et al.,2021)**.

The reaction of chloride ions with the components of concrete (mainly calcium hydroxide $Ca(OH)_2$), e.g. expansive alkaline calcium chloride $Ca(OH)_2 \cdot H_2O \cdot CaCl_2$, which increases its volume during crystallization and causes destruction of concrete, is formed during the following reactions as shown in Equation (2-1) and (2-2) **(Zych, 2015)**

$$Ca(OH)_2 + 2NaCl \rightarrow CaCl_2 + 2NaOH \qquad (2-1)$$

$$Ca(OH)_2 + CaCl_2 + H_2O \rightarrow Ca(OH)_2 \cdot H_2O \cdot CaCl_2 \qquad (2-2)$$

Chloride ions, along with carbon dioxide (CO_2), can have detrimental effects on the corrosion of steel reinforcement in concrete. In the presence of chlorides, the protective ferric oxide film that forms naturally on the surface of steel rebar during the casting of concrete can be destroyed. This film is stable in the alkaline (high pH) environment surrounding the steel rebar. When depassivation occurs, meaning the loss of the passive layer on the surface of the reinforcement, it initiates the corrosion process of the steel. Chloride ions (Cl^-) react with iron to form ferric chloride ($FeCl_2$). Subsequently, $FeCl_2$ reacts with water to produce rust ($Fe(OH)_2$), and the resulting hydrochloric acid (HCl) formation contributes to the formation of pits on the surface of the reinforcing bars. **(Kurdowski, 2014)** as illustrated in Equations (2-3), (2-4) and Figure (2-9).

$$Fe + 2Cl^- \rightarrow FeCl_2 + 2e^- \qquad (2-3)$$

$$FeCl_2 + 2H_2O \rightarrow Fe(OH)_2 \qquad (2-4)$$

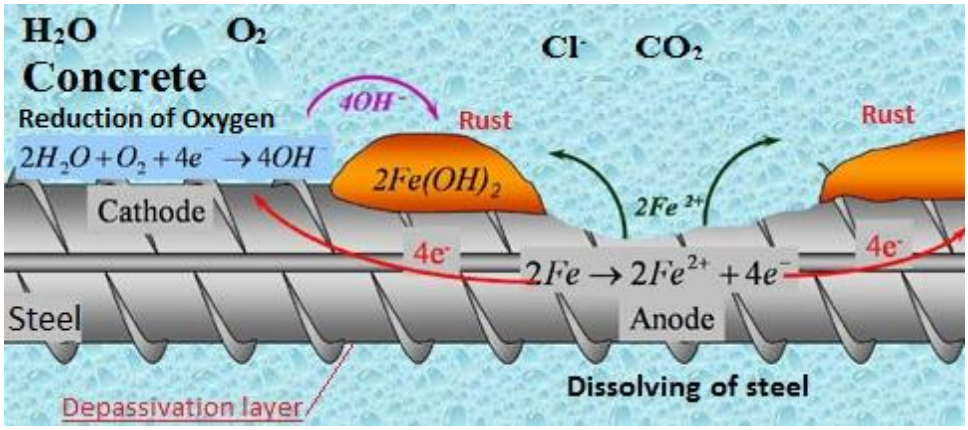

Figure 2-8: Corrosion mechanism of reinforcement in concrete (Broomfield, 2007)

There are three mechanisms for transport chloride ions into concrete:

A. Diffusion

Diffusion is the movement of ions, gases, or water vapor from areas of higher to lower concentration. In concrete, diffusion tests, including gas, water vapor, and ionic diffusion tests, study these processes **(Hearn et al., 2006)**. These tests provide insights into substance transport within the concrete matrix.

B. Absorption

Water absorption in concrete is driven by surface tension in capillaries, influenced by pore structure and moisture content. Methods like Surface Absorptivity and Drilled Hole Absorptivity tests are employed to measure water absorption, providing insights into concrete's permeability. These tests evaluate how water is absorbed by the concrete surface and through drilled holes, respectively **(Zhuang et al. 2022).**

C. Permeability

Permeability, defining fluid passage under pressure differential, allows chlorides to penetrate concrete surfaces under hydraulic head exposure. Permeability tests, commonly conducted using permeability cells, involve admitting pressurized fluid to one side of the specimen, measuring

flow at the inlet or outlet, utilizing varied cell specifications **(Skutnik, et al. 2020).**

2.8.4. Test Methods of Chloride Penetration and Concentration in Concrete

The most common techniques for measuring chloride content can be broadly classified as field and laboratory methods as shown in Figure (2-10), with field destructive tests being prevalent. These methods involve sampling from in-service structures and determining chloride profiles using chemical or physical lab techniques. Destructive techniques are primarily employed for short-term decision-making, such as repair and maintenance **(Torres-Luque, et al. 2014)**.

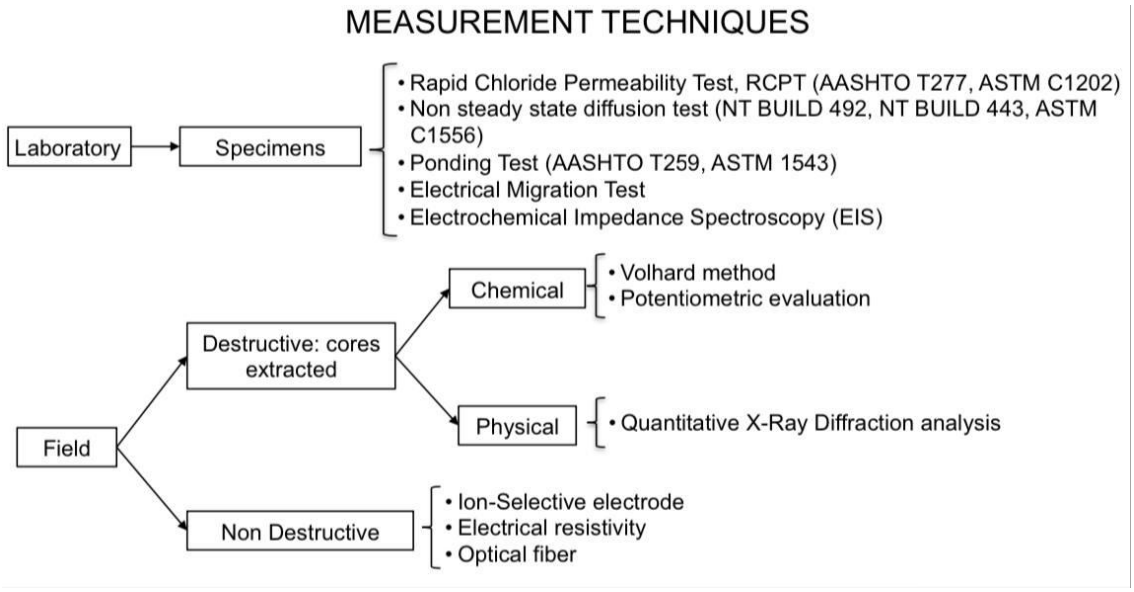

Figure 2-10: Techniques for measuring chloride content

2.9. The Effect of Nanoclay on Chloride Penetration into Concrete

The impact of chloride ingress into concrete should be studied in order to understand the behavior of concrete when exposed to chloride attack when there nano-clay is present, as **(He and Shi, 2008)** discovered nano-clay has shown greater effectiveness in reducing the chloride diffusion

coefficient of mortar compared to other types of nanomaterials. When 1% of different nanomaterials, such as Fe_2O_3, Al_2O_3, TiO_2, and SiO_2, were added to the mortar, the chloride diffusion coefficient values exhibited a significant decrease. For the control specimen (C0), the chloride diffusion coefficient was measured to be 6.82×10^{-11} m^2/s.

Upon the addition of 1% nano-SiO_2, hydrophilic nano-montmorillonite (clay-hi), and hydrophobic nano-montmorillonite (clay-ho), the chloride diffusion coefficients of the mortar decreased to 2.61×10^{-11}, 2.29×10^{-11}, and 1.64×10^{-11} m^2/s, respectively. This represents reductions of 62%, 66%, and 76% compared to the control specimen. Another study conducted by **(Niu et al., 2021)** revealed nano-clay has the potential to enhance the resistance of concrete against chloride penetration. Meanwhile, as the nano-clay concentration increased, the chloride diffusion coefficient decreased exponentially. The 28-day chloride diffusion coefficient of concrete incorporating 1, 3, 5, 7 and 9% nano-clay decreased by 27, 29, 53, 31 and 23% when compared to a plain specimen. **(Langaroudi et al. ,2018)** also discovered that adding nano-clay reduced the coefficient of chloride migration. The concrete containing 3% nano-clay had the lowest chloride migration coefficient $1.84 * 10^{-12}$ m^2/s, indicating an extremely high resistance to chloride penetration. **(Fan et al. ,2014)** In the study conducted, a mixture of ordinary Portland Cement (OPC) and kaolinite clay soil was used to create concrete and mortar with enhanced mechanical properties and resistance to chloride ion invasion. Different percentages of kaolinite clay soil (ranging from 0% to 9% by weight of cement) were added to the OPC. The results of the study showed that the incorporation of kaolinite clay soil improved the penetration resistance of cement concrete. Specifically, at 1% clay content, the chloride diffusion coefficient was reduced by 8.68% compared to the control sample without clay. Furthermore, at 5% clay

content, the chloride diffusion coefficient was reduced by a larger percentage, specifically by 18.87%. Additionally, the compressive strength of the cement concrete was also improved with the addition of kaolinite clay soil.

Chloride ingress is a significant environmental loading that weakens concrete and, as a consequence, reduces the strength, serviceability, and aesthetics of the structure. This research investigated the effects of ingress chlorides on concrete containing halloysite nanoclay, a topic that had not been previously studied.

2.10. Conclusion Remarks

Upon reviewing the previous literature, it becomes evident that:

- Halloysite is a natural, nontoxic material from kaolin group clay 1:1 layer Phyllosilicates content at the external layer silicon (S-O-S) and the inside aluminum (Al-OH) with interfacial water molecule. The chemical formula $Al_2(OH)_4.Si_2O_5 \cdot nH_2O$ which (n=2) if (HNC) hydrate named (halloysite 10 Å) and (n=0) if halloysite dehydration and have (7 Å).
- Calcine halloysite nano clay has tuber form with diameter 50-70nm for external,10-20nm for internal with 0.2-40 μm length. Because of its unique chemical and physical properties, which give it a high mechanical strength and modulus.
- Calcine halloysite nano clay is now used in a variety of fields of nanotechnology, including biomedicine, energy, and catalysis. Furthermore, HNTs are used in a variety of applications, such as environmental protection and remediation, biomedicine, chemicals, agriculture, and others.

- Chloride ions are a harmful agent that interacts with concrete, destroying it and jeopardizing the constructor's safety. Chloride comes from both the outside (de-icing, water content in concrete,) and the inside (contaminating aggregate, mixing water content chloride, and concrete itself). It enters concrete through three different mechanisms, diffusion, adsorption, and permeability.

Previous studies have primarily focused on investigating the mechanical and fresh properties of mortar, with limited research conducted on the impact of incorporating halloysite into concrete. This research aims to provide a comprehensive analysis of both the mechanical and durability properties of concrete, specifically examining the penetration of chlorides into the concrete.

Furthermore, this study addresses an aspect that has not been extensively explored thus far, which is the influence of halloysite on the dry shrinkage of concrete. Additionally, non-destructive tests will be conducted to assess the effect of halloysite on the surface hardness and microstructure of concrete. To estimate carbon emissions from concrete mixtures incorporating halloysite, the calculation of eCO_2 will also be undertaken.

Chapter Three Methodology and Experimental Works

Chapter Three
Methodology and Experimental Works

3.1. Introduction

The chapter focuses on presenting the methodology, materials, and also experimental procedures undertaken to fulfill the objectives and goals outlined in Chapter One. The primary objective of this experimental work is to investigate the impact of incorporating Halloysite Nanoclay (HNC) on various aspects of concrete performance. Specifically, the focus is on evaluating the effects of HNC on chloride penetration, corrosion, dry shrinkage, and mechanical properties of concrete.

This chapter includes two main parts; the first part includes the properties of the materials, the proportions of mixing, casting, and curing. While, in the second part, the various test procedures that were employed to achieve the aims of study. The work experimental was carried out in civil engineering department laboratories in College Engineering / University of Babylon. The experimental work of this thesis is illustrated in Figure (3-1).

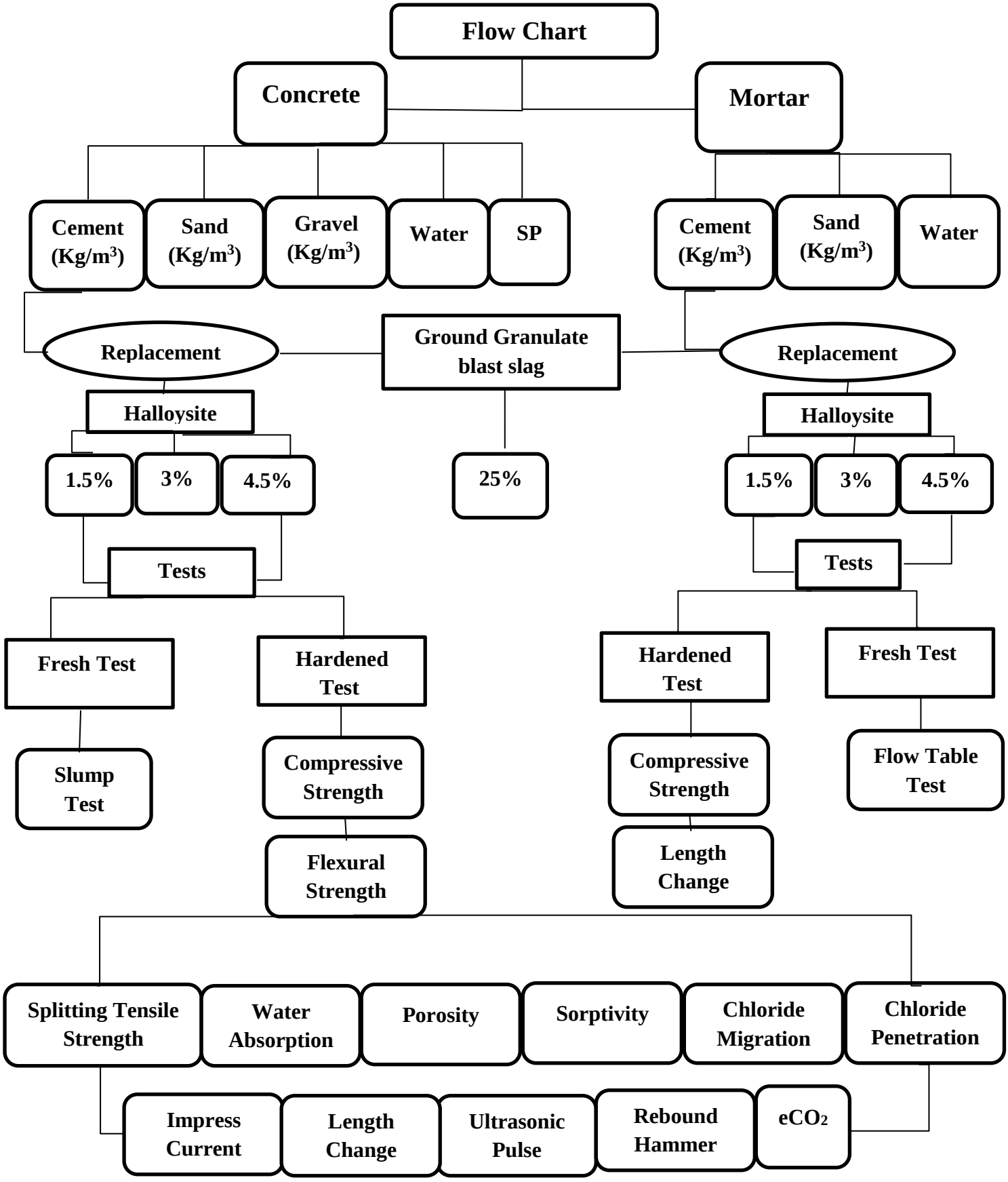

Figure 3-1: Flow Chart Experimental Work

3.2. Materials Properties

The following sections outline the materials used in the Halloysite Nanoclay (HNC) concrete mixes.

3.2.1 Cement

Iraqi ordinary Portland cement **CEM I -42.5R** originating under the trade name (Al-Mass) was used. The chemical and physical properties of this cement are shown in Tables (3-1), (3-2) and they are conformed to the Iraqi specifications **(IQS No.5/2019)**.

Table 3-1: Chemical Composition and Main Compounds of Cement*

Chemical Composition	Percentage By Weight	Limit of IQS No.5/2019
Lime (CaO)	60.7	-
Silica (SiO_2)	20.52	-
Alumina (Al_2O_3)	5.33	-
Iron oxide (Fe_2O_3)	3.98	-
Magnesia (MgO)	2.44	5.0 (max)
Sulfate (SO_3)	2.45	2.8 (max)
Loss on ignition (L.O.I)	2.55	4.0 (max)
Insoluble residue (I.R)	0.93	1.5 (max)
Main compounds (Bogue's equation)		
Tricalcium Silicate (C_3S)	49.58	-
Dicalcium Silicate (C_2S)	21.5	-
Tricalcium Aluminate (C_3A)	7.39	-
Tetracalcium Aluminoferrite (C_4AF)	12.1	-

*Chemical tests were conducted by the national center for construction laboratory at the University of Karbala.

Table 3-2: Physical Properties of the Cement*

Physical Properties	Test result	Limit of IQS 5:2019
Fineness using Blaine air permeability apparatus (cm^2 / gm)	3200	≥ 2800
Soundness using autoclave method	0.19%	≤ 0.8 %

Setting time using Vicat's instrument Initial (minute) Final (hours)	 190 4	 ≥ 45 min ≤ 10 hr
Compressive strength for cement paste cube (70.7 mm) at 2 days (MPa) 28 days (MPa)	 22.4 43.2	 ≥20 ≥42.5

*Physical tests were conducted by the national center for construction laboratory at the University of Karbala.

3.2.2. Aggregate

3.2.2.1. Fine Aggregate (I)

The fine aggregate used in this research is local natural sand from the (Al-Ekhaider) quarry, with a maximum particle size of 4.75 mm. Sieve analysis of fine aggregate was carried out according to (IQS No. 45/1984). The results indicate that the classification of fine aggregates is within the requirements of the Iraqi Standard. Table (3-3), Figure (3-2) show the sieve analysis test. The content of sulfate, clay percentage, fineness modulus, specific gravity and absorption of fine aggregate were performed according to (IQS) and the results of physical and chemical properties of fine aggregate are shown in Table (3-4).

Table 3-3: Fine Aggregate Test Result *

Sieve size(mm)	Passing %	IQS No.45/1984, zone 3
9.5	100	100
4.75	97	90-100
2.36	85	85-100
0.6	60	60-79
0.3	18	40-12
0.15	0	0-10

*test was conducted by the construction material laboratory at the University of Babylon

Table 3-4: Chemical and Physical Properties of Fine Aggregate *

Physical Properties	Test Results	Iraqi specification. 45/1984
Fineness modulus of sand	2.65	-
Specific Gravity	2.60	-
Absorption %	2.6	-
Materials finer than 75µm %	3.44	≤ 5 %
Chemical Properties		
Sulfate content%	0.33	Not more than 0.5%

*test was conducted by the construction material laboratory at the University of Babylon

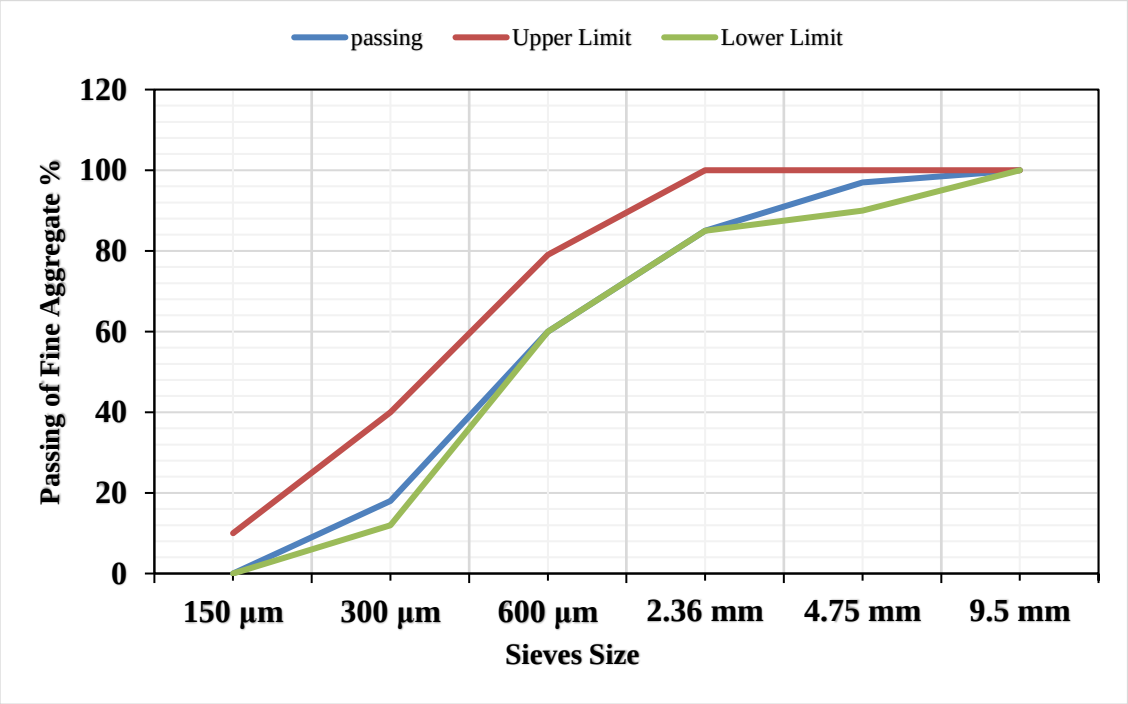

Figure 3-2: Sieve Analysis of Fine Aggregate Zone (3)

3.2.2.2. Fine Aggregate (II)

Natural silica sand is used in this study for mortar only. The sand was sieved to show the maximum particle size of sand was (4.75mm). The results indicate that the classification of fine aggregates is within the requirements of the Iraqi Standard (IQS No. 2080 /1998). as shown in Table (3-5). the sulfate content test has been carried according to and the result of SO_3 was (0.08%) and is was conformed to Iraq standard No.5. and Figure (3-3) show standard sand.

Table 3-5: Fine Aggregate Test Result *

Sieve size(mm)	Passing %	IQS No.2080/1998
4.75	97	95-100
2.36	95	95-100
1.18	91	90-100
0.6	87	80-100
0.3	43	15-50
0.15	4	0-15

*test was conducted by the construction material laboratory at the University of Babylon

Table 3-6: Chemical and Physical Properties of Fine Aggregate *

Physical Properties	Test Results	Iraqi specification. 2080/1998
Fineness modulus of Sand	1.83	-
Specific Gravity	2.67	-
Absorption %	1.02	-
Materials finer than 75µm %	1.8	≤ 5 %
Chemical Properties		
Sulfate content%	0.08	Not more than 0.5%

*test was conducted by the construction material laboratory at the University of Babylon

Figure 3-3: Standard Sand used in Mortar

3.2.2.3. Coarse Aggregate

The crashed coarse aggregate used in this research is a local natural aggregate was brought from the Al Nabai region, with a maximum size of 20 mm. Sieve analysis was performed for dry coarse aggregate and by selecting standard sieves. The results showed that the classification of coarse aggregate within the requirements of the Iraqi Standard (IQS No. 45/1984) and Table (3-7) and Figure (3-4) illustrate the sieve analysis test. The sulfate and particulate content, specific gravity accuracy and coarse aggregate adsorption were performed according to (IQS). Table (3-8) shows the physical and chemical properties of coarse aggregate

Table 3-7: Coarse Aggregate Test Result *

Sieve Size (mm)	Passing %	Limits of Iraqi spec. no.45/1984 (5-20mm)
19.5	96.19	100-95
12.5	41.28	-
9.5	30	60-30
4.75	1.61	10-0

*test was conducted by the construction material laboratory at the University of Babylon

Table 3-8: Chemical and Physical Properties of Coarse Aggregate *

Physical Properties	Test Results	Iraqi specification. 45/1984
Fineness modulus of Gravel	2.30	-
Specific Gravity	2.65	-
Absorption %	0.75	-
Bulk Density	1580 (Kg/m^3)	-
Chemical Properties		
Sulfate content%	0.009	Not more than 0.1%

*test was conducted by the construction material laboratory in University of Babylon

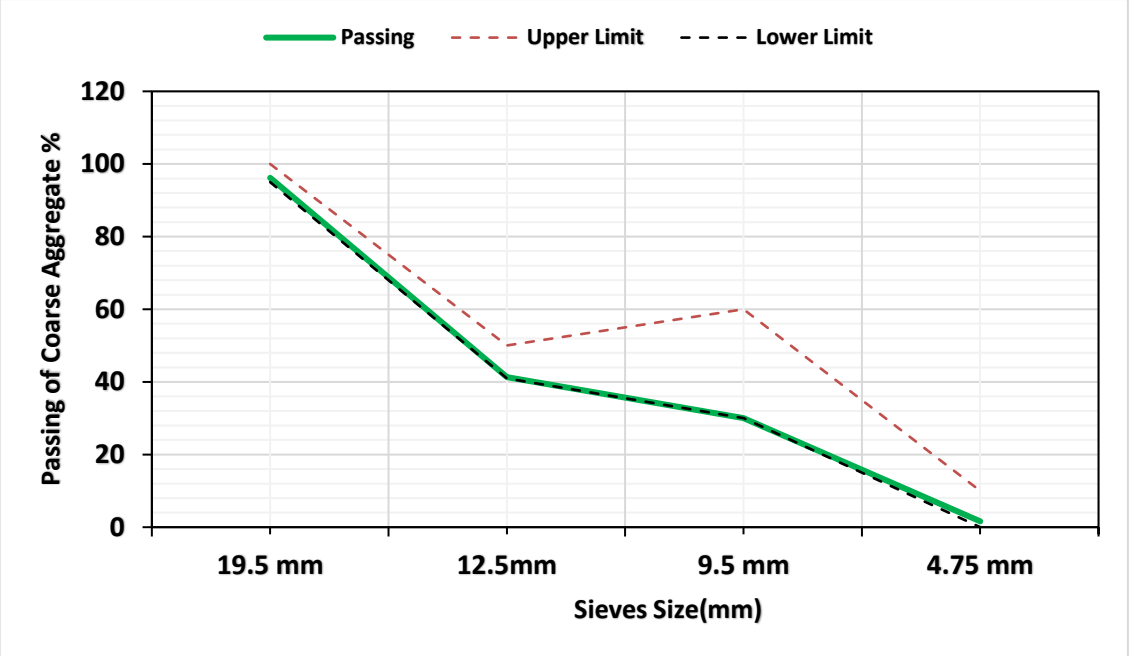

Figure 3-4: Sieve Analysis of Coarse Aggregate

3.2.3. Calcine Halloysite Nano Clay (CHNC)

Calcined halloysite tubular Nano powder from (Shijiazhuang Huabang) company in china. It has chemical formula $Al_2Si_2O_5(OH)_4.2H_2O$ with weight (294.19 g/mol) that is use in this research. The chemical and physical properties of halloysite are illustrated in Table (3-9) and (3-10) respectively. The halloysite were imported in 10 kg bags, Figure (3-5) shows the halloysite powder that is used in this study.

Table 3-9: Chemical composition of halloysite *

Oxide Composition	Test Result (%)
SiO_2	45.8
AL_2O_3	37.3
K_2O	6
Na_2O	1.2
MgO	1.2
Fe_2O_3	2.5
TiO_2	0.7

CaO	0.2

*From Manufacturer

Table 3-10: Physical Properties of Halloysite *

Properties	Specification
Purity	100%
Diameter x Length	30-70 nm x 1-3 μm, nanotube
Color	Hunter brightness (75-96)
Refractive Index	N20/D 1.54[a]
Pore volume	1.26-1.34 ml/g
specific surface area	64 m^2/g
Cation exchange capacity	8 meq/g[b]
True Specific gravity	2.53

*Manufacturer Properties

a: N is mean 20 C^o at room temperature, D- sodium doublet" wave length" (589.3nm) ,1.54:value of halloysite refractive.

b: meq/g (milli equivalents of charge (number of charges) per100g of soil).

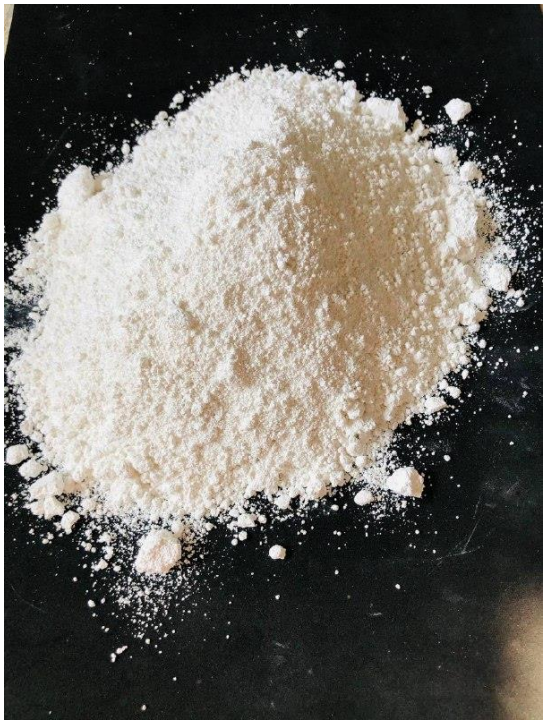

Figure 3-5*:* Halloysite Nano Powder

3.2.4. Ground Granulated Blast Furnace Slag (GGBS)

Ground Granulated Blast Furnace Slag was supplied by Hanson cement group-UK with relative density (2.90 g/cm^2). The chemical analysis and physical properties of GGBS are shown in Table (3-11) and (3-12) respectively, and it satisfied the requirement of BS-EN 15167-1: 2006 Figure (3-6) shows the GGBS powder. In this study, the percentage of replacement with cement taken was 25% by weight of cement, this percentage was used based on the previous studies **(Alwash, et al, 2023)**.

Table 3-11: Chemical Analysis of GGBS*

Chemical Composition %	Test Result (%)	Limits of BS EN 15167-1: 2006
SiO_2	35.59	
Al_2O_3	14.32	
Fe_2O_3	0.35	
CaO	41.95	
MgO	7.41	≤ 18%
MnO	0.18	
Mn_2O_3 Calc	0.20	
TiO_2	0.55	
S_t	0.94	
S^{2-}	0.90	
SO_3	0.09	≤ 2.5%
L.O.I.	0.66	≤3%
I.R.	0.18	
C	0.08	
Cl	0.01	≤ 0.1%

* Manufacturer Properties

Table 3-12: Physical Properties of GGBS*

Properties	Test Result	Limits of (Reference standard BS EN 15167-1: 2006)
Setting time using Vicat's Method Initial (min.)	190	≥150 min
Fineness (Blaine Method) m^2/km	456	≥275 m^2/kg
Expansion (mm)	0.5	-
H_2O/Standard consistency	0.3	-
Activity Index (%) at		
7day	65	≥50%
28days	90	≥50%

* Manufacturer Properties Hanson Cement Company.

Figure 3-6: GGBS powder

3.2.5. Steel Reinforcement

15 cm long ,Ø10 Steel bar embedded in the concrete samples for accelerated chloride penetration and impressed current test , the concrete cover was 2 cm. Figure (3-7) shows the steel and cover spacer used in this study.

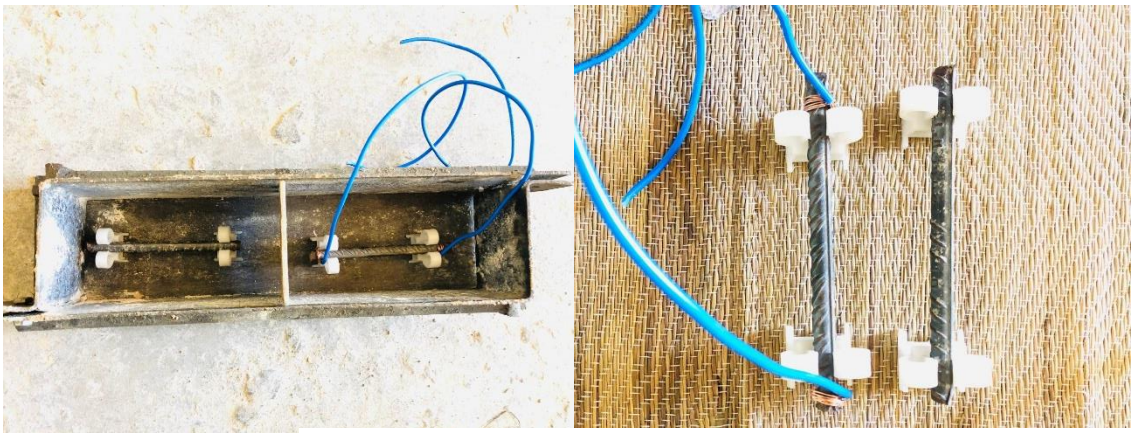

Figure 3-7*:* Steel and spacer used

3.2.6. Mixing water

Tap Water was used for all the mixes in this study water. the water was fresh and free of acids, organic matter, suspended solids, alkalis and impurities. The temperature of the mixing water was maintained at (25±2) ^{o}C.

3.2.7. High-Range Water Reducing Admixture (Superplasticizer)

Glenium 54 (G54) was used and It is a modified polycarboxylate ether based high performance concrete plasticizer conforming ASTM C 494-2017 Type A & F, chemical effect based on a unique carboxylate ether polymer with long literal chains. It is used for early and final high strength, and appears as a dark brown liquid with free chloride. In the study, concrete mixtures were prepared with the addition of Halloysite nanoclay at specific proportions. A mass ratio of 0.5% of superplasticizer by the mass of cement was used for the concrete mixture aiming for a target strength of 40MPa,

while a mass ratio of 1% of the cement was used for the concrete mixture aiming for a target strength of 50MPa.

3.3. The Optimum Proportions of Halloysite

The growing interest in nanoscience has led researchers to explore its application in the construction field, particularly by partially replacing cement with nanomaterials in order to produce mortar or concrete with improved mechanical, chemical, and physical properties. This approach also aims to reduce cement consumption.

Based on a previous study conducted by **(Allalou, 2019)**, experimental mixtures were made on cement mortars to find out the optimal proportion of halloysite that give high compressive strength and improve mortar properties such as fresh, mechanical and durability properties.

Depending on the specification (ASTM C109/C109M,2016) the mixing proportions of cement, sand and water were determined as shown in Table (3- 13), the w/cm ratio was 0.48 , three 50x50mm cube molds were used for each mixture. the proportions of HNC were 1.5,2, 3, 4.5 and 6% by weight of cement

Table 3-13: Mix Proportions for Mortar

Mix Proportions for mortar for(3) cubes of 5*5*5cm					
CHNC%	**CHNC(g)**	**cement (g)**	**sand (g)**	**Water(g)**	**w/cm**
0	**0**	**500**	**1375**	**240**	**0.48**
1.5	**7.5**	**492.5**	**1375**	**240**	**0.48**
2	**10**	**490**	**1375**	**240**	**0.48**
3	**15**	**485**	**1375**	**240**	**0.48**
4.5	**22.5**	**477.5**	**1375**	**240**	**0.48**
6	**30**	**470**	**1375**	**240**	**0.48**

The molds used for casting the mortar cubes were removed after 24hr of initial curing in a wet room with a temperature of 23±2 °C and a relative humidity of not less than 95% . The mortar cubes were then placed in a water curing basin and stored for 7 and 28 days.

After the specified curing period, the mortar samples were tested according to the ASTM C109 / C 109M standard to determine their compressive strength. The compressive strength values were measured at the end of 7 and 28 days from the time of casting. show in Figure (3-8).

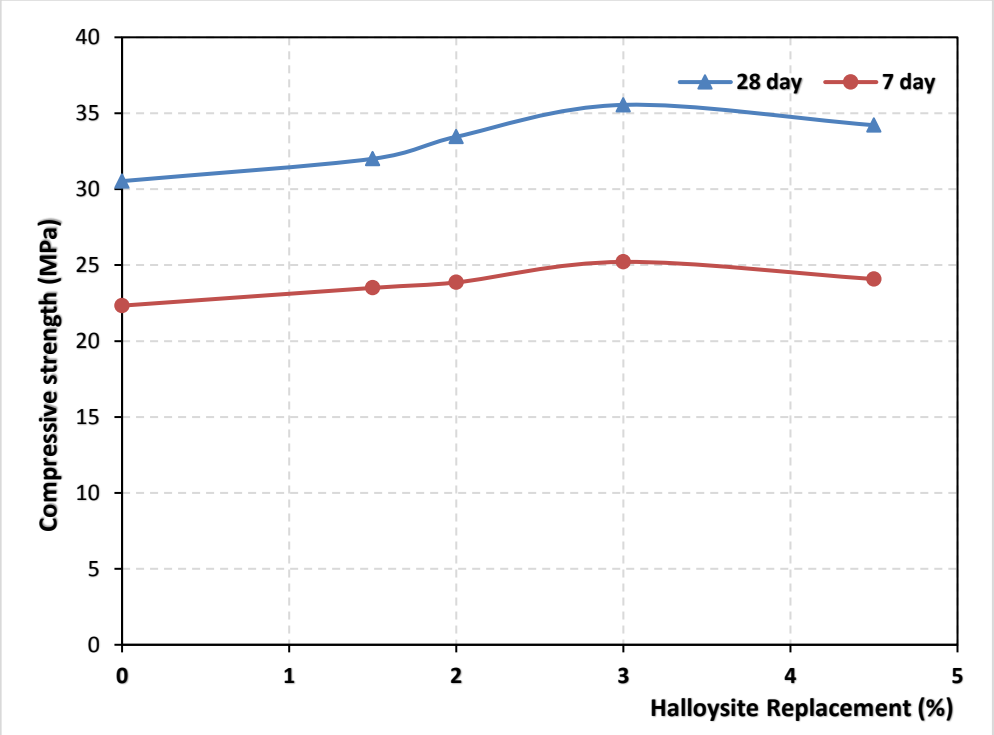

Figure 3-8: Compressive Strength of Mortar with Halloysite Percentage

3.4. Concrete Trial Mixes

Several mixing proportions from previous literature were considered in order to establish a variety of mix proportions for this study. Six experimental mixtures were made, 3 concrete mixtures and the other is a mortar. Where the first mixture (NC) targeted a compressive strength of 40MPa, and that was done by reducing the percentage of W/C = 0.5 and

using a super plasticizer at a rate of 0.5%of the mass of cement. The second mixture (HS) was done to obtain a higher strength estimated at 50MPa by using w/c=0.45 and adding a super plasticizer by 1% of the cement mass to improve the workability of the concrete mixture. As for the third mixture (GG), the cement was replaced by 25% of GGBS to reduce the amount of cement and add it to study its behavior when is added to concrete with hallyosite. This ratio of GGBS was based on previous studies **(Alwash, et al, 2023)**. As for the mortar, a ratio of 1: 2.75 cement to sand was used with two w/cm ratios. 0.5 and 0.48. The trial mix certified in this study is shown in Table (3-14).

Table 3-14: The trial mixture for concrete and mortar

Trial Mix	Content per unit volume of concrete (kg / m^3)			w/c	SP[1]	GGBS[2]%	Compressive Strength at 28 day
	Cement	Sand	Gravel				
NC	370	706	1080	0.5	0.5	0	40.92
HS	420	678.4	1080	0.45	1	0	50.11
GG	277.5	706	1080	0.5	0.5	25	41.05
Mortar mixtures							
MC	500	1375	0	0.50	0	0	24.49
MH	600	1650	0	0.48	0	0	32.22
MG	375	1375	0	0.50	0	25	25.73

[1]SP: superplasticizer with percentage of cement mass.

[2]GGBS: replacement percentage of cement mass

3.5. Mixing Procedures

The mixing process of mortar or concrete is important to obtain the homogeneity and workability required to complete the concrete mixture. Concrete was mixed in a horizontal rotary mixer with a capacity of 300kg

as shown in Figure (3- 9). Before using the new concrete mixture, it is important to remove any residual particles of concrete from the prier patch. To accomplish this, a moist cloth was utilized to clean the blades and pan of concrete mixer.

Sand and gravel were placed and mixed for a minute, then a part of the mixing water was added, and the mixer continued to rotate. After that, cement and GGBS were added to the mixtures containing it, and the mixing continued, after which the hallyosite mixture was added, the hallyosite was mixed with water in an electric mixer for two minutes before adding it to concrete mixture. For mortar mix the same producers has been followed but without adding gravel.

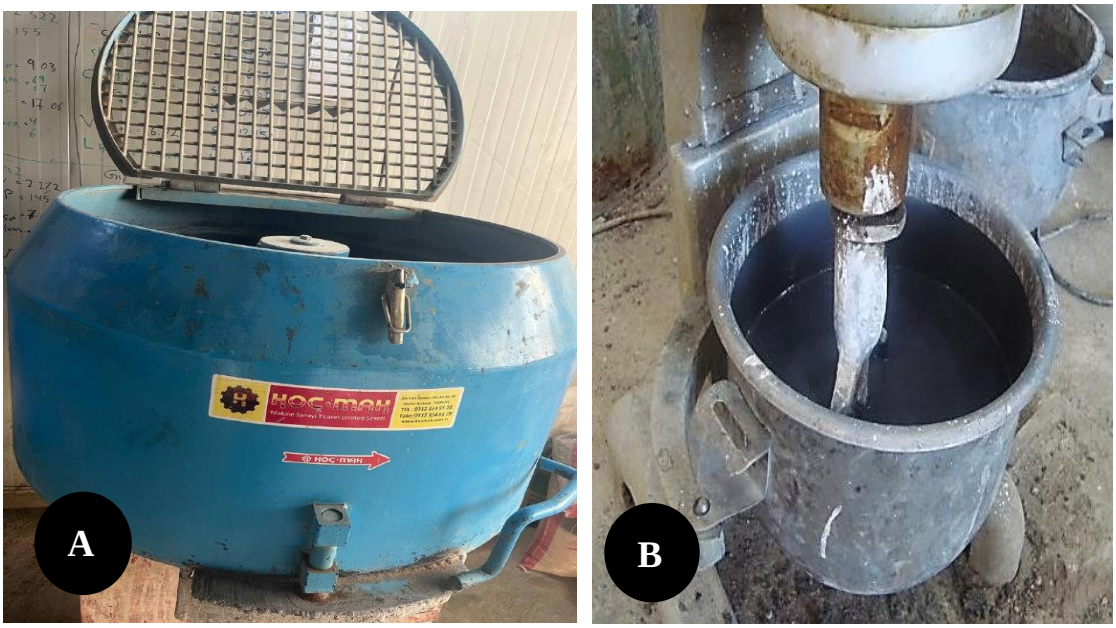

Figure 3-9: A: Mixture used to mix the concrete; B: Mixture used to mix the Mortar

3.6. Casting and Curing Procedure

Prior to casting, the necessary materials were prepared and weighed according to the required volume of the mix. Plastic and steel molds, as depicted in Figure (3-10), were used for casting all mortar and concrete specimens in this research. To minimize variation in exposure conditions, the specimens were cast within a short period of time. Before each casting, the internal face of the mold was cleaned and lubricated with oil to prevent adhesion with the hardened concrete. The molds were then placed on a horizontal surface. Once the mixing process was complete, the fresh concrete mixture was poured into the molds in three layers. Each layer was compacted by vibrating it with a rod, following the specified standards for these specimens. The compaction process ensured full compaction, as observed by checking for air bubbles on the surface. After the casting and finishing the top surface of all samples, they were covered to prevent the moisture loss. The molds were left undisturbed, as shown in Figure (3-10), and kept in a casting room at a temperature of 25±2°C for 24 hr. until demolding. The molds were demolded and the specimens were cured until the specified testing age, following the procedures outlined in Figure (3- 10).

A

B

C

Figure 3-10: A: Molds, B: casting, C:de-molding process

3.7. Mortar Tests

In this section, the tests that have been conducted in this research will be presented.

3.7.1. Flow Table Test

Flow tests is employed for determine consistency of mortars and done according to (ASTM C1437). The flow table apparatus consists of two parts, part of a vibrator and the second part of the mold which is conical in cast bronze or brass. Where the diameter of the upper part is (70.0 + 1.3 mm) and the lower diameter is (100.0 + 1.3 mm) with a height of [50.0 + 0.5 mm], mold shall have a minimum wall thickness of [5mm] as shown in Figure (3-11). The mortar sample was placed in the mold, 25 stacks are compacted, the entire mold is filled, the surface is polished, and the diameter is measured, after which the mold is lifted and the diameter is measured.

Figure 3-11: Flow Table Test

3.7.2. Compressive Strength

The compressive strength test was accomplished according to (BS EN 12390-Part 3:2019). Three cubes of (50x50x50 mm) for each mixture were cast and cured to determine the compressive strength. The compressive strength test was determined by testing three cubes at ages of (7, 28, and 90 days) using a digital testing machine with a capacity of (2000 kN), The loading rate applied during the test was set at 0.3 MPa/sec.

3.7.3. Length Change

The test was carried out according to (ASTM C157 / 157M-08), the sample placed in two approximately equal layers and each layer is stacked with rod and then after merging completed, straighten out the excess material. Immediately after pouring is finished, loosen device by fixing the measuring screws in place at each end. In order to prevent any restriction on the measurement studs before test samples are disassembled. And the mold used for this test has two prisms (2.5x2.5x28cm) for each mix, at ages (at first day after demolding ,7,14, 28 and every14 day until reach to 18 week). Figure (3-12) shows the samples of mortar.

Figure 3-12: Mortar samples

3.8. Concrete Tests

In this section of the chapter, the tests that have been conducted in this scientific research will be presented

3.8.1. Fresh Test (Slump Test)

Slump test was carried out according to (ASTM C143/C143M – 15). The mold of slump used is metallic, with a conical shape the top diameter is 100 mm, and the bottom is 200mm diameter, and the height is 300 mm. To measure the slump of freshly mixed concrete, a sample of the concrete is placed and compacted within a mold shaped like the frustum of a cone, as illustrated in Figure (3-13). The mold is then lifted vertically, and the concrete is allowed to settle. The vertical distance between the original position and the displace position of the center of the top surface of the concrete is measured and recorded as the slump of the concrete. This measurement provides an indication of the workability and consistency of the concrete mixture.

Figure 3-13: Slump test core

3.8.2. Hardened Tests

three groups will be considered in this section: mechanical properties, durability and non-destructive test).

3.8.2.1. Compressive Strength

The compressive strength test was accomplished according to (BS EN 12390-Part 3:2019). Three cubes of (100x100x100 mm) for each mixture were cast and cured to determine the compressive strength. The compressive strength test was determined by testing three cubes at ages of (7, 28, and 90 days) using a digital testing machine with a capacity of (2000 kN), The loading rate applied during the test was set at (0.3 MPa/sec). Figure (3-14) shows the compressive strength test machine.

Figure 3-14: Compressive strength testing machine

3.8.2.2. Flexural Strength

The flexural tensile strength of concrete was performed on 100x100x400 mm concrete prisms using a digital testing machine of 2000kN capacity. The flexural strength of the prisms was tested using the third point loading according to the ASTM specification (BS EN 12390-Part 5:2019) for (7,28, and 90) days as shown in Figure (3-15). The average flexural strength of three prisms for each mix and age was recorded. Modulus of rupture was calculated from the simple beam bending formula:

a. If the fracture initiates in the tension surface within the middle third of the span length, then:

$$\mathbf{R = \frac{PL}{bd^2}} \qquad (\mathbf{3-1})$$

Where:
R = modulus of rupture, (MPa)

L = span length, (mm)

P = maximum applied load, (N),

d = average depth of specimen, (mm)

b = average width of specimen, (mm)

b. If the fracture occurs in the tension surface outside the middle third of the span length by not more than 5% of the span length, then:

$$\mathbf{R = \frac{3Pa}{bd^2}} \qquad (\mathbf{3-2})$$

Where:

a = average distance between line of fracture and the nearest support measured on the tension surface of the prism, (mm).

Figure 3-15: Flexural test

3.8.2.3. Splitting Tensile Strength

The splitting tensile strength was performed according to (BS EN 12390-Part 6:2010). Three (100x200 mm) cylindrical concrete specimens performed for each mix at ages (7, 28, and 90 days) were loaded continuously up to failure. Two bearing strips of 3 mm thick of plywood, 25 mm wide and 200 mm length were placed below and above the specimen

which was placed between the bearing blocks of the testing, an electrical testing machine with a capacity of 2000kN as shown in figure (3-16).

The average splitting tensile strength of three cylinders was adopted for every mix. The splitting tensile strength was calculated by using the following formula:

$$\mathbf{T = \frac{2P}{\pi l d}} \qquad (\mathbf{3-3})$$

Where:

T: Splitting tensile strength (MPa),

P: Maximum applied load in splitting test (N),

d: Diameter of cylinder (mm),

I: Length of cylinder (mm).

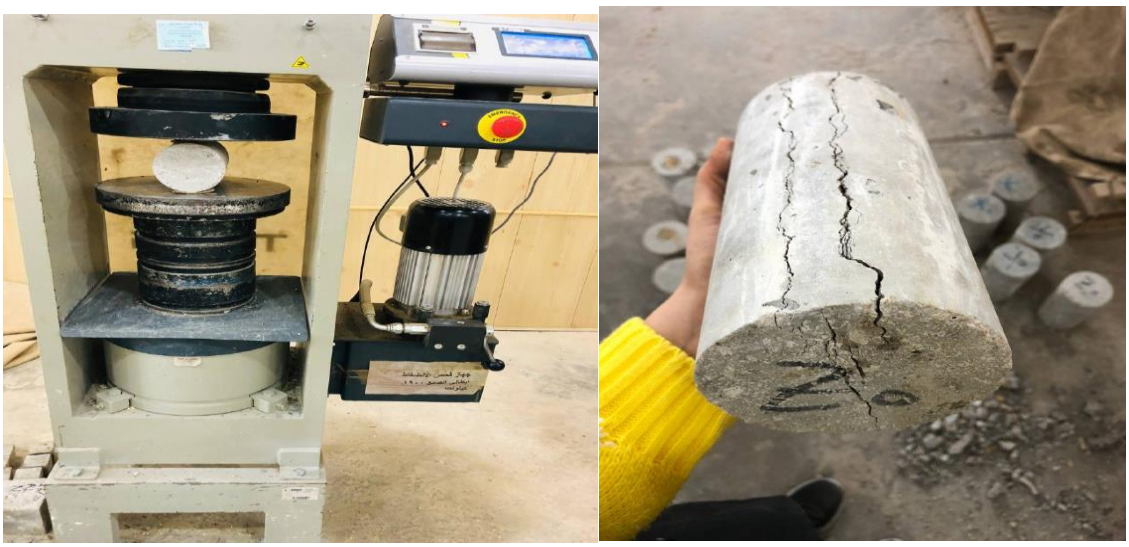

Figure 3-16:Splitting tensile strength machine

3.8.2.4. Absorption and Porosity

According to (ASTM C642-13), the water absorption test of concrete was performed. Cube samples measuring (100x100x100mm) were subjected to drying at a temperature of 100 +10 °C for 24 hours. The weight of the samples in their dry state was measured and recorded as Wd. Subsequently, the samples were immersed in water with a water level maintained at 25 ± 5 mm above the surface of the samples. At intervals of 7, 28, and 90 days, the samples were removed from the water, and their weights were measured and recorded as Ws. To determine the absorbed water content and porosity of the samples, additional measurements were taken. The weight of the sample immersed in water (Ww) was measured as shown in figure (3-17). The absorbed water content was calculated using Equation (3-4), and the porosity was calculated using Equation (3-5). These calculations were performed relative to the dry weight of the sample at each respective time point.

$$\textbf{Water absorption } (\%) = \frac{\mathbf{Ws - Wd}}{\mathbf{Wd}}\mathbf{x100} \qquad (3-4)$$

$$\textbf{porosity } (\%) = \frac{\mathbf{Ws - Wd}}{\mathbf{Ws - Ww}}\mathbf{x100} \qquad (3-5)$$

Where:

Ws: Weight of sample in case of surface saturated dry (SSD),

Wd: Dry weight of the sample,

Ww: Submerged weight of sample.

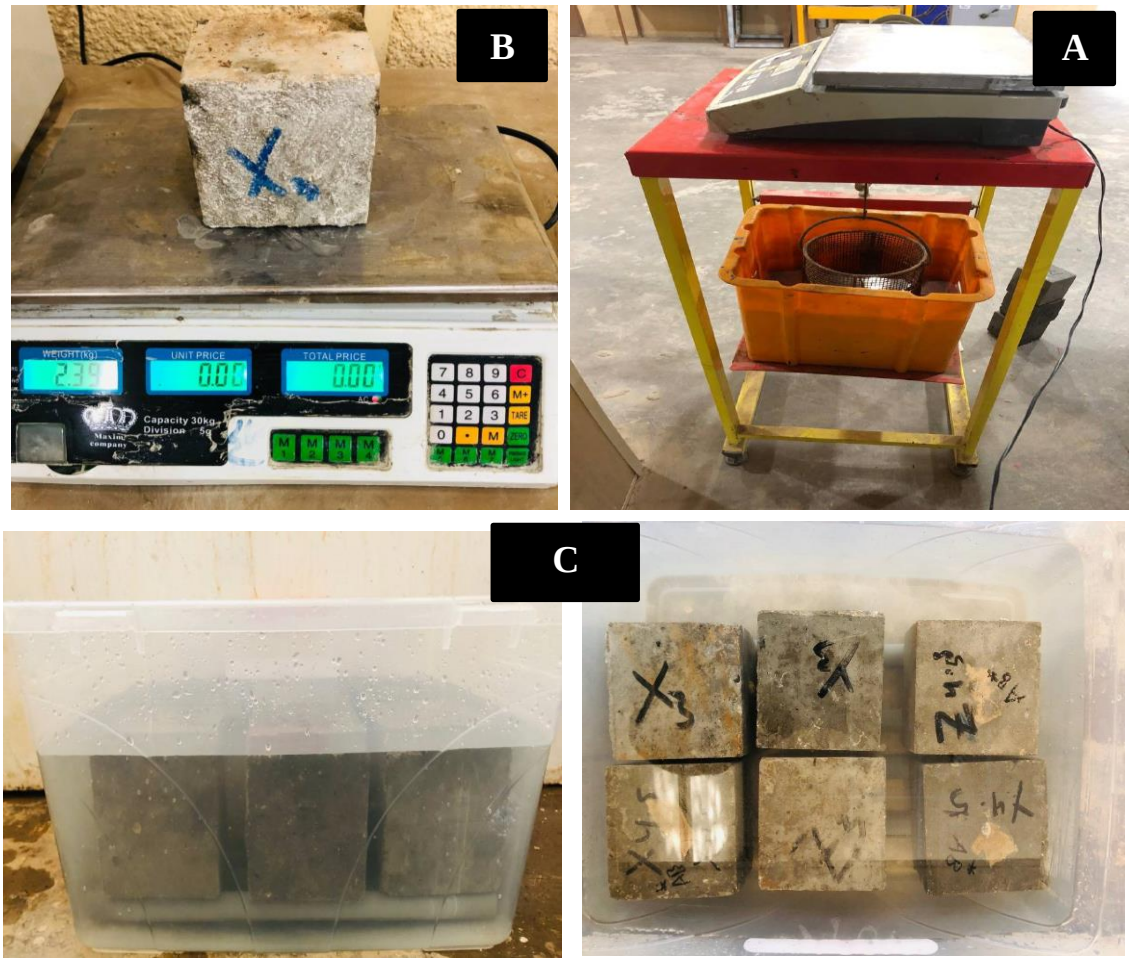

Figure 3 -17: Total Absorption of concrete A: Aqueous balance to weigh the sample in case(submerged); B: Sample weight in case (SSD)and(Dry); C: Samples completely immersed in water

3.8.2.5. Sorptivity

The surface absorption of the concrete was carried out according to the (ASTM C 1585-13). where, a concrete sample was taken with dimensions (100x100x100mm) and cured in water for 28 days. The test performed for a period of 7,28,90 days, and immersed in water at a distance of 5 mm as shown in Figure (3- 18) measurements were calculated. surface absorption was determined according to Equation (3-6)

$$\textbf{Sorptivity (I)} = \frac{\textbf{mt}}{\textbf{a} * \textbf{d}} \qquad (\textbf{3} - \textbf{6})$$

Where

m_t: the change in specimen mass in grams, at the time t،

a: exposed area of the specimen, mm^2

d: density of the water, g/mm^3

Figure 3-18: Sorptivity test for concrete

3.8.2.6. Chloride Migration Coefficient

The chloride penetration test was conducted according to specified NT-Build 492. For each concrete mix and at the ages of 28 and 90 days, three cylindrical specimens measuring 100 mm in diameter and 200 mm in thickness were prepared. These specimens were used to assess the penetration of chlorides into the concrete. Initially the specimens were split into two parts with dimensions of (100 x 50mm), where the middle part of the cylinder was taken. Then, the sample was placed in a vacuum and the air

was withdrawn for 3 hours, after which the intake valve was closed and a valve was opened to withdraw water containing hydrated lime (8 g of hydrated lime with 10 liters of water) and saturated for 18 hours. After that, the samples were placed in sleeve rubber, and the ends were sealed tightly. In the upper part, an anode electrode was placed, and a sodium hydroxide solution was added in an amount of 300 ml (0.3M). As for the lower part, it was placed on the cathode electrode, which is a bucket containing water and sodium chloride, NaCl (solution 10%). Connect the cathode to the negative pole and the anode to the positive pole of the DC power supply .

Figure (3- 19) shows the realization of the first stage of the test, in which the concretes are exposed to chlorides. After being exposed to ionic migration, the samples were diametrically broken and 0.1 M $AgNO_3$ solution was sprayed on them to check the chloride penetration depth.

Then, calculate the migration coefficient according to Equation (3-7):

$$D_{nssn} = \frac{0 \cdot 0239(273 + T)L}{(U - 2)t}\left(X_d - 0 \cdot 0238\sqrt{\frac{(273 + T)L\,X_d}{U - 2}}\right) \quad (3 - 7)$$

Where:

D_{nssn}: non-steady state diffusion coefficient ($\times 10^{-12}$ m^2/s);

T = average value of the initial and final temperatures in the anolyte solution (ºC);

L = thickness of the specimen (mm);

U = absolute value of the applied voltage (V);

X_d = average value of the penetration depths (mm);

and t = test duration (h).

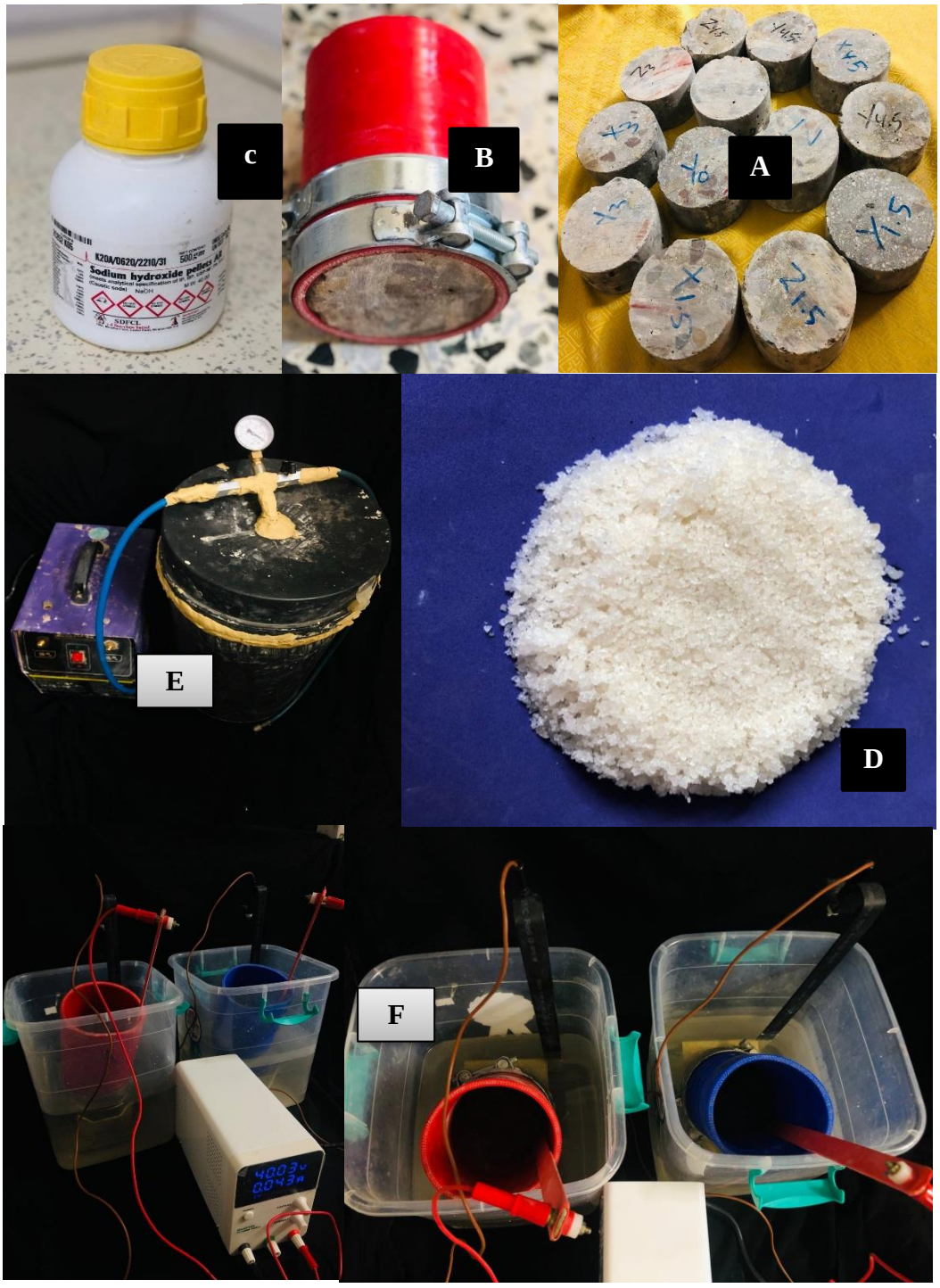

Figure 3-19: Migration equipment test used:

A: Split samples used for testing; B: sleeve rubber; C: Sodium hydroxide; D: Natural Sodium Chloride Salt; E: Vacuum; F: Migration equipment's

3.8.2.7. Accelerated Chloride Penetration

Three samples of concrete prism of (100x100x200mm) for each mixture. The sample is cast and cured for (28day), steel reinforcement of Ø10 with 15mm length implants in concrete with 2cm cover and weigh before being put in mold. After curing, the sample was put in solution of 5% sodium chloride and the side of specimen sealed with epoxy form all side except the lower side. The sample was exposed to wetting and drying cycles every 14 days in chloride solution and one week out of it for a period of 120 days **(Lu, 2015)**. At the end of exposure to chloride solution, the specimens were split in two halves. The steel bar was removed, cleaned and weighed, and concrete pierces deeply at interval of 0-1, 1-2, 2-4, 4-6cm powder taken to measure the chloride concentration (chemical test) according to BS EN 14629: 2007 to find the diffusion coefficient and surface concentration of chloride according to BS EN 12390-11:2015. The second half of the specimen was sprayed with silver nitrate with 0.1 M and measured the depth of chloride penetration (x_d). Figure (3-20) shows the specimen that used to measure chloride penetration and concentration. Depending on Equation (3-8) "error function solution" the diffusion coefficient (Da) and the concentration of chlorides on the surface (Cs) were calculated:

$$C_{(x;t)} = Ci + (Cs - Ci) \cdot \left[1 - \text{erf}\left(\frac{x}{2 * \sqrt{Da * t}}\right)\right] \qquad (3-8)$$

Where:

$C_{(x, t)}$: represents the chloride concentration at a specific position (x) within the concrete at a given time (t).

C_i: is the initial chloride concentration at the surface of the concrete.

C_s: is the chloride concentration at an infinite depth or the "source" concentration.

erf: is the error function, which is a mathematical function used to describe the cumulative distribution of a Gaussian distribution.

D_a: is the chloride diffusion coefficient, which is a material property representing the rate of chloride ion movement in the concrete.

t: is the time duration.

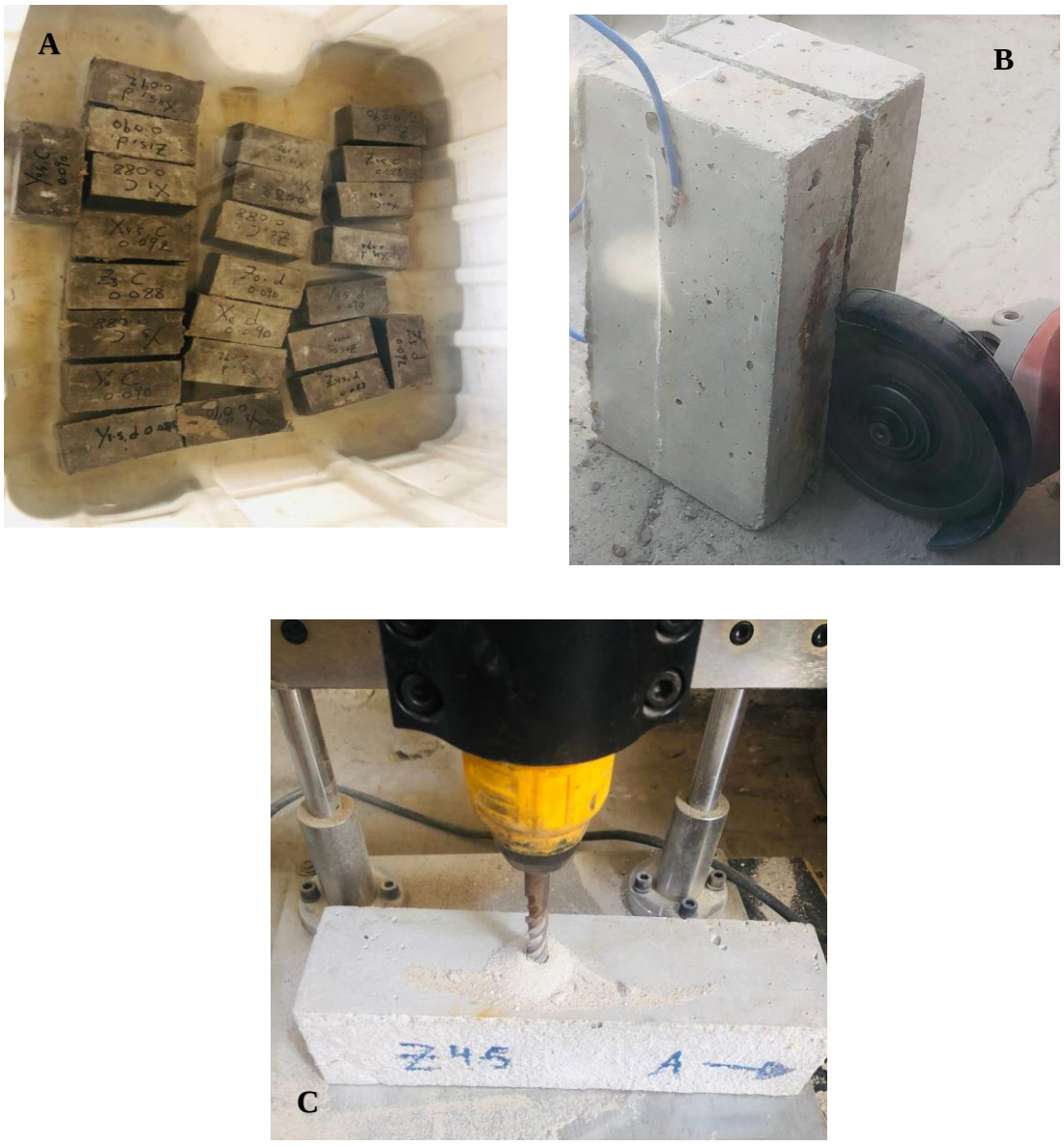

Figure 3-20: A: Sample immersed in 5% salt and coated with epoxy; B: Split the samples; C: powdered extraction

3.8.2.8. Impressed Current for Corrosion

Two specimen of concrete prism of (100x100x200mm) for each mix. At the first, the steel bar was weigh and implants in concrete with 2cm cover with length 15cm and then sample is cast and cured for (28day). After 28 days, the samples was placed in solution containing 5% sodium chloride. At the bottom of the sample, a grid of steel is placed, connected with wires and connected to the DC power supply, where it represents the cathode electrode. As for the electrical wires in the sample, a variable resistance of 1 kΩ was placed in it and connected to the power supply as an anode electrode. Then, the current was applied while maintaining the voltage constant as shown in Figure (3-21). The duration was 26 days, it was calculated according to Faraday's Law and achieve 10% of corrosion. After this period of time, the specimens were split in two halves, the steel was removed, cleaned and weighed. While, the second half of the specimen was sprayed with silver nitrate and measures the depth of chloride penetration in this case of exposure

$$t = \frac{m * z * F}{M * I} \qquad (3-9)$$

Where:

T=time (second)

M=mass loss due to corrosion (gm)

Z=valance (2)

F=Faradays constant (96480 A.sec.)

M=atomic weight of metal (55.85)

I=Imposed current (A)

Density of steel rebar=7.85gm/cm^3

Mass of the rebar=7.85x π x 0.5^2 x 15=92.48 gm

10% degree of corrosion=0.1x 92.48=9.248gm

Apply corrosion current density=0.3 mA/cm^2

I=0.3 x 2 x π x 0.5 x 15=14.137 mA

$$t = \frac{9 \cdot 248 * 2 * 96480 * 1000}{55 \cdot 85 * 14 \cdot 137} = 2260136 \cdot 537\ sec$$

$$t(day) = \frac{2260136 \cdot 537}{3600 * 24} = 26\ day$$

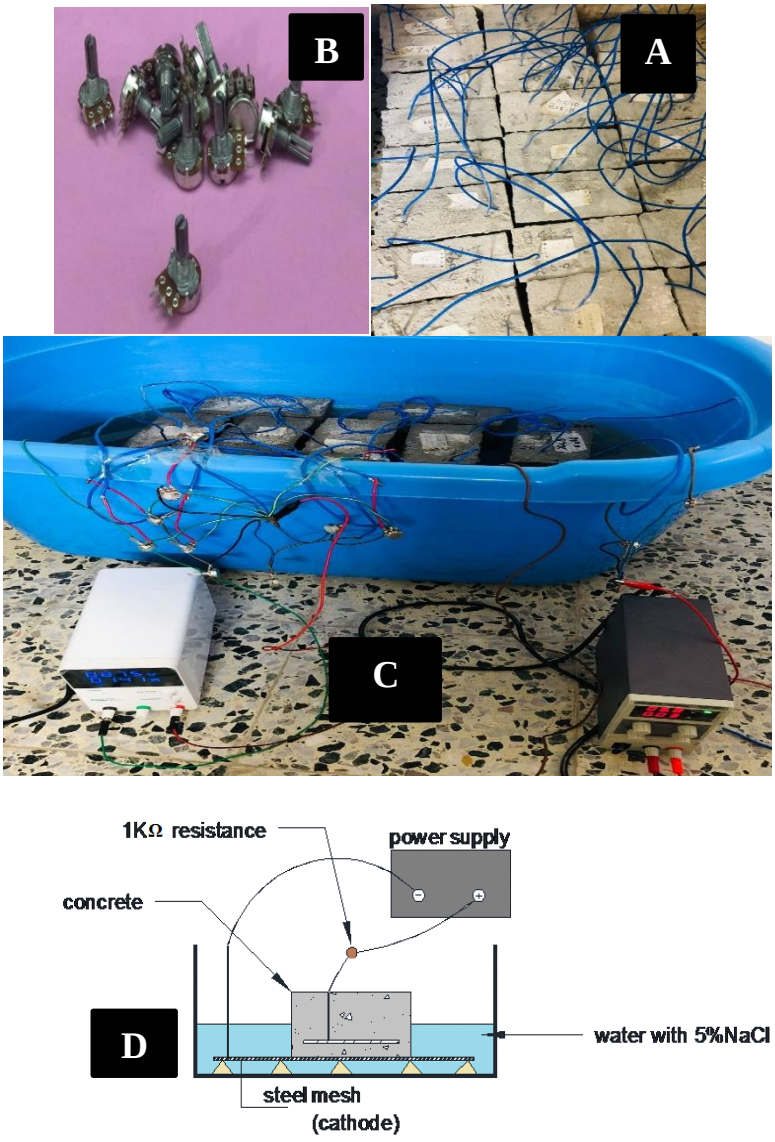

Figure 3-21:Impress current test

A: Concrete sample after 28-day curing; B: Resistance 1kΩ; C: Illustration of the connection process; D: Impressed current connection

3.8.2.9. Length Change

This test was used to determine the change in length caused by non-external causes applied forces and temperature changes in hydraulic unreinforced cement samples of mortar and concrete made in the laboratory, they are exposed to controlled conditions of [18 to 24 ° C] temperature and humidity [50+4%]. The test was carried out according to (ASTM C157 / 157M-08), the sample is taken for concrete and mortar and placed in two approximately equal layers and each layer is stacked with rod and then after merging completed, straighten out the excess material. Immediately after pouring is finished, loosen device by fixing the measuring screws in place at each end. In order to prevent any restriction on the measurement studs before test samples are disassembled. The mold used for this test has two prisms for each concrete mix with dimensions (7x 7 x 28cm) for concrete, at ages (at first day after demolding ,7,14, 28 and every14 day until reach to 18 week). Figure (3-22) shows the comparator length device and the tank treatment for specimen.

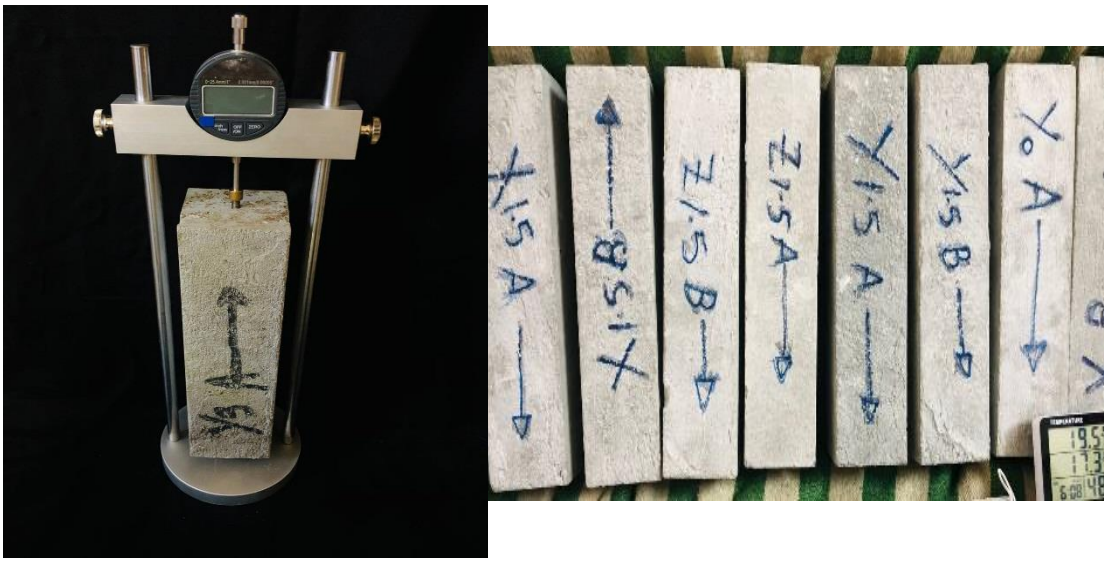

Figure 3-22: the length change frame and dial gauge with the tank treatment for specimen

3.8.2.10. Ultrasonic Pulse Velocity

In the cube samples measuring 100x100x100 mm, longitudinal stress waves were generated by an electro-acoustical transducer. These stress waves were then transmitted through the concrete specimen by maintaining contact with one surface. After traversing through the concrete, the pulses were received and converted into electrical energy by a second transducer located a distance (L) from the transmitting transducer as shown in Figure (3- 23). This test was carried out according to the specification (ASTM C597-16). The transit time (T) was measured electronically. The pulse velocity (V) is calculated by dividing L by T as shown in Equation (3-10):

$$\mathbf{V = \frac{L}{T}} \qquad (\mathbf{3-10})$$

Where:

V = pulse velocity, m/s

L = distance between centers of transducer faces, m, and

T = transit time, s.

Figure 3-23: Ultrasonic Pulse Velocity Test

3.8.2.11. Rebound Hammer Test

A cube (100x100x100mm) was used for this examination, where the tool was held firmly and the direction of the piston was perpendicular to the surface of the sample and the piston was gradually pushed towards the test surface until the hammer collided and the number was read back to the nearest integer. (3) readings were taken for one sample and an average of the readings was taken. This test done according to specification (ASTM C805/C805M-13a). Figure (3- 24) shows the hammer test device.

Figure 3-24: Rebound Hammer Test

Chapter Four

RESULTS AND DISCUSSION

Chapter Four
Results and Discussion

4.1. Introduction

The primary objective of this research is to investigate the effect of replacing different percentages (1.5%, 3%, and 4.5%) of calcined halloysite nanoclay to concrete on its ability to resist chloride penetration. This chapter presents and discusses the results obtained from the experimental programme of the study, including an assessment of the fresh properties of the concrete, such as its workability and the flow table of mortar.

Furthermore, chapter four also presents an analysis of the chloride migration test results, impressed current test results, and a chloride penetration test results. These tests could evaluate the effectiveness of halloysite nanoclay in preventing chloride ions from penetrating into the concrete. In addition, this chapter will discuss other tests, such as the strength of concrete and shrinkage, which are important properties that should be considered when designing and constructing durable concrete structures.

4.2. Fresh Properties

Fresh properties refer to the state of concrete when it is freshly mixed and still in a plastic state. Workability is one of the key properties and often evaluated to refers to the ease with which the concrete can be placed and compacted in its final location. The slump test and flow table test are commonly used for assessing workability of mixtures.

4.2.1. Workability

Workability describes as the ability of fresh concrete and mortar to easily mix, placed, and finished without loss of homogeneity.

When calcined halloysite nano clay is replace by cement of concrete mixes, it tends to reduce the slump, which is evident in all mixtures tested (NC1.5,

GG1.5, NC3, GG3, NC4.5, and GG4.5) with reduction (12.5, 15.38, 25, 23.07, 37.5, and 24.61%) respectively as shown in Figure (4-1). This reduction in workability can be attributed to the high surface area and small particle size of the CHNC, which reduces the amount of free water in the mixture. Additionally, the silica in halloysite can formation of calcium silicate hydrate (C-S-H) products, which can lead to the absorption of water and further reduction in slump **(Farzadnia et al. ,2013)**. Similarly, the addition of Ground Granulated Blast Furnace Slag (GGBS) to concrete Z mixture can also reduce the workability due to its higher surface area compared to cement, estimated at 4560 cm^2/g for GGBS and 3200 cm^2/g for cement **(see Table (4-1))**. The rough surface texture of GGBS particles can also increase water absorption, which further reduces workability. In a study by **(Allalou et al., 2019)**, it was observed that the addition of GGBS reduced the slump of concrete mixes.

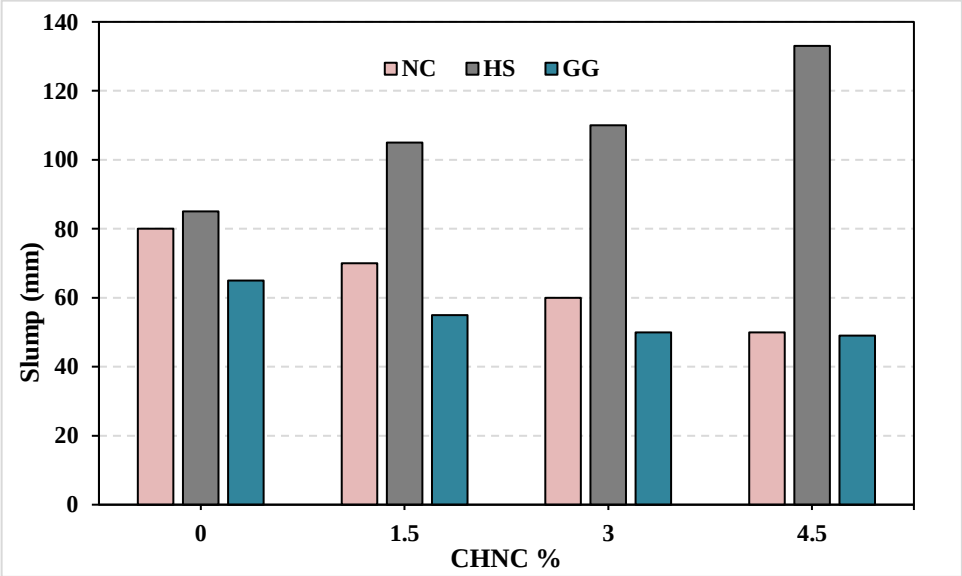

Figure 4-1: Slump test result for concrete mixtures

The workability of concrete and mortar can be influenced by various factors, including the composition of the mixture. When the concrete mixture contains a high amount of cement, there is a tendency for the workability to increase. This was observed in mixtures HS1.5, HS3, and HS4.5, which

showed a continuous increase in workability values of 23.5%, 29.41%, and 55.88%, respectively, despite the presence of different proportions of halloysite. This increase in workability can be attributed to the lower water-cement ratio in these mixtures and the higher percentage of plasticizer used that work to disperse the cement particles in the mix, allowing for more efficient water usage and reducing the amount of water needed to achieve a desired consistency, which helped to increase the slump. This effect is demonstrated in Table (4-1) and has been observed by **Vandhiyan (2018).** Similar effects have been observed for mortar mixes MC, MH, and MG, as shown in Figure (4-2).

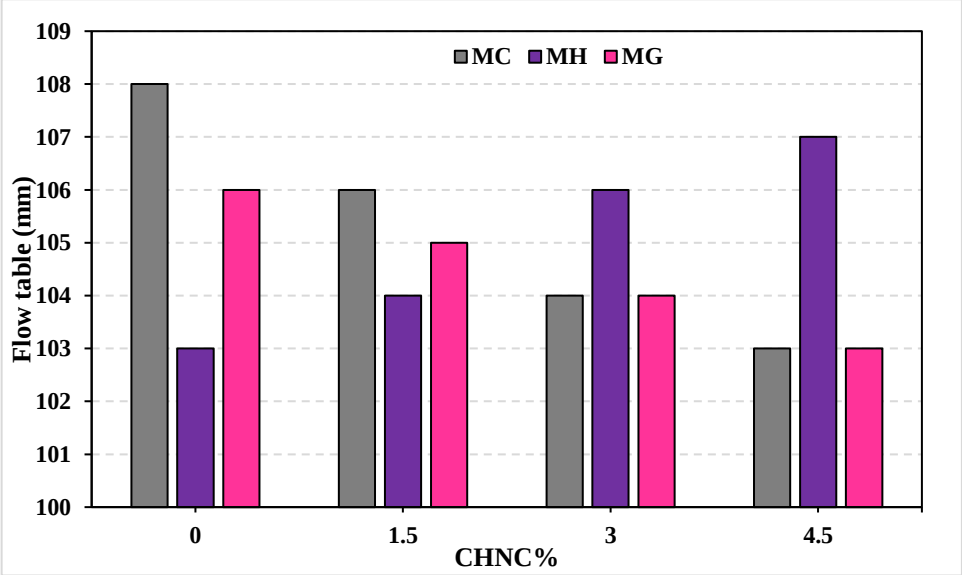

Figure 4-2: Flow table test result for mortar

Table 4-1: Slump and Flow Table Result

Slump of Concrete (mm)					Flow Table of Mortar (mm)				
Mix	CHNC%				Mix	CHNC%			
	0	1.5	3	4.5		0	1.5	3	4.5
NC	80	70	60	50	MC	108	106	104	103
HS	85	105	110	133	MH	103	104	106	107
GG	65	55	50	49	MG	106	105	104	103

4.3. Effect of Halloysite and GGBS on the Hardend Properties of Concrete

The performance of concrete is evaluated according to its mechanical properties, which include compressive, flexural and spilling tensile strength and in the following sections, the results of these properties will be presented and discussed.

4.3.1. Compressive Strength

Concrete gains strength over time as the hydration process progresses and the cementitious materials binding together. The compressive strength tests measure the maximum load concrete or mortar sample can withstand before failure, indicating its structural integrity and load-bearing capacity. It is one of the most important properties of concrete that should be studied.

The compressive strength test was conducted at the age of 7,28 and 90 days for the three mixtures of both concrete and mortar, and the results were obtained as follows.

4.3.1.1. Compressive Strength for Concrete

The test results for each of the NC, HS, GG mixtures showed an increase in compressive strength with the replacement of CHNC as shown in Figure (4-3) and Table (4-2). Where it was found that 1.5% of CHNC in all mixtures had a slight increase in compressive strength compared to the control mixture, but the 3 and 4.5% replacement of CHNC was the increase values higher. In mixture NC when cement was replaced with 3% CHNC, there was an increase in compressive strength, the increase in strength compared to the control mixture was (22.05%, 4.88%, 9.55%) for 7, 28, and 90 days, respectively. Similarly, at 4.5% substitution, the increase in strength was (27.85%, 8.47%, and 11.60%) for the same time periods. This improvement can be attributed to the excellent adsorption property of the calcined material, which facilitated water absorption, swelling, and expansion, as a result, the pores are filled, the microstructure is strengthened, and the overall strength increased (**Rooj, 2011).**

When the cement in the HS mixture was replaced by CHNC, there was a noticeable improvement in the compressive strength at different time intervals. Specifically, replacing 3% of CHNC resulted in an increase in compressive strength by (7.29%, 11.35%, and 11.30%) at 7, 28, and 90 days respectively. Similarly, at a replacement ratio of 4.5%, the compressive strength increased by (10.28%, 13.16%, and 18.14%) for the same time intervals. This indicates that the addition of CHNC positively influence the compressive strength of the HS mixture.

The behavior of the third mixture, which included GGBS (GG), exhibited a similar pattern to the other mixtures. When 3% CHNC was added, there was a percentage increase in compressive strength of (8.20%, 8.54%, and 6.36%) at 7, 28, and 90 days respectively. Similarly, at a replacement ratio of 4.5%, the increase in compressive strength was (17.14%, 12.86%, and 14.26%) for

the same time intervals. This trend can be attributed to the high pozzolanic activity of calcined halloysite nano clay present in concrete. When cement reacts with water and forms a C-S-H gel along with Ca $(OH)_2$, CHNC interacts with Ca $(OH)_2$ and facilitates the formation of additional C-S-H gel. This mechanism helps control and enhance the strength of the mixture (**Chithra, 2016)**.

Also when comparing NC Mixture with the GG mixture containing GGBS for the control mixture without adding Halloysite, note that adding GGBS at a percentage of 25% worked to increase the compressive strength by a percentage 7.90, 0.83 and 7.44% for 7, 28 and 90 days, the reason is that GGBS supports configuration of C_3S and C_2S because the hydraulic activity is high for slag **(Shi, 2004)**.

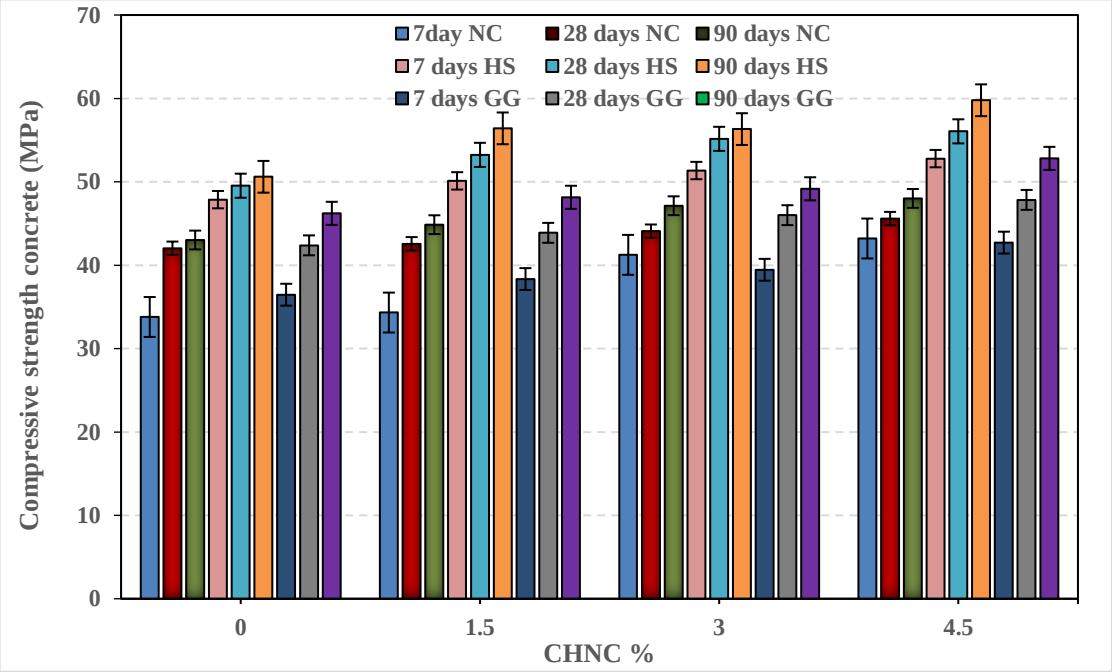

Figure 4-3: The result of compressive strength test for concrete

Table 4-2: Compressive strength result for concrete

Mix	Age (days)	CHNC %			
		0	1.5	3	4.5
		Compressive Strength (MPa)			
NC	7	33.79	34.32	41.24	43.20
	28	42.03	42.57	44.08	45.59
	90	43.02	44.86	47.13	48.01
HS	7	47.86	50.11	51.35	52.78
	28	49.53	53.23	55.15	56.05
	90	50.6	56.41	56.32	59.78
GG	7	36.46	38.34	39.45	42.71
	28	42.38	43.88	46	47.83
	90	46.22	48.14	49.16	52.81

4.3.1.2. Compressive Strength for Mortar

Compressive strength tests were performed on mortar cubes (5*5*5cm) at 7, 28, and 90 days for three different mixtures with four replacement percentages of CHNC ,0, 1.5, 3 and 4.5% as depicted in Figure (4-4) and Table (4-3). The first mixture, MC, was designed to have a target strength of 20 MPa. The second mixture, MH, aimed a strength of 30 MPa. The third mixture, MG, had the same target strength as MC but incorporated a 25% replacement of GGBS. The test results revealed that replacing CHNC positively influenced the compressive strength of the three mixtures. In the three mixtures, the substitution of 1.5% of CHNC resulted in a slight increase in compressive strength compared to the control mixture. However, when the replacement percentages were increased to 3% and 4.5%, there was a clear and significant improvement in compressive strength.

For the MC mixture, at a replacement of 3%, the compressive strength achieved an increase by 21.13%, 25.68%, and 21.14% at 7, 28, and 90 days respectively. Similarly, at a replacement of 4.5%, the increase in compressive strength was 41.48%, 31.48%, and 30.07% for the same time intervals. These improvements can be attributed to the formation of additional products, C_3ASH_6 and C_2ASH_8, which contribute to the overall strength enhancement **(Razzaghian et al., 2018)**.

The MH mixture also demonstrated an increase in compressive strength when replaced with 3% and 4.5% of CHNC. At 3% replacement, the compressive strength increased by 14.79%, 15.25%, and 21.80% at 7, 28, and 90 days respectively. With a replacement of 4.5%, the increase in compressive strength was 19.34%, 22.44%, and 26.46% for the same aging periods. The additional products of C-S-H are believed to play a role in strengthening the mixtures and contributing to the observed increase in compressive strength **(Morsy,2010)**.

In the case of the MG mixture, there was also an increase in compressive strength when CHNC was replaced at 3% and 4.5%. At a 3% replacement, the compressive strength increased by approximately 8.90%, 23.45%, and 20.67% at 7, 28, and 90 days respectively. Similarly, at a 4.5% replacement, the increase in compressive strength was 21.51%, 30.84%, and 27.16% for the same time periods. This increase in compressive strength can be attributed to the combined effect of CHNC and GGBS. The presence of CHNC contributes to the formation of C-S-H (calcium silicate hydrate), which improves the microstructure of the concrete. Additionally, GGBS further enhances the strength due to its pozzolanic properties and the formation of additional C-S-H. The combined effect of CHNC and GGBS may improve the bonding, reduce porosity, and enhance overall strength in the MG mixture. Overall, the use of CHNC in combination with GGBS has

a positive impact on compressive strength by promoting the formation of C-S-H and improving the microstructure of the concrete **(Allalou et al., 2019)**.

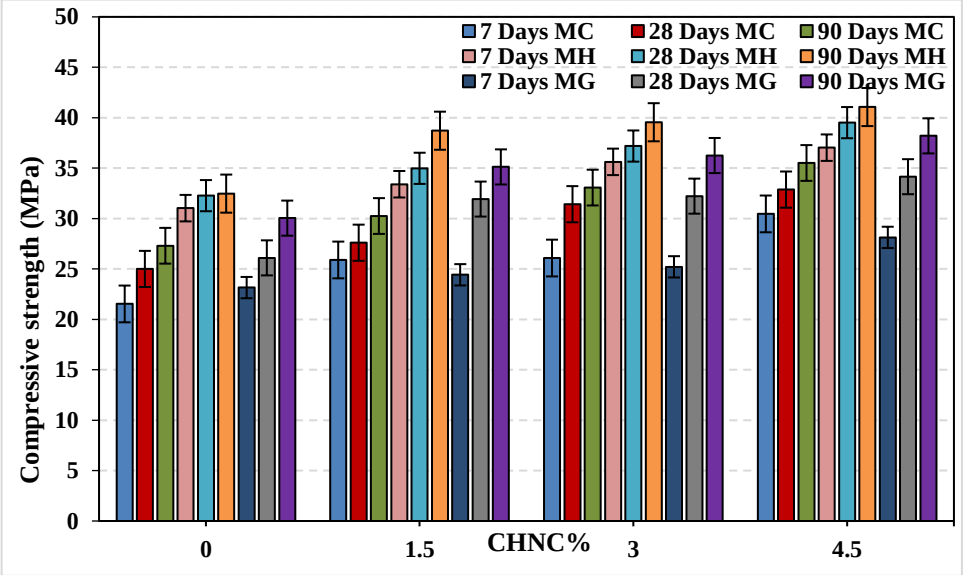

Figure 4-4: The result of compressive strength test for mortar

Table 4-3: Compressive strength for mortar

Mix	Age (days)	CHNC %			
		0	1.5	3	4.5
		Compressive strength (MPa)			
MC	7	21.53	25.89	26.08	30.46
	28	25.00	27.60	31.42	32.87
	90	27.30	30.25	33.07	35.51
MH	7	31.03	33.4	35.62	37.03
	28	32.27	34.98	37.19	39.51
	90	32.47	38.71	39.55	41.06
MG	7	23.15	24.42	25.21	28.13
	28	26.10	31.93	32.22	34.15
	90	30.04	35.12	36.25	38.20

4.3.2. Flexural strength

It shows the ability of unreinforced concrete or slab to resist bending, and is considered an indirect tensile test. The inclusion of CHNC in the concrete mixture enhanced the flexural strength properties. As a result of its known unique properties such as high aspect ratio and reinforcement properties, it improves the load-bearing capacity and resistance to bending forces in concrete. The addition of 1.5% CHNC to all the mixtures resulted in a slight increase in comparison to the control mixture as shown in Figure (4-5) and Table (4-4). However, the percentage of 3% and 4.5% replacement showed a significant improvement in flexural strength.

For the NC mixture, at a 3% replacement of CHNC, the increase in flexural strength was approximately (24.44%, 21.01%, 6.21%) at 7, 28, and 90 days respectively. Similarly, at the same ages, the increase in flexural strength for a 4.5% replacement was (53.93%, 29.64%, and 14.05%). This increase is due to increase the high aspect ratio of nano materials that allows for a more effective dispersion and distribution within the concrete matrix. When uniformly dispersed, these nano materials create a three-dimensional reinforcement network that maybe act as additional reinforcement, improving the load-bearing capacity of the concrete. The incorporation of high aspect ratio nano materials in concrete can enhance the interfacial bonding between the cementitious matrix and the aggregates. This improvement in bonding can strengthen the interface and help to increase the resistance of crack propagation, which increase the flexural strength **(Razzaghian et al., 2021)**.

In the case of the HS mixture, the increase in flexural strength with a 3% replacement of CHNC was approximately (11.49%, 8.17%, 6.38%) at 7, 28, and 90 days. With a 4.5% replacement, the increase in flexural strength was (51.88%, 9.07%, and 7.13%) at the same ages. It is observed that the increase

in flexural strength was higher in the early ages, particularly at 7 days, compared to the later ages. This can be attributed to the continued hydration and rapid formation of C_3ASH_6, which contributes to the increased strength during the early stages of concrete curing (**Singh , 2015)**. Additionally, the unstable crystalline state of the calcined halloysite further enhances the pozzolanic activity, leading to increase the flexural strength.

In the GG mixture, which incorporates both GGBS and CHNC, exhibited an increase in flexural strength. At a 3% replacement of CHNC, the flexural strength increased by approximately (15.70%, 6.60%, 3.38%) at 7, 28, and 90 days respectively. Similarly, at a 4.5% replacement, the increase in flexural strength was (31.41%, 7.72%, and 4.33%) for the same time intervals. The main reason of this increase in flexural strength can be attributed to the combined effect of GGBS and CHNC in the mixture. The GGBS, is being a pozzolanic material, may enhance the formation of calcium silicate hydrate (C-S-H) gel, which contributes to improve strength. The addition of CHNC further enhances the pozzolanic activity and promotes the formation of additional C-S-H, leading to increase the flexural strength. The combination of GGBS and CHNC results in a synergistic effect on the microstructure of the concrete, enhancing the bond between cementitious materials and aggregates **(Allalou et al., 2019)**. This improvement of microstructure contributes to the observed increase in flexural strength in the GG mixture. As well as the addition of GGBS to concrete, which increased the flexural by (21.63, 33.58, 20.75%) compared with the reference mixture NC without replacing halloysite.

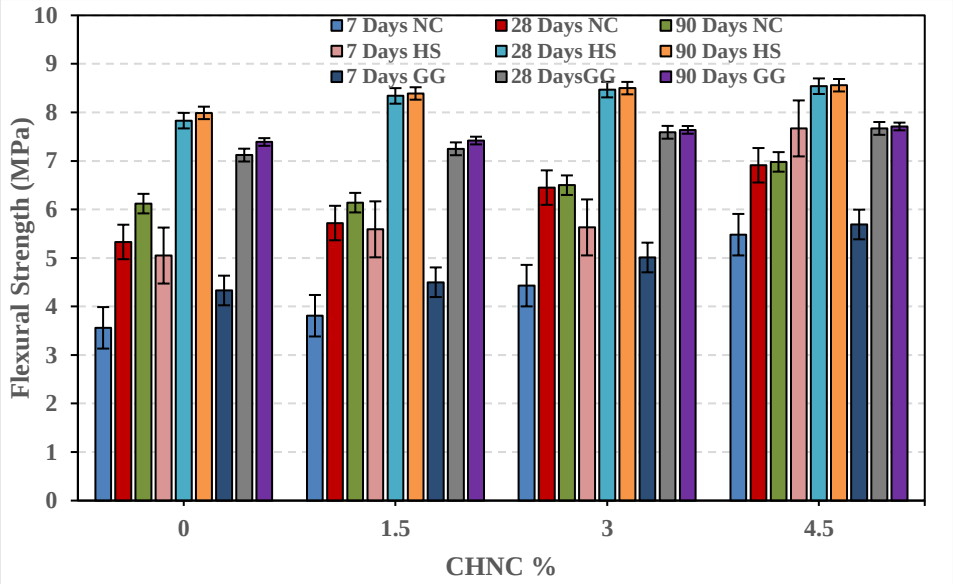

Figure 4-5*:* Flexural Strength result of concrete

Table 4-4: The result of flexural strength test

Mix	Age (days)	CHNC %			
		0	1.5	3	4.5
		Flexural strength (MPa)			
NC	7	3.56	3.81	4.43	5.48
	28	5.33	5.72	6.45	6.91
	90	6.12	6.14	6.50	6.98
HS	7	5.05	5.59	5.63	7.67
	28	7.83	8.34	8.47	8.54
	90	7.99	8.39	8.50	8.56
GG	7	4.33	4.50	5.01	5.69
	28	7.12	7.25	7.59	7.67
	90	7.39	7.42	7.64	7.71

4.3.3. Splitting Tensile Strength

It is an indirect method for measuring the tensile strength of concrete. Calcined halloysite, when it is incorporated into concrete, contributes to enhance its tensile strength. The results of this test are presented in Figure (4-6) and Table (4-5).

The test results of splitting strength indicate that the inclusion of calcined halloysite in different mixtures resulted in a slight increase in tensile strength when replaced at 1.5%. For the NC mixture, a 3% replacement of CHNC led to an increase of approximately (3.38%, 4.78%, 7.48%) in tensile strength at 7, 28, and 90 days respectively. Similarly, at a 4.5% replacement, the increase was (7.32%, 7.58%, and 8.03%) for the same age intervals.

In the case of the HS mixture, the increase in tensile strength with a 3% replacement of CHNC was approximately (14.12%, 22.62%, 24.15%) at 7, 28, and 90 days. With a 4.5% replacement, the increase was (19.02%, 28.34%, and 25.72%) for the same age intervals. Calcined halloysite exhibits unique characteristics as a nanomaterial. It possesses both pozzolanic properties, interacting with $Ca(OH)_2$, and a distinctive tubular fiber-like shape that acts as a bridge within the concrete matrix. The tubular shape of calcined halloysite enables it to connect cracks and prevent the propagation of micro-cracks. This bridging effect contributes to the improvement of tensile strength. Furthermore, calcined halloysite, is being a calcined material with high pozzolanic activity, may enhance the microstructure of the concrete. This improvement in microstructure results in increase the tensile strength. Overall, the combination of the tubular shape, bridging effect, and pozzolanic activity of calcined halloysite leads to the observed increase in tensile strength in the concrete mixtures **(Al-Salami et al, 2013)**. In the case of the GG mixture that contains GGBS, the inclusion of 3% CHNC resulted in an increase in tensile strength of approximately (10.03%,

7.10%, 5.95%) at 7, 28, and 90 days. Similarly, a 4.5% replacement of CHNC led to an increase of (14.75%, 7.92%, and 10.24%) for the same age intervals. The increase in tensile strength can be attributed to the combined effect of CHNC and GGBS in promote the formation of calcium silicate hydrate (C-S-H) gel within the concrete matrix. The increase in formation of C-S-H gel improves the bonding between the cementitious matrix and aggregates, making the concrete more resistant to cracking and improving its overall tensile strength.

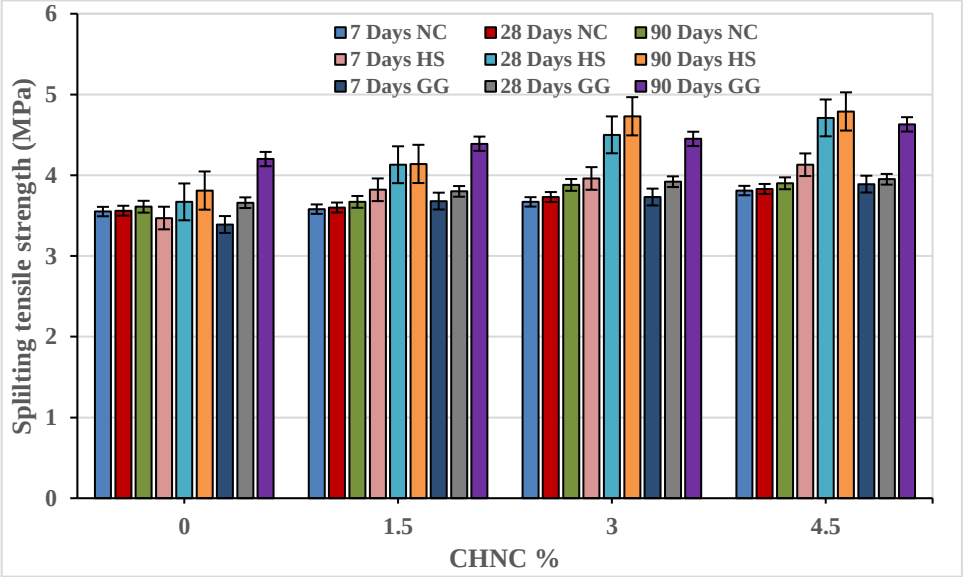

Figure 4-6: Splitting tensile strength for concrete

Table 4-5: Splitting tensile strength result for concrete

Mix	Age (days)	CHNC %			
		0	1.5	3	4.5
		Splitting tensile strength (MPa)			
NC	7	3.55	3.58	3.67	3.81
	28	3.56	3.60	3.73	3.83
	90	3.61	3.67	3.88	3.90
HS	7	3.47	3.82	3.96	4.13
	28	3.67	4.13	4.50	4.71
	90	3.81	4.14	4.73	4.79
GG	7	3.39	3.68	3.73	3.89
	28	3.66	3.80	3.92	3.95
	90	4.20	4.39	4.45	3.63

4.3.4. The Water absorption

The results of total water absorption of concrete for each of the admixtures NC, HS and GG for different percentage of CHNC at 7,28 and 90 days are presented in Table (4-6) and Figure (4-7).

The results showed that the replacement of calcined halloysite with cement reduced the water absorption, as there was a decrease in the results of the mixture NC samples for the three percentage. The ratio 1.5% had a slight decrease in water absorption by (0.54, 1.67 and 2.81%), however there was a clear decrease in water absorption of concrete samples having 3 and 4.5 % of the CHNC compared with the control mixture by (25.20, 24.44 and 25 %) for samples with CHNC 3 % and (28.46, 28.89 and 31.74) for samples with CHNC 4.5% at 7,28,90 days respectively. This reduction in water

absorption is an indication of the improvement of the porous structure of concrete containing CHNC with high proportions **(Razzaghian et al., 2021).**

As for the GG mixture, there was a decrease in the reference mixture containing GGBS with the NC reference mixture by about (14.63, 13.61and 15.17%), and this is due to the pozzolanic activity of GGBS, which works to improve the binding properties of the matrix and reduce the water absorption, also pore refinement and the formation of discontinuous pores in concrete **(Li, 2003)**. Also, CHNC has a considerable role when adding it with the GGBS, as both the ratio of 3 and 4.5 % worked to reduce the amount of water absorption percentage (18.41, 17.36 and 16.32%) for 3% CHNC and (32.70, 31.38 and 35.43%) for 4.5% of CHNC at 7, 28 and 90 days this due to the nanoscale size of halloysite, they can penetrate into small spaces between cement particles and fill voids, leading to the more dense structure with lesser pores. The combined effect of halloysite nano particles and GGBS can significantly enhance the properties of concrete structures and reduce their water absorption. Halloysite nano particles can fill voids and improve the packing density of the concrete, while GGBS can increase the amount of C-S-H gel and reduce the porosity of the cementitious material. This can lead to a denser and more durable concrete structure with lower water absorption.

As for the HS mixture, it was noticed that it has less absorbency because it has a high-strength concrete with less w/c compared with other mixtures. And the addition of CHNC has an additional and clear improvement in reduce the water absorption of concrete for both the ratio of 3 and 4.5% due to the decrease in interconnected voids and provide a dense matrix and the reduction was 39.88, 36.86 and 36.04 for 3% CHNC and 42.99, 33.01 and 29.55% for 4.5% at 7, 28, 90 days respectively.

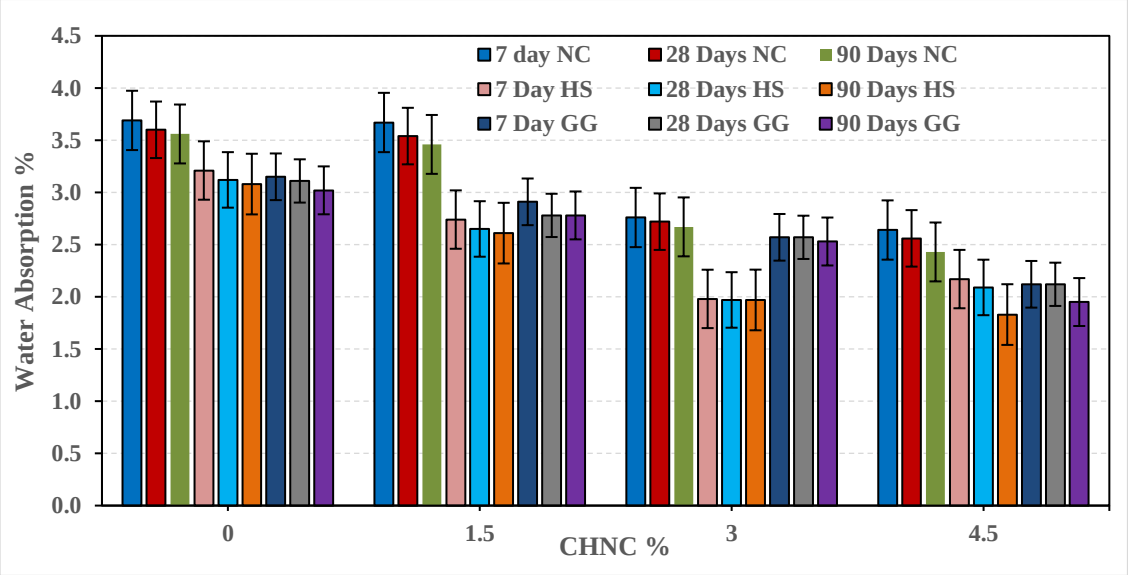

Figure 4-7: The water absorption test result

Table 4-6: Total water absorption test

Mix	Age (days)	CHNC %			
		0	1.5	3	4.5
		Water Absorption (%)			
NC	7	3.69	3.67	2.76	2.64
	28	3.60	3.54	2.72	2.56
	90	3.56	3.46	2.67	2.43
HS	7	3.21	2.74	1.98	2.17
	28	3.12	2.65	1.97	2.09
	90	3.08	2.61	1.97	1.83
GG	7	3.15	2.91	2.57	2.12
	28	3.11	2.78	2.57	2.12
	90	3.02	2.78	2.53	1.95

4.3.5. Porosity

Porosity of concrete containing CHNC in different percentage was performant at 7, 28 and 90 days, the result are illustrated in Table (4-7) and Figure (4-8).

The results showed that the NC mixture has a significant reduction in the porosity of concrete samples having 3 and 4.5 % of the CHNC compared with the control mixture by (24.70, 23.72 and24.14%) for samples with CHNC 3 % and (27.32, 27.98 and31.50%) for samples with CHNC 4.5% at 7,28 and 90 days respectively. The best percentage was 4.5%, and as mentioned previously, the reason is due to the improvement of the concrete microstructure and the high fill ability of the concrete **(Razzaghian et al., 2021)**.

As for the GG mixture, there was a decrease in the control mixture containing GGBS with the NC control mixture, and this is due to the pozzolanic activity of GGBS, the reduction was (14.85, 13.75 and 15.81%). It can be seen that the GGBS shows its effect more at later ages. Also, CHNC has a considerable role when adding it with the GGBS, as both the ratio of 3 %(17.57, 16.78 and 14.99%) and 4.5 %(30.82, 30.18 and33.92%) performed to reduce the amount of porosity at 7,28 and 90 days.

As for the HS mixture, it was noticed that it has less porosity and the addition of CHNC has an additional and clear improvement in reducing the porosity of concrete for both the ratio of 3 and 4.5% due to the decrease in interconnected voids and provide a dense matrix and the reduction was (37.31, 36.30 and36.35%) for 3% CHNC and (31.07, 32.27 and39.46%) for 4.5% at 7, 28, 90 days respectively.

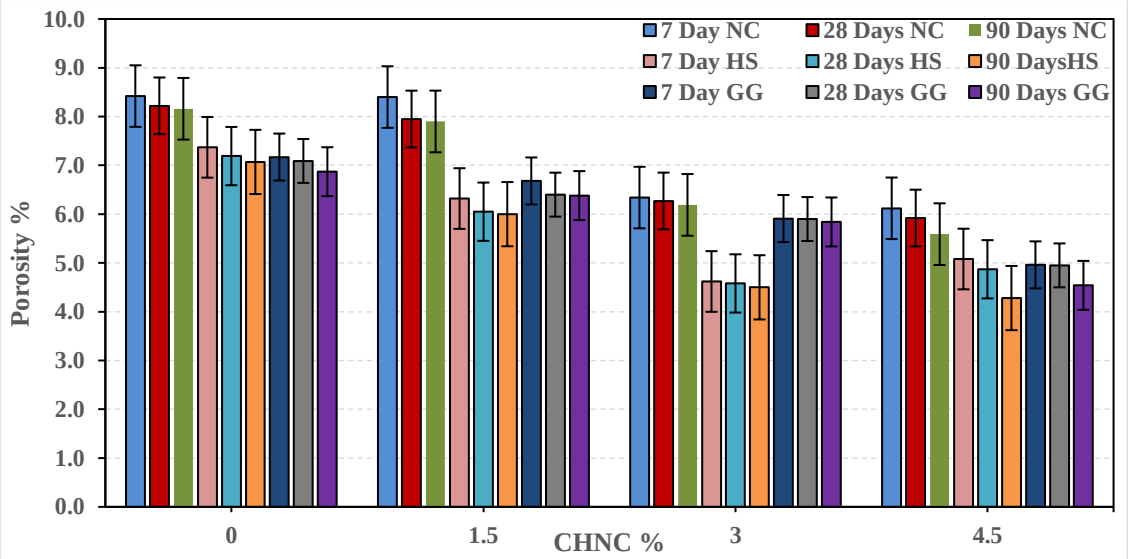

Figure 4-8: The porosity of concrete result

Table 4-7: Porosity test result

Mix	Age (days)	CHNC %			
		0	1.5	3	4.5
		Porosity (%)			
NC	7	8.42	8.40	6.34	6.12
	28	8.22	7.95	6.27	5.92
	90	8.16	7.90	6.19	5.59
HS	7	7.37	6.32	4.62	5.08
	28	7.19	6.05	4.58	4.87
	90	7.07	6.00	4.50	4.28
GG	7	7.17	6.68	5.91	4.96
	28	6.09	6.40	5.90	4.95
	90	6.87	6.38	5.84	4.54

4.3.6. Sorptivity

The results of sorptivity of concrete replaced by CHNC in different percentage are shown in Table (4-8) and Figure (4-9).

According to these results shown, there is a significant decrease in the surface absorption of concrete in the percentage of 3 and 4.5% for NC mixture about (20, 21.21 and 21.88%) for 3% replacement, and (28.57, 30.30 and 37.50%) for 4.5% at 7, 28 and 90 days. This reduction is due to the decrease in the number and size of the pores in the concrete as a result of the fact that CHNC is fineness material that penetrates between the pores to fill them owing to formation of a new gel. The large reduction was with 4.5% replacement as the more replacement in normal concrete, the more pores are filled and the sorptivity value decreases **(Farzadnia et al. ,2013)**.

As for the HS mixture, there was also a clear decrease in the sorptivity and the best percentage was with 3% replacement of CHNC by (57.14, 42.86 and 42.86%) at 7, 28 and 90 days. The decrease in sorptivity can be attributed to the interaction between CHNC and the concrete matrix, which leads to reduce the pore connectivity and a denser matrix.

As for the GG mixture has same result of NC mixture, 3 and 4.5% of CHNC was a decrease in the sorptivity values about (21.88, 13.33 and 16.67%) for 3% of CHNC and (37.50, 16.67 and 16.67%) at 7, 28 and 90 days for 4.5% the highest reduction was in 4.5%, and the reason of this is the CHNC interacts with the calcium oxide (CaO) present in the GGBS to form an additional product of C-S-H gel that fills the pores and reduces sorptivity **(Allalou et al., 2019)**.

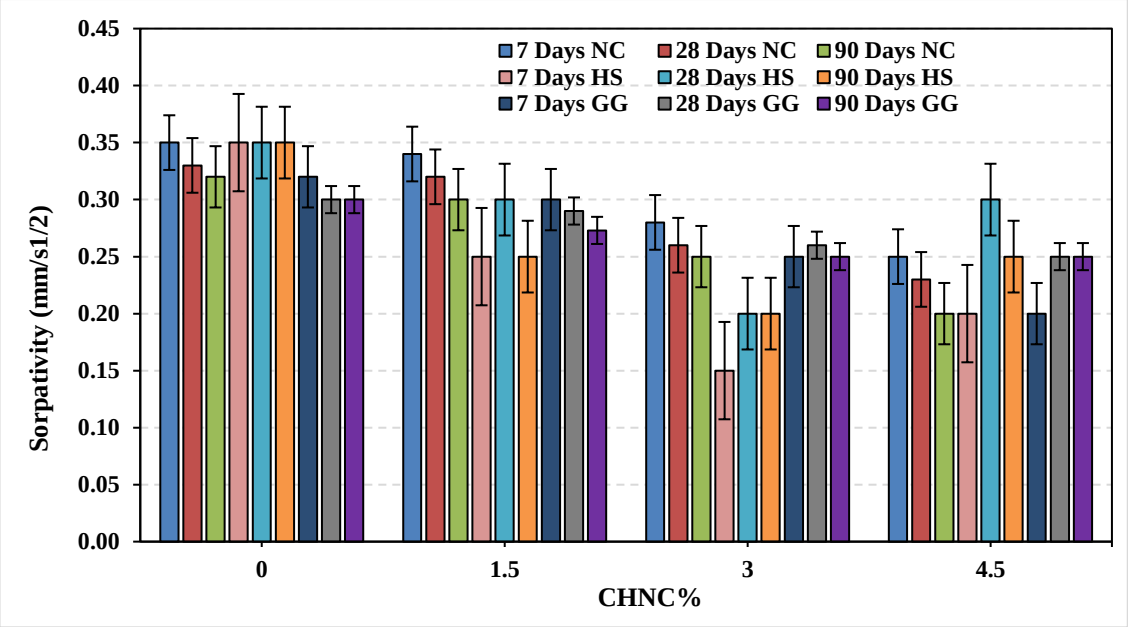

Figure 4-9: The effect of CHNC % on sorptivity test in concrete mixtures

Table 4-8: The results of sorptivity test

Mix	Age (days)	CHNC %			
		0	1.5	3	4.5
		Sorptivity ($mm/s^{1/2}$)			
NC	7	0.35	0.34	0.28	0.25
	28	0.33	0.32	0.26	0.23
	90	0.32	0.30	0.25	0.20
HS	7	0.35	0.25	0.15	0.20
	28	0.35	0.30	0.20	0.30
	90	0.35	0.25	0.20	0.25
GG	7	0.32	0.30	0.25	0.20
	28	0.30	0.29	0.26	0.25
	90	0.30	0.273	0.25	0.25

4.3.7. Chloride Migration Coefficient (D_{nssm})

In Figure (4-10) and Table (4-9), the results of chloride migration coefficient test at the age of 28 and 90 days are illustrated. It is noted that the values of the migration of chloride depth at the age of 90 days were lesser than values at 28 days for all mixtures. Secondly, the different percentage of CHNC replacement decrease the penetration of chloride in concrete samples as shown in Figure (4-11). As there was a clear decrease in D_{nssm} in the mixture HS which it is classified as a high strength concrete, and the decrease was 15% lesser than the control mixture at 28 days, the reason of this reduction is to the nanomaterials have small size and they have a high filling ability, as they can fill the pores due to generation of new gel of this material **(Ganesh, 2016)**.

Also, in the mixture GG containing GGBS, the reduction in D_{nssm} was 9.31% compared with the control mixture at 28 days. The reason of reduction in D_{nssm} is due to grain size of the GGBS granules, they are smaller than the cement particle, therefore according to the micro-filling characteristic of GGBS, they would fill the voids in microstructure of cementitious past and bind with the aggregate, which makes the concrete more compact and thus lesser penetration of aggressive materials into the concrete **(Ahmad et al, 2021).** This effect is clear through the results of the absorption test of concrete, where, as previously shown, a clear decrease of the mixture containing GGBS in 90 days compared with the control mixture by 15.17%.

CHNC has a significant effect in reduceing the migration coefficient as the replacement percentage increased. Where the results showed that the lowest diffusion coefficient was at the replacement of CHNC 4.5%. Where the amount of decrease in the mixture was NC at the age of 90 days, about (21.21%), compared to 28 days, and also 45.30% and 54.18% for each of

HS and GG mixture respectively. This indicates that concrete containing halloysite is more resistance to chloride penetration.

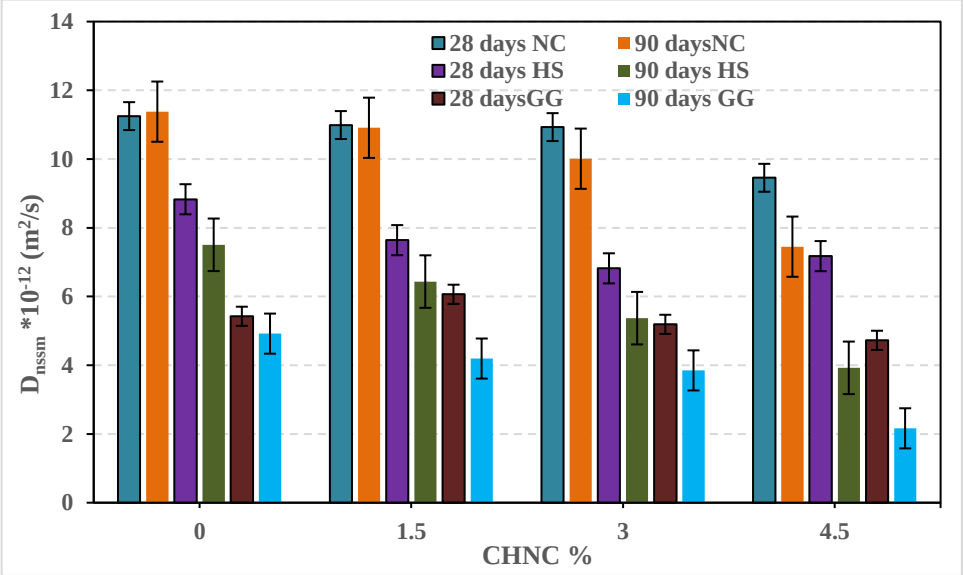

Figure 4-10: Chloride migration depth with CHNC percentage at 28 and 90 days

Table 4-9: Chloride migration coefficient test result

Mix	Age(days)	D_{nssm}*10^{-12} (m^2/s)			
		CHNC %			
		0	1.5	3	4.5
X	28	11.25	10.99	10.93	9.46
	90	11.38	10.91	10.01	7.45
Y	28	8.83	7.64	6.82	7.18
	90	7.51	6.44	5.37	3.93
Z	28	5.43	6.07	5.19	4.73
	90	4.92	4.20	3.85	2.17

The penetration of chloride ions mainly affects the water absorption and the microstructure of the concrete, and CHNC has a clear effect on reduction of the water absorption due to increase the amount of CHNC replacement. The reason is due to the decrease in the capillary pores of the concrete as a result of the continuation of the hydration process, because the CHNC reacts with calcium hydroxide to form additional gel products that fill the pores, thus the concrete is less water absorption.

Figure 4-11: Chloride migration depth at A: 28 and B: 90 days

4.3.8. Chlorides Attack

4.3.8.1. Chloride Penetration

The result of chloride penetration shown in Figure (4-12) and Table (4-10). After exposing the samples to a cycle of wetting and drying in a saline solution for 120 days, the sample was spilt into two parts and the first part of it was sprayed with silver nitrate ($AgNO_3$) with 0.1 M to determine the depth of penetration of the chloride ions **(He & Shi, 2011)** as shown in

Figure (4-12). The results showed that the amount of penetration (X_d) decreased at 1.5 and 3% for all the three mixtures by (15.72, 4.59, 9.15 mm) for 1.5% of CHNC and (9.88, 3.12, 6.14 mm) for 3% compared with control mixture (16.81, 8.08, 11.97 mm) for NC, HS, GG mixture. While the amount of penetration returned to the rise when the replacement increased to 4.5% by (12.79, 9.86, 8.27 mm).

Figure 4-12: Chloride penetration depth after 120 days

Table 4-10: Chloride penetration depth after 120 days

Mixture	CHNC %	Avg. X_d (mm)
NC	0	16.813
	1.5	15.723
	3	9.877
	4.5	12.789
HS	0	8.079
	1.5	4.587
	3	3.115
	4.5	9.862
GG	0	11.971
	1.5	9.151
	3	6.137
	4.5	8.269

4.3.8.2. Chlorides Concentration in Concrete Contain CHNC

The concentration of chlorides is determined using the nitration method, where silver nitrate reacts with sodium chloride, leading to the formation of a silver chloride precipitate the solution is titrated using Ammonium thiocyanate solution. Throughout the titration process, the solution retains its pale yellow color, indicating the presence of excess (unreacted) silver ions. These silver ions react with the thiocyanate ions to form a precipitate of silver thiocyanate as shown in equation below.

$$Ag^{+} + Cl^{-} \rightarrow AgCl$$

$$Ag^{+} + SCN^{-} \rightarrow AgSCN$$

$$Fe^{3+} + SCN^{-} \rightarrow [FeSCN]^{2+}$$

Powder samples were collected from different depths within the concrete specimens, specifically at depths interval of 0-1, 1-2, 2-4, 4-6 cm. These powder samples underwent a chemical examination based on the specifications outlined in **BS EN 14629(2007)**. The obtained results are

presented in Table (4-11). The results showed that the surface layer of the concrete and the initial depths exhibited a noticeable concentration of chloride ions .This can be attributed to the capillary suction characteristic of concrete when exposed to a cycled drying and wetting. During the wetting phase, water carrying dissolved chlorides infiltrates the concrete, depositing chloride ions. As the concrete dries, capillary suction draws the moisture towards the surface, resulting in the migration of chloride ions towards the concrete's outer layers **(Lu, 2015).** As the depth increases, the chloride concentration is reduced due to the capillary suction effect gradually reduces because the migration of chloride ions towards the surface diminishes. The addition of nanomaterials would reduce the concentration of chlorides entering the concrete compared to the control mixture.

Where the chloride concentration of depth (0-1, 1-2, 2-4, 4-6 cm) in the NC mixture decreased by (11.14, 10.14, 28.63,0.00%) for 1.5% of CHNC and (27.75, 60, 42.74, 0.00%) for 3% and (22.27, 40, 28.629, 0.000%)as shown in Figure (4-13) this attributed to the improvement in microstructure and dense the concrete because the halloysite work as a pozzolanic material, it can form additional products of the C-S-H that fill the capillary pores and voids, which reduces the chance of chlorides penetration into the concrete.

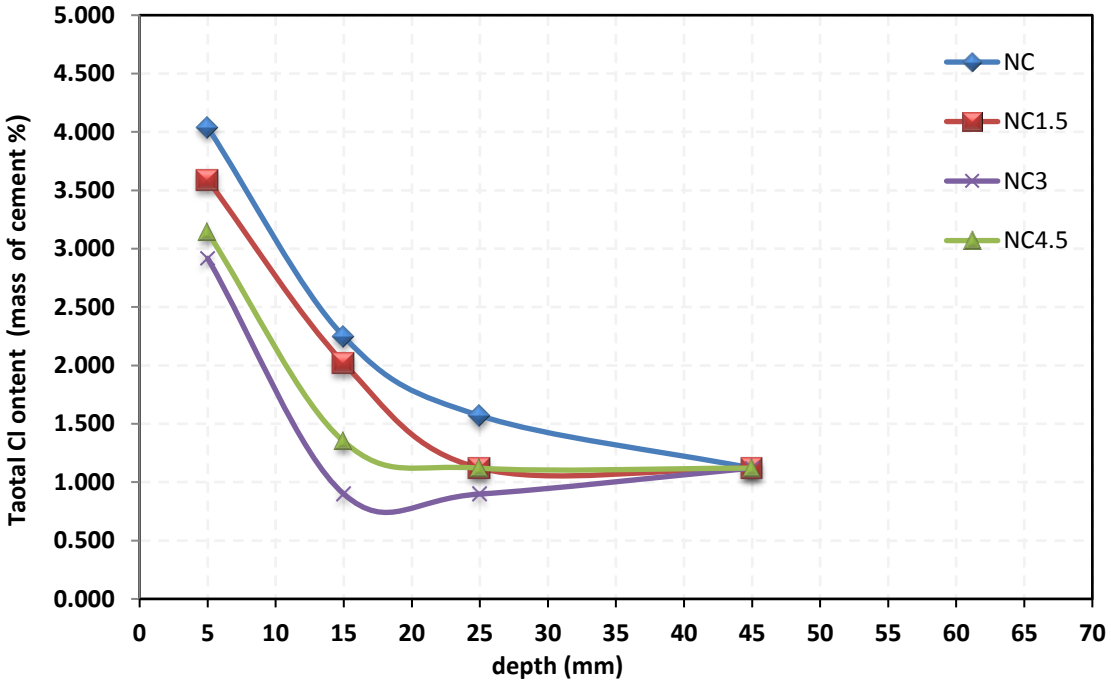

Figure 4-13: Chloride concentration (by mass of cement) with depth for NC mixture

As for HS mixture there was also decrease in Cl^- when replacing (1.5, 3 and 4.5%) of CHNC by cement as shown in Figure (4-14), for 1.5% the reduction about (45.83, 42.74, 42.74 and 0.00%) for 0-1, 1-2 ,2-4 and 4-6cm, also for 3% (58.28,50, 42.74 and19.77%) for same depth and (54.17, 64.31, 57.26 and19.77%)for 4.5% compared to control mixture at same depth.

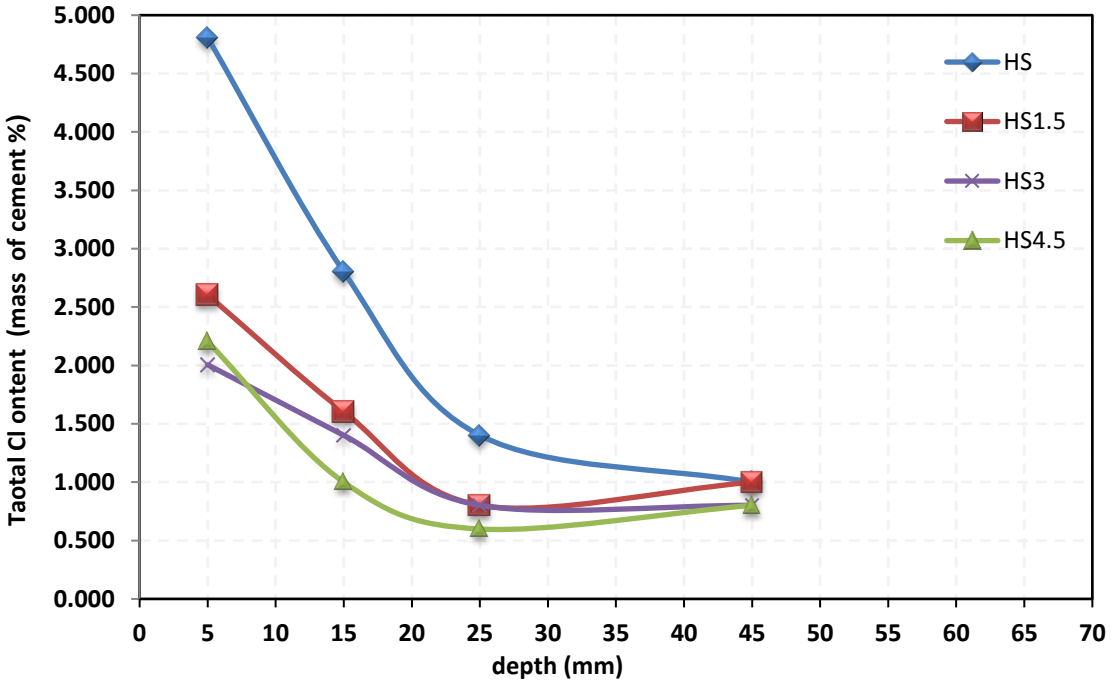

Figure 4-14: Chloride concentration (by mass of cement) with depth for HS mixture

As for the mixture GG there was also a decrease in the concentration of chlorides upon replacement with halloysite compared to the control mixture. The concentration decreased at 1.5% (6.77%) in 0-1 cm depth only, and (13.35, 50.23, 57,26, 0.00%) for 3% at 0-1, 1-2, 2-4 and 4-6cm depth as shown in Figure (4-15). The reason is due to the fact that both GGBS and halloysite worked to reduce the sorptivity and absorption of concrete as a result of their effectiveness in improve the microstructure of concrete.

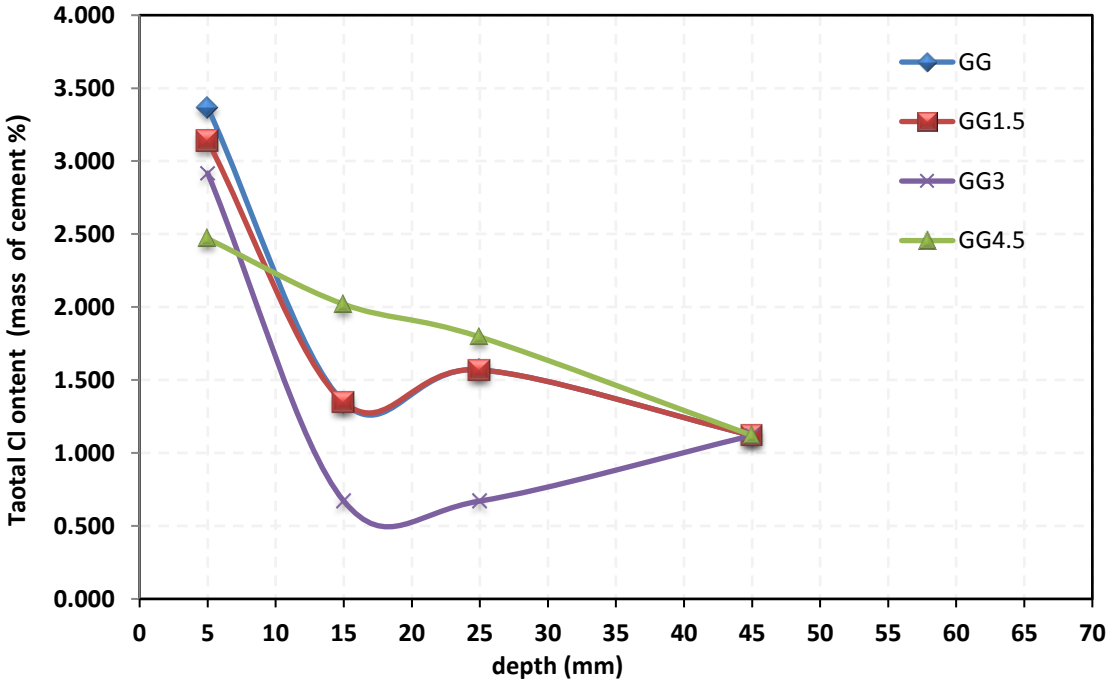

Figure 4-15: Chloride concentration (by mass of cement) with depth for GG mixture

Table 4-11: Chloride concentration of concrete with depth

Mix	CHNC	Cl^- Concentration % (by mass of cement)				
		Depth(mm)				
		0-10	10-20	20-40	40-60	Ref
NC	0	4.039	2.247	1.570	1.120	0.671
	1.5	3.589	2.019	1.120	1.120	0.671
	3	2.918	0.899	0.899	1.120	0.671
	4.5	3.139	1.348	1.120	1.120	0.899
HS	0	4.808	2.802	1.401	1.000	0.599
	1.5	2.605	1.605	0.802	1.000	0.599
	3	2.006	1.401	0.802	0.802	0.599
	4.5	2.203	1.000	0.599	0.802	0.599
GG	0	3.367	1.348	1.570	1.120	1.120
	1.5	3.139	1.348	1.570	1.120	1.120
	3	2.918	0.671	0.671	1.120	0.671
	4.5	2.468	2.019	1.795	1.120	0.671

4.3.8.3. Chloride Diffusion Coefficient and Surface Chloride

The process of calculating and evaluating the penetration and distribution of chloride ions inside the concrete is an important factor, as it is represented by apparent diffusion coefficient, D_a that refers to the rate of penetration of chlorides into the concrete and the ease of their movement within the pores with time, and C_s it represents the accumulated concentration of chlorides on the surface of the concrete at duration of exposure to chloride attack. An equation of Fick's second law was adopted to estimate each of the D_a, C_s and the results are listed in a Table (4-12) (calculation of D_a and C_s are shown in **Appendix -A**). The results indicated that the halloysite reduced the diffusion of chlorides and decreases the concentration of chloride at the surface, the incorporation of halloysite in concrete has a positive effect on chloride ingress control. The tubular structure and unique properties of halloysite, such as its ability to fill pores and reduce permeability, likely contribute to this effect **(Kiran et al, 2021).** Moreover, the influence of nucleation and the presence of filling and pozzolanic nanomaterials leads to the formation of additional hydrates within the concrete. This process contributes to the improvement of the microstructure by densifying it and purifying the pores. As a result, the penetration of chlorides into the concrete is reduced **(He, & Shi, 2008)**.

Table 4-12: Chloride factor Da and Cs

Mixture	CHNC%	D_a ($x10^{-11}$) (m^2/sec)	C_s (By mass of cement)	C_i^* (By mass of cement)
NC	0	3.90	3.797	0.671
	1.5	3.70	3.481	0.671
	3	2.50	3.165	0.671
	4.5	5.00	2.848	0.899
HS	0	5.90	3.390	0.599
	1.5	3.50	2.542	0.599
	3	3.60	2.147	0.599
	4.5	4.50	2.825	0.599
GG	0	1.50	2.278	1.120
	1.5	2.20	1.899	1.120
	3	1.00	1.899	0.671
	4.5	4.70	0.490	0.106

* **Initial chloride concentration of concrete before exposure to chloride attack**

4.3.9. Chloride Penetration Depth of Impressed Current Test

The impress current test is a try of simulation of the corrosion process of reinforcing steel by accelerated method, which is an electrochemical process that was carried out to find out the effectiveness of halloysite in concrete mixture by reducing corrosion in embedded steel bar. One of the main causes of corrosion is the penetration of chlorides into the concrete. Where it was observed that the amount of penetration of chlorides into concrete containing CHNC by 1.5, 3 and 4.5% as shown in Figure (4-16), (4-17) and Table (4-13). It was found that the depth of penetration for all mixtures containing 1.5 and 4.5% decreased from the amount of penetration, but the percentage of 3% was the best percentage ever, as the amount of decrease was 23.38 and 34.59 % for NC and HS mixture respectively. This is due to

the fact that CHNC would reduce the pores in the concrete, and thus reduces penetration.

As for the percentage of 4.5%, despite the decrease in the depth of penetration by a slight amount from the control mixture, but its values were higher than 1.5 and 3% it is possible that the reason could be due to when the halloysite interacted with $Ca(OH)_2$ to form new products of C-S-H an excess amount of silica would be formed that would accumulate the quantity together to form granules of large size distributed inside the concrete, which weakens the bonding between the components of the matrix and thus gives a harmful adverse effect on the concrete **(Zhang, 2012)**. This behavior is close to the behavior of nano silica.

As for mixture GG, the combined effect of each of halloysite and GGBS had a significant effect on reduceing the depth of penetration by 19.62 mm, with a decrease percentage of 36.69%. The reason is that both halloysite and GGBS have the ability to fill, also **Cheng et al. (2011)** claimed that GGBS cement pastes do not contain Portlandite for a percentage of 25% and needle shape of ettringite, in addition, halloysite reaction with $Ca(OH)_2$ which formed more C-S-H and both effect means concrete very compacted microstructure.

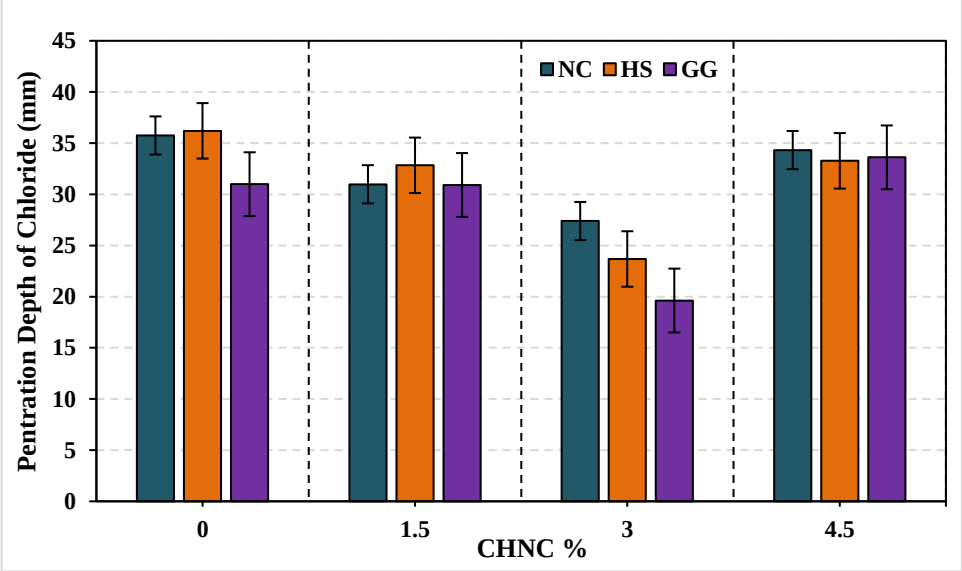

Figure 4-16: Depth penetration of chlorides for NC, HS and GG mixtures due to impressed current

Table 4-13: Chloride penetration depth at 26 days (X_d)

Mix	Chloride penetration depth (Xd) (mm)			
	CHNC %			
	0	1.5	3	4.5
NC	35.73	30.98	27.39	34.32
HS	36.2	32.83	23.68	33.27
GG	30.99	30.91	19.62	33.61

Figure 4-17: Chloride penetration depth at 26 days under impressed current

4.3.9.1. Evaluation of Corrosion Rate and Mass Loss of Steel Exposed to Corrosive Conditions

The presence of reinforcement steel bar embedded in concrete with high alkalinity of pores solution (pH 12-13) forms the passive protective film (PPF) spontaneously. This film, which is self-generated soon after the hydration of cement has started. When chloride ions penetrate the concrete and reach the layer of concrete neighbouring of the reinforcing steel rebar,

this layer of protection surrounding the rebar is broken down and destroyed due to chloride ions and carbonation and the surface of the steel becomes an anode electrode, which triggers an electrochemical reaction. This reaction leads to the corrosion of the reinforcing steel, resulting in the steel turning from its original color to a black or red rust color, and pits begin to form on the surface of the steel. An example of this can be seen in Figure (4-18), which depicts reinforcing steel bars that have been exposed to the effects of corrosion.

Figure 4-18: The reinforcing steel bars that exposed to the effects of corrosion due to impressed current

The corrosion rate was calculated to estimate the damage to the reinforcing steel using the following Equation (4-3) **(Vedalakshmi, 2010)**:

$$Corrosion\ Rate(C \cdot R) = \frac{87 \cdot 6 * W}{D * A * T} \qquad (4-3)$$

Where:

W: Loss in weight (gm); D: Density of steel (gm/cm^3) =7.85; A: Area (cm^2); T= Time (hr).

According to the results presented in Figure (4-19) and Table (4-14), the addition of halloysite nanoparticles with a concentration of 1.5% and 3% by weight of cement resulted in a decrease in the rate of corrosion in all three concrete mixtures (NC, HS, GG). This decrease in the rate of corrosion is attributed to the formation of a denser microstructure in the concrete due to the presence of halloysite nanoparticles. However, when the concentration of halloysite was increased to 4.5%, the rate of corrosion increased again in all three mixtures.

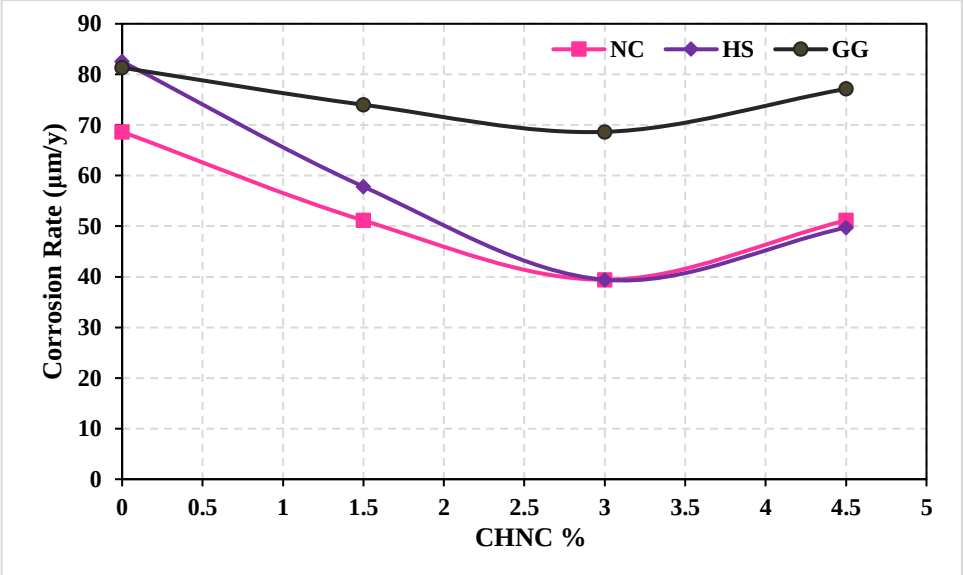

Figure 4-19: Corrosion rate of concrete for NC, HS, GG mixture

Table 4-14: Value of corrosion rate

Mix	Corrosion Rate in (µm/year)				Condition of rebar
	CHNC (%)				
	0	1.5	3	4.5	
NC	68.641	51.139	39.415	51.139	Low Corrosion activity (23-58)
HS	82.533	57.823	39.415	49.730	Low Corrosion activity (23-58)
GG	81.315	74.002	68.641	77.137	Moderate Corrosion activity (58-174)

The weight loss of the steel sample provides a measure of the extent of corrosion that has occurred. The amount of weight loss in the reinforcing steel due to corrosion was determined by calculating the difference in weight

between the initial weight of the steel sample and the weight after exposure to the corrosive environment. This weight loss can be calculated using the following Equation (4-4):

$$Weight\ Loss\ \% = \frac{W_{initial} - W_{final}}{W_{initial}} * 100 \qquad (4-4)$$

where:

$W_{initial}$ is weight of bar before the test, W_{final} is weight of bar after the test.

According to the findings of the study, the use of 3% of CHNC resulted in the lowest percentage of weight loss for all three concrete mixtures tested. This reduction in weight loss was particularly significant for mixtures NC and HS, with a decrease of 41.30% and 49.74% respectively, while mixture GGshowed a decrease of 13.32% as shown in Figure (4-20) and Table (4-15). The results indicate that halloysite is effective in reducing pores and creating a dense matrix, which helps to preserve the reinforcing steel and reduce damage to the steel bar.

The reduction in weight loss can be attributed to the ability of halloysite to act as a filler material, filling in the gaps between the cement particles and creating a more tightly packed concrete structure. This dense structure helps to reduce the amount of moisture that can penetrate the concrete, which can lead to the corrosion of the reinforcing steel and other forms of damage.

In addition to reduce weight loss, the use of halloysite can also improve the overall durability of concrete. By reducing the amount of damage to the steel bar, the concrete is better able to withstand the stresses and strains of use over time, which can increase its longevity and reduce the need for costly repairs or replacement.

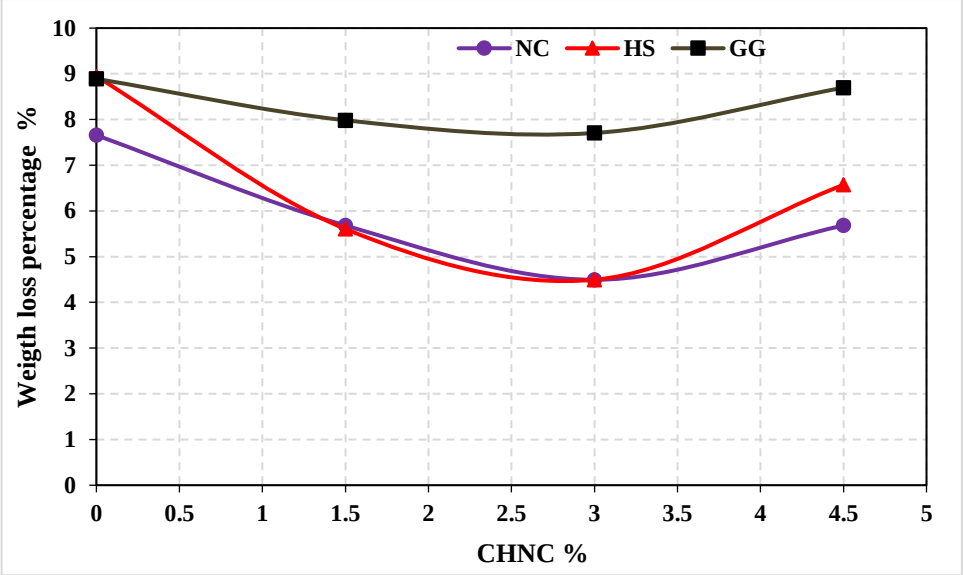

Figure 4-20: Weight loss of steel reinforcement for different mixture due to accelerated corrosion (impress current)

Table 4-15: Weight loss of steel rebar corroded

Mix	Weight Loss Percentage %			
	CHNC%			
	0	1.5	3	4.5
NC	7.66	5.68	4.50	5.68
HS	8.94	5.61	4.50	6.57
GG	8.89	7.98	7.71	8.70

During the corrosion process of reinforcing steel, the volume of corrosion products or rust can be formed on the surface of the steel increases, which would generate an internal pressure on the surrounding concrete of rebar. This increase in an internal pressure is more tensile strength capacity of concrete that can cause cracks to form along the face of the concrete parallel to the reinforcing steel, as well as cracks on the sides of the area surrounding the reinforcing steel bar. These cracks can lead to a reduction in the strength and durability of the concrete, as well as the potential for further corrosion to occur.

4.3.10. Length Change

The length change test was conducted on both concrete and mortar samples, with the addition of halloysite in percentages of 1.5%, 3%, and 4.5%. The results of the test are as follows.

4.3.10.1. Length Change for Concrete

After the hydration process of concrete, the capillary pores of the concrete start to release water due to evaporation and absorption by the surrounding materials. This loss of water creates internal stresses within the concrete, which can lead to cracking if the stresses become too high and over the tensile strength capacity **(Taylor, & Wang, 2014)**. This phenomenon is known as length change, and it occurs in hardened concrete. During the early stages of hydration (24h, 7, 14 and 28 days) during the cement reacts with water to form hydration products, the expansion may occur in the concrete as shown in Figure (4-21).

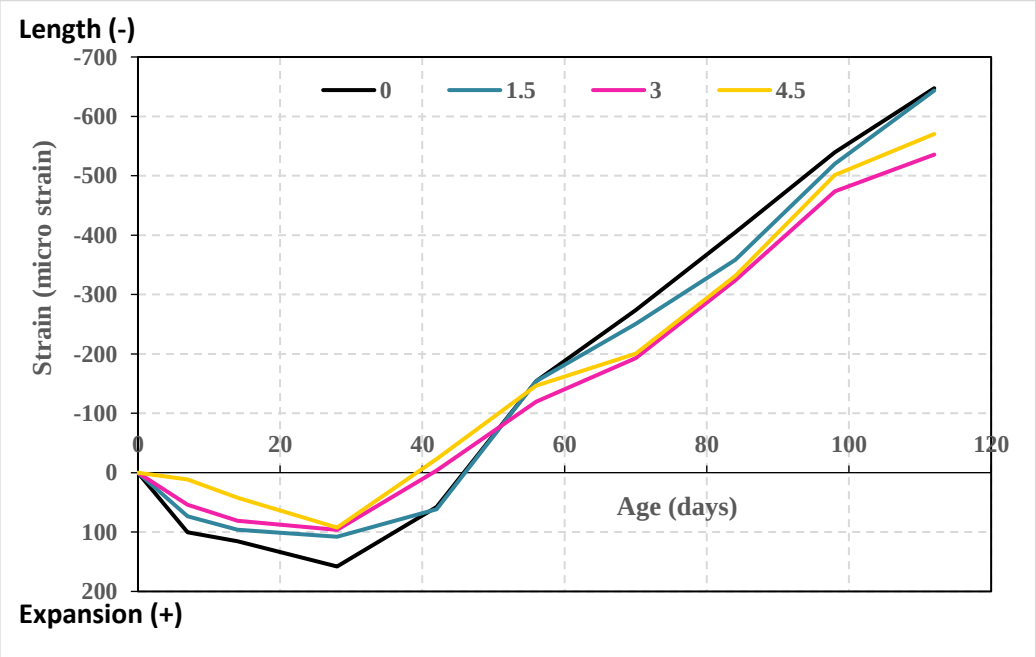

Figure 4-21: Expansion and Length Change for NC mixture

Test results showed that the addition of CHNC in different proportions reduced the length change of concrete. Figure (4-22) and Table (4-16) shows

that the NC mixture that contain 1.5, 3 and 4.5% of CHNC all worked to reduce length for all ages. Despite the fact that the length was constantly increase with age, but at the same time CHNC worked to reduce the amount of length compared to the control mixture, there was a slight decrease in length from the control mixture for 1.5 % of CHNC. However, the biggest reduction in length was at 3% (46.15, 30, 39.24, 93.33, 22.5, 29.58, 20, 12.14 and 17.26%) at 7, 14, 28, 42, 56, 70, 84, 98 and 112 days respectively. The reason of reduction is that CHNC creates a denser and more compact microstructure for the concrete, which reduces the evaporation of water from within the concrete **(He & Shi 2008).**

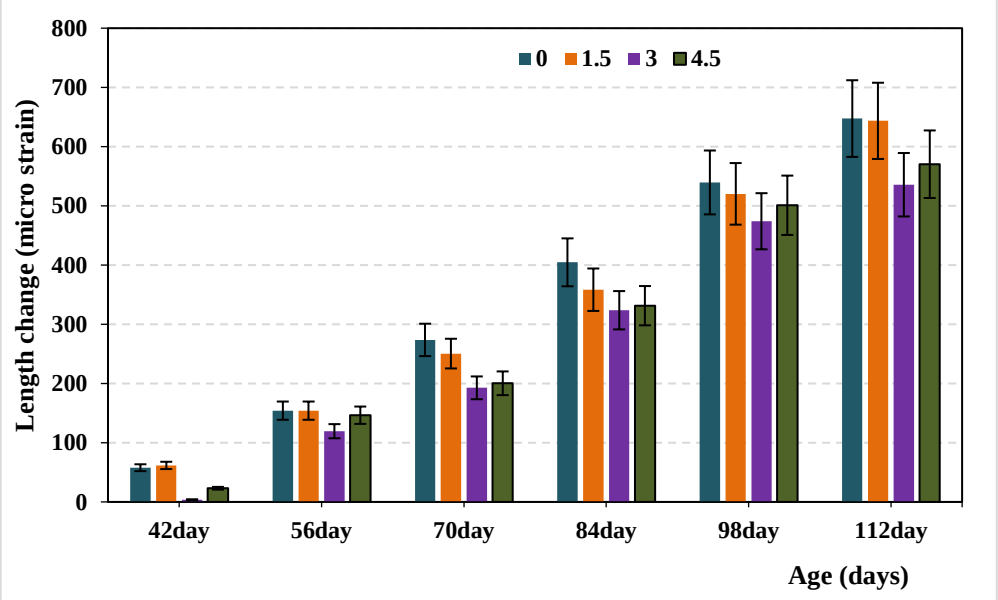

Figure 4-22: Length Change Result for NC Mixture

As for the HS mixture as shown in Figure (4-23) and Table (4-16), the CHNC had a greater effect in reducing length than the NC mixture. There was little decrease for 1.5% CHNC and the largest decrease was for 3% also, the reduction was (0, 5.26, 27.27, 97.37, 311.11, 80.5, 68.18, 59.17 and 58.17%) at 7, 14, 28, 42, 56, 70, 84, 98 and 112 days respectively compare to control mixture. The first reason can be attributed to the fact that the amount of w/c ratio in this mixture is less than other mixtures, as the

decrease in water less available for evaporation which reduces length. The second reason is that it is possible that CHNC, due to its distinctive absorption property, acts as a sponge to absorb the free water present in the concrete, which reduces length, in addition to its role in improving the microstructure of concrete **(Elzokra, 2020)**.

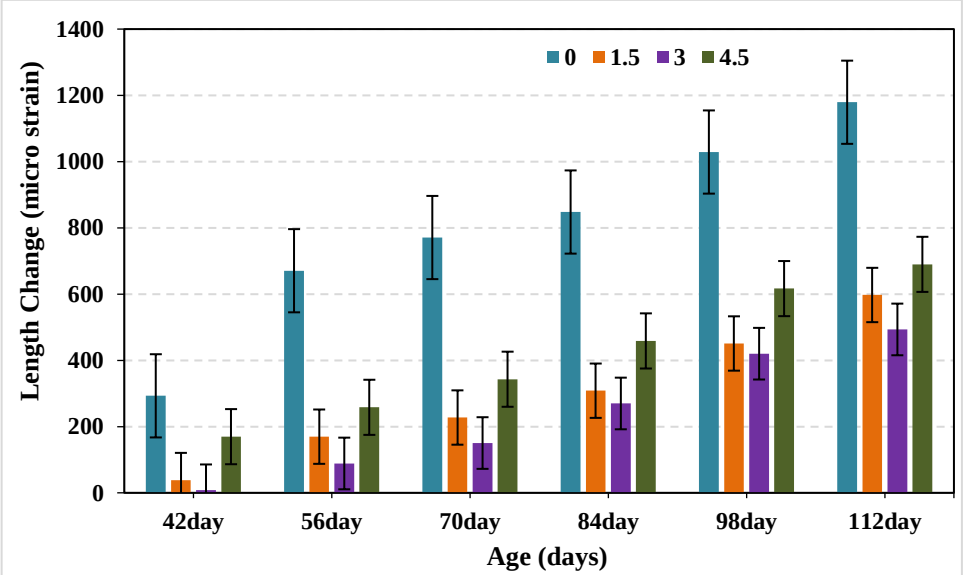

Figure 4-23: Length Change result for HS mixture

As for the mixture GG that containing GGBS, the test results shown in Figure (4-24) showed that the reference mixture GG worked to reduce length of concrete compared to the reference mixture NC by - (46.15, 43.33, 51.22, 46.67, 60, 22.54, 0.95, 47.86 and 35.12 %) at 7, 14, 28, 42, 56, 70, 84, 98 and 112 days respectively. This is due to that the GGBS can help reduce the length by reducing water demand and dense the microstructure of concrete. Also it is noted that the addition of halloysite to the concrete containing GGBS reduced the length of the different proportions of halloysite. The percentage 1.5% of CHNC showed a decrease in length with age (64.29, 58.82, 60, 77.27, 26.56, 26.44, 6.73, 34.78 and 28.19) at 7, 14, 28, 42, 56, 70, 84, 98 and 112 days respectively. Also there was a reduction in length of concrete with 3% CHNC replacement by approximate (3.35, 5.81, 1.04, 27.27, 85.93, 74.71, 36.53, 46.85 and 44.49) at the same age. During the

drying process, the larger pores within the concrete tend to empty first, followed by progressively smaller pores. As the moisture content decreases, capillary pores begin to form within the remaining pores. But when both CHNC and GGBS present in concrete it works to fill and occupy some of the pore spaces and limiting the movement of water and reducing the overall evaporation rate this due to the filling ability for both CHNC and GGBS. It can be seen that the replacement of 4.5% of CHNC, it increased the length of all mixtures. The reason of the increase is to increase the amount of nanoparticles and the distances between them become narrower. This may be due to the filling effect of the nanoparticles or their tendency to agglomerate. Thus, there is less space available for calcium hydroxide $Ca(OH)_2$ crystal growth as it generates pressure inside the concrete that works on cracking and evaporation of water and thus increasing length **(Jalal, 2013).** These results may lead to the decrease in crystal quantity resulting from the limited space prevents proper hydration and formation of a dense, well-connected structure this leads to length **(Jalal, 2013)**.

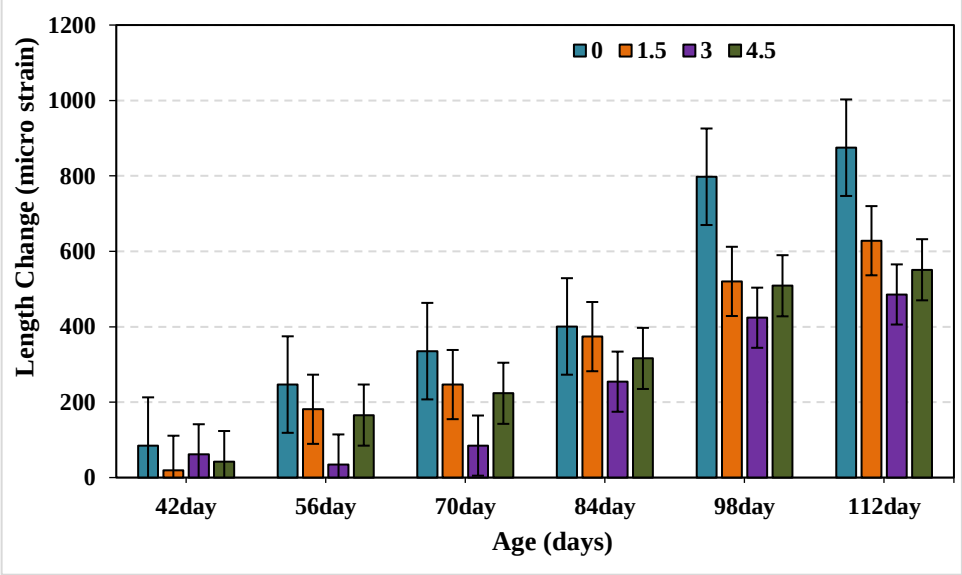

Figure 4-24: Length Change result for GG mixture

Table 4-16: Expansion and Length Change result for NC, HS, GG mixture

Mixture	CHNC%	Length Change (micro strain) at age								
		7 days	14 days	28 days	42 days	56 days	70 days	84 days	98 days	112 days
NC	0	100.19	115.60	157.99	57.80	-154.1	-273.60	-404.62	-539.49	-647.39
	1.5	73.21	96.33	107.89	61.65	-154.14	-250.48	-358.38	-520.23	-643.54
	3	53.94	80.92	96.33	-3.85	-119.46	-192.67	-323.69	-473.98	-535.64
	4.5	11.56	42.38	92.48	-23.12	-146.43	-200.38	-331.40	-500.96	-570.32
HS	0	50.09	73.21	84.77	-292.87	-670.52	-770.71	847.78	-1028.90	-1179.19
	1.5	26.97	26.97	65.51	38.53	-169.55	-227.36	-308.28	-450.86	-597.30
	3	50.09	69.36	107.89	7.71	-88.63	150.28	-269.74	-420.03	-493.25
	4.5	26.97	61.65	0	-169.56	-258.18	-342.96	-458.57	-616.57	-689.78
GG	0	53.95	65.51	77.071	-84.78	-246.62	-335.26	-400.77	-797.68	-874.75
	1.5	19.27	26.97	30.83	19.26	-181.12	-246.62	-373.79	-520.23	-628.13
	3	154.14	165.70	177.26	61.65	-34.68	-84.77	-254.33	-423.89	-485.54
	4.5	15.41	11.56	53.94	-42.38	-165.70	-223.51	-315.99	-508.67	-551.05

(+) refers expansion strain

(-) refers Length Change

4.3.10.2. Length Change for Mortar

Length Change test was carried out on the mortar mixtures as well, where 1.5, 3 and 4.5% of the CHNC were replaced, and an improvement was shown in all mixtures. Also, in the early ages of the mortar, expansion of all mixtures occurred as a result of the interaction of water and cement, as shown in Figure (4-25).

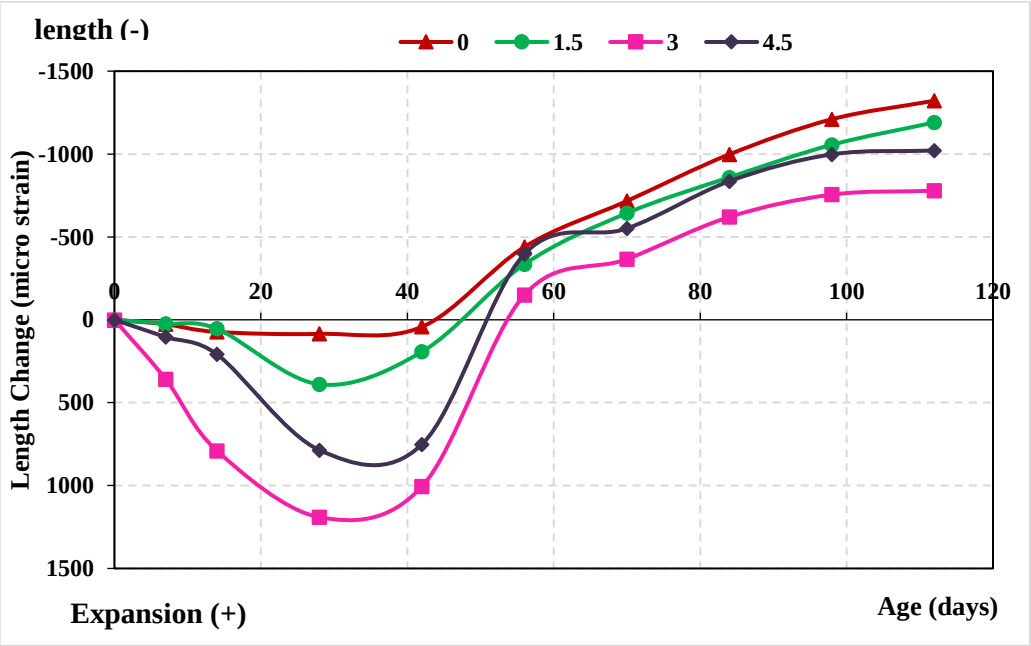

Figure 4-25: Expansion and Length Change for MH mixture mortar

The test results for mixture MC indicate that the addition of CHNC led to a decrease in length compared to the control mixture. The reduction in length was more significant when 3% of CHNC was used compared to the 1.5% replacement. The test result of CHNC percentages at different time intervals are provided in Figure (4-26) and Table (4-17). For example, at 42 days, the length reduction with 3% CHNC was approximately 67.50%, compare to control mixture. Similarly, at 56, 70, 84, 98, and 112 days, the reduction percentages with 3% CHNC were 44.44%, 39.5%, 27.70%, 30.56%, and 30.56%, respectively. This can be attributed to the CHNC reacting with the components of the cement and these reactions can lead to the formation of

additional hydration products that contribute to better length performance **(Singh, 2015)**.

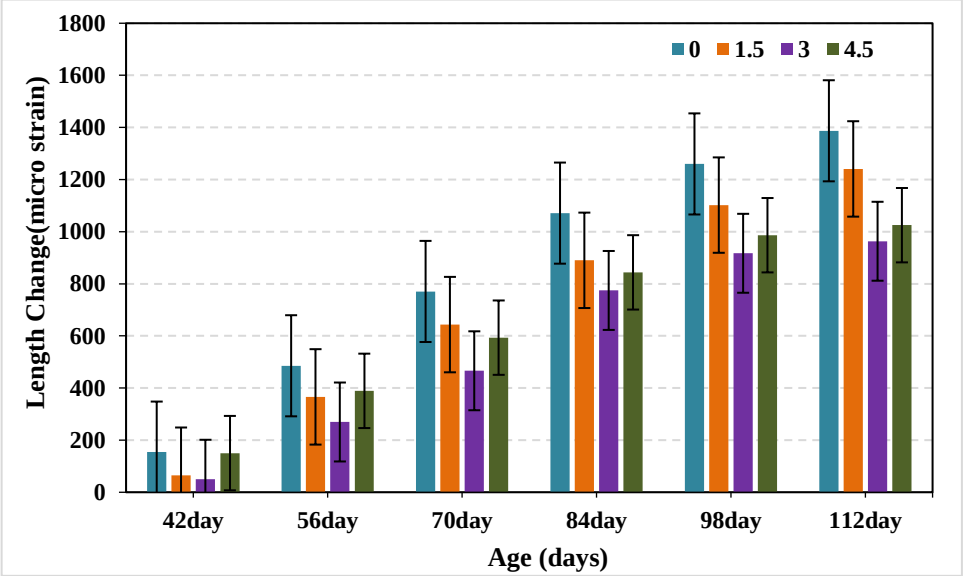

Figure 4-26: Length Change of mortar for MC mixture

In the case of mixture MH as shown in Figure (4-27) and Table (4-17), the addition of CHNC had a greater impact on reduction of length change compared to mixture MC. The results show that the reduction in length change was relatively small when 1.5% CHNC was added, but the largest decrease occurred when 3% CHNC was used. The reduction percentages at different time intervals.

For example, at 42 days, the Length reduction with 3% CHNC was approximately 38.21%, similarly, at 56, 70, 84, 98, and 112 days, the reduction percentages with 3% CHNC were 65.79%, 48.92%, 37.84%, 37.58%, and 41.12%, respectively, compared to the control mixture.

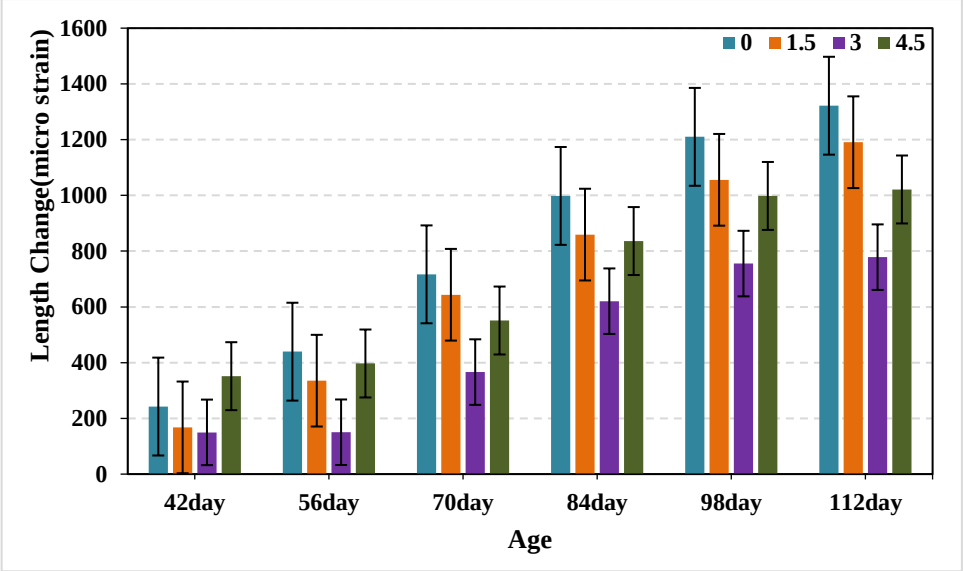

Figure 4-27: Length Change of mortar for MH mixture

As for the mixture MG that containing GGBS, the test results shown in Figure (4-28) showed that the percentage 1.5% of CHNC showed a decrease in length. Also there was a reduction in length of concrete with 3% CHNC replacement by approximate (64.63, 67.92, 46.5, 28.14, 32.94 and 37.17) at age 42, 56, 70, 84, 98 and 112 days respectively, and this due to filling effect and pozzolanic activity for both GGBS and CHNC that improves microstructural of mortar.

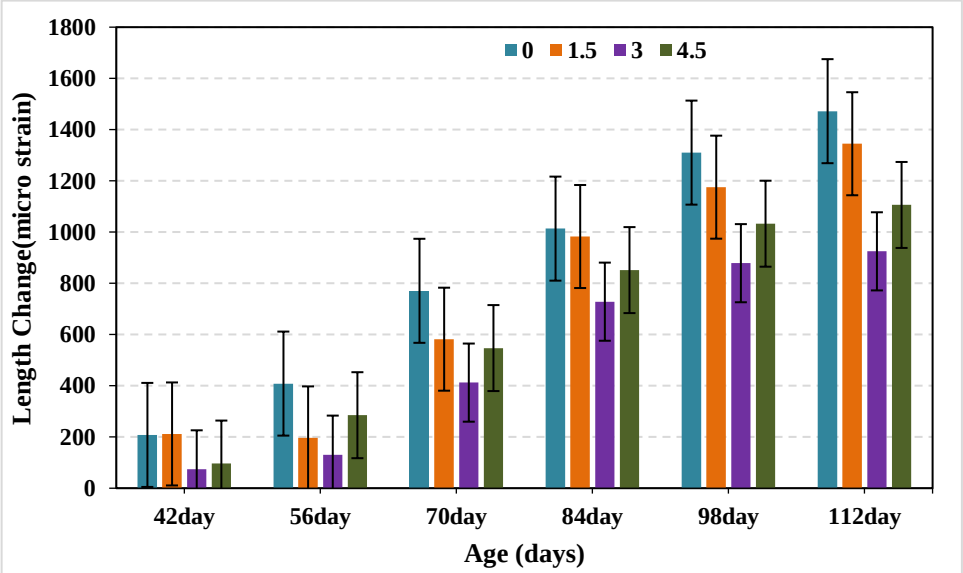

Figure 4-28: Length Change of mortar for MG mixture

Table 4-17: Expansion and Length Change result for MC, MH, MG mixture mortar

Mix	CHNC(%)	Expansion and Length Change (microstrain) at								
		7 days	14 days	28 days	42 days	56 days	70 days	84 days	98 days	112 days
MC	0	61.66	96.34	177.26	154.14	-485.55	-770.71	-1071.29	-1260.12	-1387.28
	1.5	34.68	38.54	107.89	65.51	-366.088	-643.55	-890.17	-1102.12	-1240.85
	3	273.60	281.31	335.26	50.096	-269.75	-466.28	-774.56	-917.15	-963.39
	4.5	211.95	219.65	235.067	150.29	-389.21	-593.45	-843.93	-986.51	-1025.048
MH	0	26.97	73.22	84.78	242.39	-439.31	-716.76	-998.073	-1210.019	-1321.77
	1.5	23.12	53.95	389.21	167.68	-335.26	-643.55	-859.34	-1055.88	-1190.75
	3	358.38	789.98	790.75	149.78	-150.29	-366.088	-620.42	-755.29	-778.42
	4.5	104.046	208.092	786.13	351.45	-396.92	-551.059	-836.22	-998.073	-1021.19
MG	0	123.314	165.70	238.92	208.092	-408.48	-770.71	-1013.49	-1310.21	-1472.061
	1.5	46.24	57.80	235.067	211.95	-196.53	-581.89	-982.66	-1175.34	-1344.89
	3	350.67	373.79	435.45	73.60	-131.021	-412.33	-728.32	-878.61	-924.86
	4.5	211.95	242.77	300.58	96.34	-285.16	-547.21	-851.64	-1032.76	-1105.97

(+) refers expansion strain

(-) refers length change

4.3.11. Nondestructive Test (NDT)

These tests are a group of techniques used to evaluate the properties of materials or structures without causing damage or altering the integrity of the tested material. In the field of civil engineering, NDT is widely used to assess the quality and performance of concrete structures such as bridges, buildings, and pavements.

4.3.11.1. Ultrasonic Pulse Velocity(UPV)

Ultrasonic testing is a non-destructive testing method that is commonly used to assess the quality and integrity of concrete structures. As mentioned previously, the addition of CHNC to concrete can improve the microstructure of concrete, therefore, the replacement of CHNC and GGBS can also affect the results of ultrasonic testing as shown in Figure (4-29) and Table (4-18).

At lower percentages of calcined halloysite nano clay 1.5%, the ultrasonic test results may show an improvement in the quality of the concrete. The UPV was increased 2.45 % than the control mixture for all ages. Also the CHNC percentage of 3% increase 2.45% at 7 days and 5.02% at 28 and 90 days. Also for 4.5% the increase was 2.45% for all age curing at NC mixture. The mixture HS was the same effect of NC mixture except that the rate of increase is 5.02% for 7,28 and 90 days at 4.5% replacement of CHNC. This is because the addition of nano clay can enhance the homogeneity and cohesiveness of the concrete, and lead to an increase in the speed of sound waves through the concrete. The improved homogeneity can also lead to a reduction in the number and size of defects in the concrete, which can be detected by ultrasonic testing. The GG mixture with GGBS there was an increase in the control mixture about 2.45% compared to NC mixture control mixture. This an increase in the speed of sound waves through the concrete. That is attributed to improve homogeneity and reduce porosity of the

concrete can lead to a reduction in the number and size of defects in the concrete, which can be detected by ultrasonic testing **(Loke, 2022).**

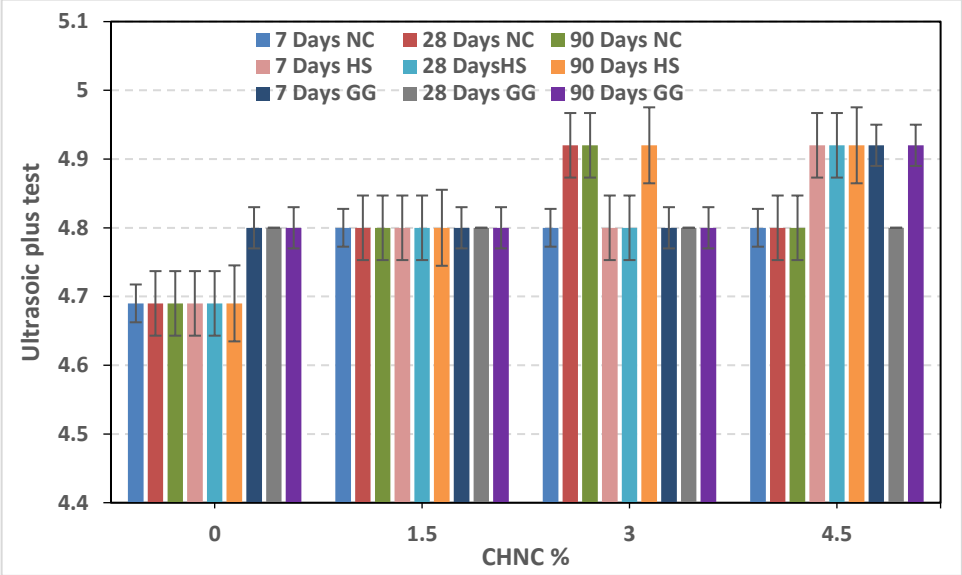

Figure 4-29: Ultrasonic test of concrete with CHNC

Table 4-18: Ultrasonic test result of concrete with CHNC

Mixture	Age (days)	Ultrasonic plus velocity (km/sec)			
		CHNC %			
		0	1.5	3	4.5
NC	7	4.69	4.80	4.80	4.80
	28	4.69	4.80	4.92	4.80
	90	4.69	4.80	4.92	4.80
HS	7	4.69	4.80	4.80	4.92
	28	4.69	4.80	4.80	4.92
	90	4.69	4.80	4.92	4.92
GG	7	4.80	4.80	4.80	4.92
	28	4.80	4.80	4.80	4.80
	90	4.80	4.80	4.80	4.92

4.3.11.2. Rebound Hammer Test

This is one of the non-destructive testing method used to assess the surface hardness and quality of concrete and also to evaluate the properties of buildings after aging. Figure (4-30) and Table (4-19) show the test result of concrete containing CHNC in different percentage. The addition of CHNC to concrete had a positive effect, as it increased the rebound number as the replacement increased. The results showed a slight increase in the replacement rate of 1.5%, the rebound number (RN) of all concrete mixtures, the increase at (10, 2.86, 2.78) at NC mixture and (5.00, 4.76, 2.22) at HS mixture and (2.70, 2.56, 15.79) at GG mixture at 7, 28 and 90 days. As for the replacement percentages 3 and 4.5% of CHNC, they increased the hardness of the concrete surface more than the first percentage 1.5% and the control mixture, where the amount of increase was for the percentage of 3% about (30, 17.14, 25%) for NC mixture and (10, 9.52, 11.11) for HS mixture and (8.11, 5.13, 26.32) for GG mixture at 7, 28 and 90 days comparing to control mixture the reason for increase surface hardness for concrete contain CHNC due to improvement in the (ITZ) transition zone region between the cement paste and aggregate that make concrete more strong and increase of rebound number. **(Haw, 2020)** investigated the combined effect of concrete HNC and metakaolin, it was found that both materials worked to intensify the region of ITZ and improve the strength. The 4.5% CHNC was the higher rebound number about (36.67, 20, 30.56%) for NC mixture and (12.50, 7.14, 20%) for HS mixture this is attributed to CHNC can act as a nucleating agent, accelerating the hydration process of cement, resulting in a more complete and rapid formation of calcium silicate hydrate (C-S-H) gel. This gel is responsible for the binding of cement particles, which leads to a denser and stronger concrete, and can also contribute to an increase in the rebound number **(Heikal, 2016)**. Also for GG mixture, the increase percentage in RN

was (10.81, 10.26, 26.32%) at 7, 28 and 90 days compared with control mixture.

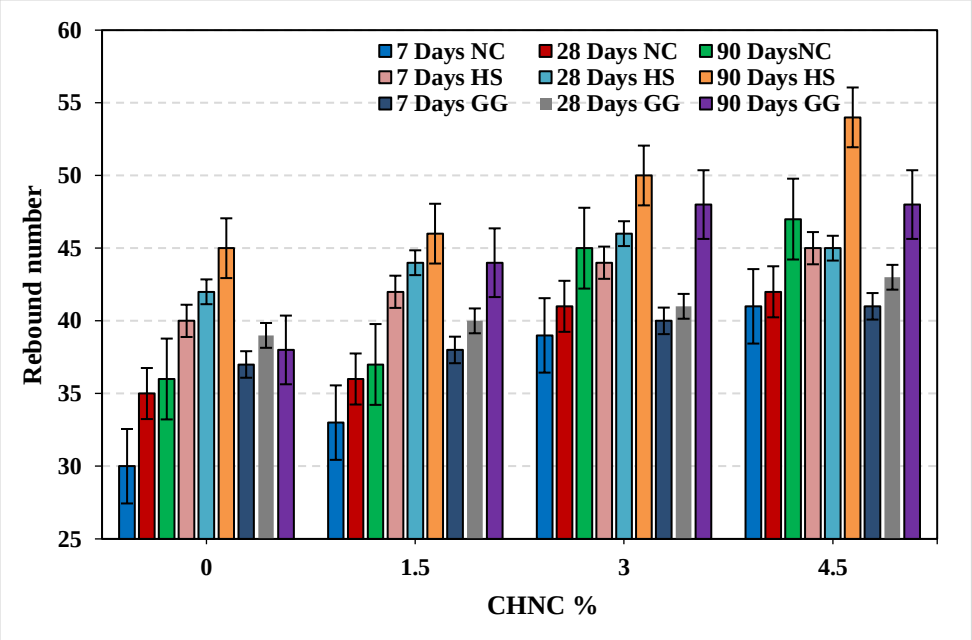

Figure 4-30: Rebound number of concrete with CHNC

Table 4-19: Rebound number result of concrete with CHNC

Mix	Age (days)	CHNC %			
		0	1.5	3	4.5
		Rebound Number			
NC	7	30	33	39	41
	28	35	36	41	42
	90	36	37	45	47
HS	7	40	42	44	45
	28	42	44	46	45
	90	45	46	50	54
GG	7	37	38	40	41
	28	39	40	41	43
	90	38	44	48	48

4.3.12 Sustainability of Concrete Containing Halloysite Nano clay and Ground Granulate Blast Slage

The sustainability of concrete is a topic of growing importance in the construction industry. While concrete is a widely used material due to its strength, durability, and versatility. Its production can have significant environmental impacts. Cement is a key ingredient in concrete and is responsible for a significant portion of its carbon footprint. Cement production is energy-intensive and releases a substantial amount of carbon dioxide (CO_2) during the calcination of (limestone and clay) and the combustion of fossil fuels. In 2021, global cement production 4.4 billion tons, with clinker estimated at 3.7 billion metric tons, contributing 7% to 8% of CO_2 emissions (**Statista, 2022)**. In China, the cement industry released 858.2 million metric tons of carbon dioxide ($MtCO_2$) into the atmosphere in 2021. China and India are mainly responsible for the overall increase in

global CO_2 emissions **(Hosseinzadeh Zaribaf, 2017)**. This problem has become more serious than before due to the increase in human activity in the industry and the resulting emissions of carbon dioxide and many other gases that increase global warming and environmental pollution. There is a demand to provide alternatives to reduce the use of cement while at the same time preserving its properties. There are efforts to develop and use alternative cementitious materials such (fly ash, silica fume and GGBS) that have a lower carbon footprint compared to traditional Portland cement. Also nanomaterials were introduced as an alternative to Portland cement to meet the technical requirements of cement in addition to reducing costs and emissions. Each of the two materials used, GGBS and Halloysite nano clay, are materials with a low carbon foot print, the production of GGBS requires less energy compared to the production of cement. As a byproduct of the iron and steel industry, GGBS is obtained through a process that releases less CO_2 compared to the production of cement. The amount of emissions is caused by the rapid cooling process and transportation for grinding. Therefore, incorporating GGBS in concrete can lower the embodied CO_2 emissions associated with the material **(Black, 2016)**. Also halloysite nano clay considered a natural material that maybe reduce this emissions. The material itself liberates the emission of 0.004 tons of carbon dioxide, which is simply a result of crushing, transportation and storage **(Black, 2016)**.

To clarify the effect of halloysite and GGBS in reducing the emission of CO_2 when it is incorporated into concrete, emission data were prepared based on the experimental work. eCO_2 is defined as the emission of carbon dioxide as a result of burning fossil fuels, as well as from the manufacture of cement and is calculated by multiplying the amount of emission CO_2 for each substance multiplied by the mass of the substance as shown in Equation (4-6) **(Purnell & Black, 2012)**.

$$eCO_2 = CO_2\ emission * Mass\ of\ constituent \qquad (4-6)$$

As shown in Figure (4-31) and Table (4-20) carbon dioxide embodied (eCO_2) in the three concrete mixtures contains three percentages of halloysite nano clay (0 ,1.5, 3, and 4.5%). The NC mixture it shows an eCO_2 ratio 0.151/kg, and upon the introduction of halloysite, there was a decrease in the value of the CO_2 emission as the amount of replacement with cement increased, and the decrease was (1.32, 3.31 and4.64%) (1.5,3 and 4.5%) respectively. As for the HS mixture design, it had the same effect in reduce CO_2 emission as the percentage increased (1.78, 2.96 and 4.73%) for (1.5, 3, and 4.5%) halloysite nano clay. Although the amount of replacement with halloysite was very small, and the decrease in the amount of carbon dioxide emission is also small, but as a nano material, it is effective in reducing atmospheric CO_2 emissions if the replacement value is increased to higher percentages, and therefore it will have a clear benefit in reducing this emission and its harm. The GG mixture which contain GGBS shown that the replacement of the GGBS reduced the emission of CO_2 by 24.21% compared to the reference mixture of NC. The addition of halloysite to the GG mixture in proportions (1.5, 3 and 4.5%) decreased CO_2 by (1.437, 2.875 and 4.313%) compared to the control mixture.

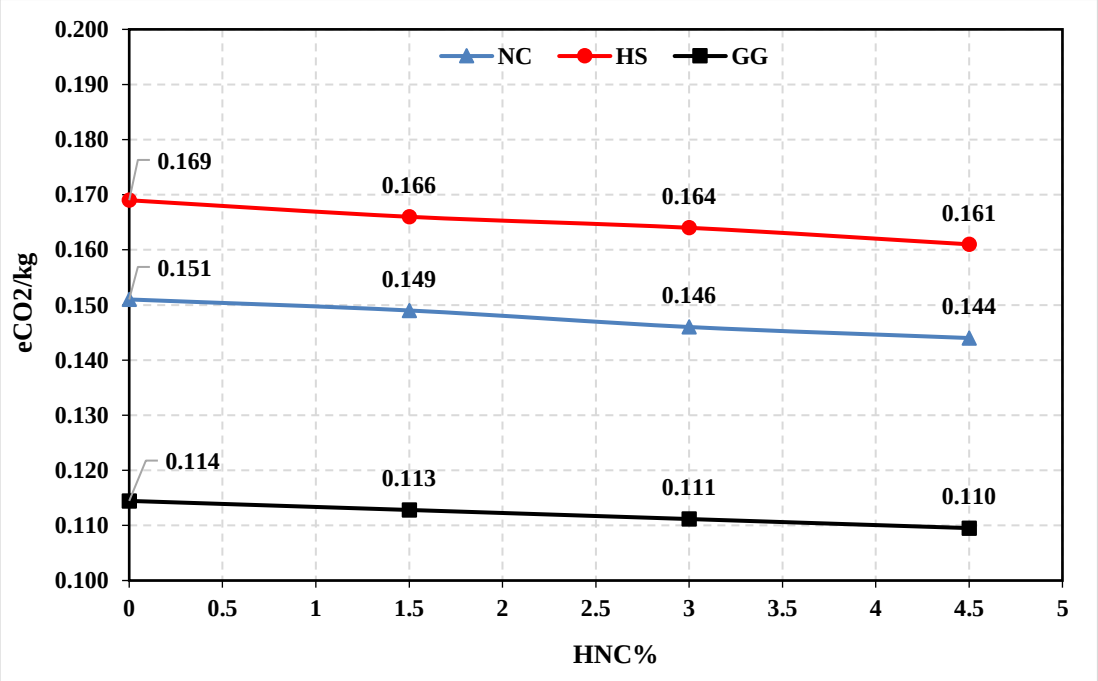

Figure 4-31 eCO_2 of concrete for NC, HS, GG mixture

Table 4-20: eCO_2 for concrete contain halloysite and GGBS

Mixture	Cement	Water	FA	CA	SP	Halloysite	GGBS	eCO_2/kg
NC	344.1	0.185	3.53	5.4	0.0185	0	0	0.151
HS	390.6	0.189	3.39	5.4	0.042	0	0	0.169
GG	258.08	0.185	3.53	5.4	0.0185	0	0.925	0.114
NC1.5	338.94	0.185	3.53	5.4	0.0185	0.0222	0	0.149
HS1.5	384.74	0.189	3.39	5.4	0.042	0.0252	0	0.166
GG1.5	254.21	0.185	3.53	5.4	0.0185	0.016652	0.925	0.113
NC3	333.78	0.185	3.53	5.4	0.0185	0.0444	0	0.146
HS3	378.88	0.189	3.39	5.4	0.042	0.0504	0	0.164
GG3	250.33	0.185	3.53	5.4	0.0185	0.0333	0.925	0.111
NC4.5	328.62	0.185	3.53	5.4	0.0185	0.0666	0	0.144
HS4.5	373.02	0.189	3.39	5.4	0.042	0.0756	0	0.161
GG4.5	246.46	0.185	3.53	5.4	0.0185	0.04996	0.925	0.110

Chapter Five
Conclusion and Recommendations

Chapter Five

Conclusion and Recommendations for Further Studies

5.1.Conclusions

Depending on the results obtained from the experimental work and analyze experimental results to understand the behavior of enhanced halloysite nanoparticles in concrete under external corrosive chloride attack.

The following conclusions are drawn:

5.1.1. Fresh and Hardened Properties of Concrete and Mortar

- The addition of CHNC to the mixture NC and GG reduced workability for both concrete and mortar, and the greater the amount of replacement, the greater decrease in workability. The slump of the mixture HS increased as a result of the effect of both the superplasticizer and the increase in the cement content.
- The employ of halloysite had a role in increase the compressive strength for both concrete and mortar. The higher the substitution ratio of halloysite, the higher the compressive strength
- Also, there was an increase in the flexural strength of the concrete containing both halloysite and GGBS. As the replacement (1.5, 3 and 4.5 %) increased, the flexural strength increased (53.93%, 29.64%, and 14.05%) replacement was 4.5% at NC mixture.
- When replace the CHNC with cement there was increase in the splitting tensile strength at 4.5% replacement of HS mixture, the increase was (19.02%, 28.34%, and 25.72%).
- It was observed that when adding 1.5 and 3% of halloysite, it reduced shrinkage compared to the control mixture, although it increased with age. It can be seen that when replacing 4.5% of CHNC, it increases the

shrinkage of all mixtures, the reason being that as the amount of nanoparticles increases, the distances between them become narrower. This may be due to the filling effect of the nanoparticles or their tendency to agglomerate.

- The addition of halloysite to the GG mixture in proportions (1.5, 3 and 4.5%) decreased CO_2 by (1.437, 2.875 and 4.313%) compared to the control mixture.

5.1.2. Durability of concrete

- An improvement in concrete microstructure, enhancing its durability, was observed. Water absorption and porosity decreased notably in mixtures with halloysite replacement. Concrete samples containing 3% and 4.5% CHNC exhibited significant reduction in water absorption compared to the control mixture at 7, 28, and 90 days (25.20%, 24.44%, 25% for 3% CHNC; 28.46%, 28.89%, 31.74% for 4.5% CHNC).
- Likewise, the sorptivity that was performed on concrete had good results, as the values decreased when replaced by different proportions of halloysite, decrease in GG mixture (21.88, 13.33 and 16.67%) for 3% of CHNC and (37.50, 16.67 and 16.67%) at 7, 28 and 90 days for 4.5%.
- The impact of halloysite on the migration coefficient was more pronounced at 90 days compared to 28 days. Higher replacement rates, particularly with CHNC 4.5%, significantly enhanced concrete resistance to chloride diffusion, showing reductions of 21.21% for NC, 45.30% for HS mixture, and 54.18% for GG mixture at 90 days.
- According to the impressed current test, the depth of penetration of the chloride for concrete mixtures with 3% CHNC as the amount of decrease was 23.38 and 34.59 % for NC and HS mixture respectively.
- The result of the chemical analysis of the concrete powder showed that the concentration of chlorides decreases with increasing depth as a result of reducing the effect of the capillary suction process.

- Halloysite worked when replaced with cement by lowering the concentration of chloride.

5.1.3. Non-Destructive tests

- When conducting the ultrasonic pulse velocity, an increase in the ultrasonic was observed as a result of the improvement of the microstructure of the concrete and the reduction of the pores when the concrete was replaced with halloysite and GBBS as well.
- The addition of CHNC to concrete positively impacted the rebound number, increasing with higher replacement rates. At 4.5% CHNC, the rebound numbers rose significantly, reaching 36.67% for NC mixture and 20% for HS mixture.

5.2.Recommendations for Further Studies

While this study provided insights into several properties of concrete with the addition of halloysite nanoclay, it also highlighted the need for further research to fully understand the effect of halloysite on concrete. It is suggested:

- Using halloysite with cement as an additive during the cement manufacturing process and studying the mechanical properties and durability.
- Studying the effect of carbonation and sulfate attack on concrete - containing halloysite.
- The use of halloysite with other nanomaterials as substitutes in concrete.
- Examining the environmental aspect of halloysite in reduction CO_2 in a broader context.
- Studying both of the thermal insulation property and the microstructure of concrete containing halloysite.

References

Ahmad, J., Kontoleon, K. J., Majdi, A., Naqash, M. T., Deifalla, A. F., Ben Kahla, N., ... & Qaidi, S. M. (2022). A comprehensive review on the ground granulated blast furnace slag (GGBS) in concrete production. Sustainability, 14(14), 8783.

Ahmad, J., Martínez-García, R., Szelag, M., de-Prado-Gil, J., Marzouki, R., Alqurashi, M., & Hussein, E. E. (2021). Effects of Steel Fibers (SF) and Ground Granulated Blast Furnace Slag (GGBS) on Recycled Aggregate Concrete. Materials, 14(24), 7497.

Al-Adwane, O., Al-Mallah, A., & Hussein, A. (2023). Transform of kaolinite in Iraqi kaolin clay to halloysite by intercalation reaction. Iraqi Geological Journal, 56(1D), 260–271. https://doi.org/10.46717/igj.56.1d.19ms-2023-4-28

AL-Ameeri, A. S., Rafiq, M. I., & Tsioulou, O. (2021). Combined impact of carbonation and crack width on the Chloride Penetration and Corrosion Resistance of Concrete Structures. Cement and Concrete Composites, 115, 103819.

Al-Bassam, K. S. (2007). Mineral resources. *Iraqi Bulletin of Geology and Mining*, (1), 145-168.

Al-Bassam, K. S., & Tamar-Agha, M. Y. (1998). Genesis of the Hussainiyat ironstone deposit, Western Desert, Iraq. *Mineralium Deposita*, *33*(3), 266-282.

Allalou, S., Kheribet, R., & Benmounah, A. (2019). Effects of calcined halloysite nano-clay on the mechanical properties and microstructure of low-clinker cement mortar. Case Studies in Construction Materials, 10, e00213. https://doi.org/10.1016/j.cscm.2018.e00213

Al-Salami, A. E., Morsy, M. S., Taha, S., & Shoukry, H. (2013). Physico-mechanical characteristics of blended white cement pastes containing thermally activated ultrafine nano clays. Construction and Building Materials, 47, 138-145.

Alwash, S. S., Al-Ameeri, A., & Mattar, S. G. (2023). Assessing the effect of corrosion on optimised low carbon concrete. Materials Today: Proceedings. https://doi.org/10.1016/j.matpr.2023.04.653

Andrade, F. A., Al-Qureshi, H. A., & Hotza, D. (2011). Measuring the Plasticity of Clays: A Review. Applied Clay Science, 51(1-2), 1-7 .

Arivalagan, S. (2014). Sustainable studies on concrete with GGBS as a replacement material in cement. Jordan journal of civil Engineering, 8(3), 263-270.

ASTM C 143/C 143M. (2016). Standard test method for slump of hydraulic cement concrete, Annual Book of ASTM Standards, vol. 04.02 American Society for Testing and Materials, Philadelphia.

ASTM C 1585 - 13 Standard test method for measurement of rate of absorption of water by hydraulic cement concretes. Annual Book of ASTM Standards, vol. 04.02 American Society for Testing and Materials, Philadelphia.

ASTM C 230-1997 Standard specification for sample and testing fly ash or natural pozzolan for use as a mineral admixture in Portland cement, Annual Book of ASTM Standard 04.01, American Society for Testing and Materials, Philadelphia.

ASTM C109/C109M-2016. Standard Test Method for Compressive Strength of Hydraulic Cement Mortars (Using 2-in. or [50-mm] Cube Specimens). ASTM International, West Conshohocken, PA.

ASTM C1202-94 , (1994).Standard Test Method for Electrical Indication of Chloride's Ability to Resist Chloride .Annual Book of ASTM Standards V 04.02, ASTM, Philadelphia, pg. 620-5.

ASTM C597 - 16, (2016). Standard Test Method for Pulse Velocity Through Concrete American Society of Testing and Materials, Annual Book of ASTM Standard 04.01, American Society for Testing and Materials, Philadelphia.

ASTM C642-13, (2013). Standard test method for density, absorption and voids in hardened concrete. ASTM International, West Conshohocken, PA, USA.

ASTM C805/C805M-13a, (2013). Standard Test Method for Rebound Number of Hardened Concrete, ASTM International, West Conshohocken, PA.

ASTM International. Standard Test Method for Density, Absorption, and Voids in Hardened, Annual Book of ASTM Standard 04.01, American Society for Testing and Materials, Philadelphia.

Aydın, S., & Baradan, B. (2014). Effect of activator type and content on properties of alkali-activated slag mortars. Composites Part B: Engineering, 57, 166-172.

Baalbaki, O., 2003. Use of recycled waste paper in concrete hollow blocks. In: Proceedings of the 9th Arab Structural Engineering Conference, November 29December 1, Abu Dhabi, UAE, pp. 11731180. ISBN: 9948-02-099-5

Bheel, N., Abbasi, S. A., Awoyera, P., Olalusi, O. B., Sohu, S., Rondon, C., & Echeverría, A. M. (2020). Fresh and hardened properties of concrete incorporating binary blend of metakaolin and ground granulated blast furnace slag as supplementary cementitious material. Advances in Civil Engineering, 2020.

Black, L. (2016). Low clinker cement as a sustainable construction material. Sustainability of Construction Materials, 415-457.

Boukendakdji, O., Kadri, E. H., & Kenai, S. (2012). Effects of granulated blast furnace slag and superplasticizer type on the fresh properties and compressive strength of self-compacting concrete. Cement and concrete composites, 34(4), 583-590.

Broomfield, J. P. (2007). Corrosion of steel in concrete: understanding, investigation and repair. Second edition,Taylor &Francis, London.

BS EN 12390, Part 11:2015, Testing hardened concrete: Determination of the chloride resistance of concrete unidirectional diffusion. BSI Stand Publishing.

BS EN 12390-19 Part 3. 2019. Testing Hardened Concrete Compressive Strength of Test Specimens. BSI Stand Publishing .

BS EN 12390-5. 2019. Testing Hardened Concrete Part 5 Flexural Strength of Test Specimens. BSI Stand Publishing . 1-22.

BS EN 12390-6. 2010. Testing Hardened Concrete — Part 6: Tensile Splitting Strength of Test Specimens. BSI Stand Publishing .3(1):10.

BS EN 14629. (2007)., Products and systems for the protection and repair of concrete structures-Test methods-Determination of chloride content in hardened concrete. BSI Stand Publishing, 3.

BS EN 15167-1:2006, (2006). Ground granulated blast furnace slag for use in concrete, mortar and grout. Definitions, specifications and conformity criteria. BSI Stand Publishing.

Cao, Y., Bao, J., Zhang, P., Sun, Y., & Cui, Y. (2022). A state-of-the-art review on the durability of seawater coral aggregate concrete exposed to marine environment. Journal of Building Engineering, 105199.

Cheng, A., Hsu, H. M., & Chao, S. J. (2011). Properties of concrete incorporating bed ash from circulating fluidized bed combustion and ground granulates blast-furnace slag. Journal of Wuhan University of Technology-Mater. Sci. Ed., 26, 347-353.

Chithra, S., Kumar, S. S., & Chinnaraju, K. (2016). The effect of Colloidal Nano-silica on workability, mechanical and durability properties of High Performance Concrete with Copper slag as partial fine aggregate. Construction and Building Materials, 113, 794-804.

Chris DeArmitt. (2015). Halloysite, https://phantomplastics.com/wp-content/uploads/2022/06/Halloysite-Handbook-Phantom-Plastics-v1.50-Web.pdf

Cravero, F., & Churchman, G. J. (2016). The origin of spheroidal halloysites: a review of the literature. Clay Minerals, 51(3), 417-427.

De Weerdt, K., Wilson, W., Machner, A., & Georget, F. (2023). Chloride profiles – What do they tell us and how should they be used? Cement and Concrete Research, 173, 107287. https://doi.org/10.1016/j.cemconres.2023.107287

Decker, M., Grosch, R., Keßler, S., & Hilbig, H. (2020). Chloride migration measurement for chloride and sulfide contaminated concrete. *Materials and Structures*, *53*(4).

Dungca, J. R., Edrada, J. E. B., Eugenio, V. A., Fugado, R. A. S., & Li, E. S. C. (2019). The combined effects of nano-montmorillonite and halloysite nanoclay to the workability and compressive strength of concrete. *GEOMATE Journal*, *17*(59), 173-180.

EN 206-1:2000. Concrete – Part 1: Specification, performance, production and conformity (PN-EN 206-1:2003P – in Polish).

Elzokra, A. A. E., Al Houri, A., Habib, A., Habib, M., & Malkawi, A. B. (2020). Shrinkage behavior of conventional and nonconventional concrete: A review. Civil Engineering Journal, 6(9), 1839-1851.

Fan, Y., Zhang, S., Kawashima, S., & Shah, S. P. (2014). Influence of kaolinite clay on the chloride diffusion property of cement-based materials. *Cement and Concrete Composites*, *45*, 117-124.

Farzadnia, N., Ali, A. A. A., Demirboga, R., & Anwar, M. P. (2013). Effect of halloysite nanoclay on mechanical properties, thermal behavior and microstructure of cement mortars. *Cement and concrete research*, *48*, 97-104.

Ganesh, P., Ramachandra Murthy, A., Sundar Kumar, S., Mohammed Saffiq Reheman, M., & Iyer, N. R. (2016). Effect of nanosilica on durability and mechanical properties of high-strength concrete. *Magazine of Concrete Research*, 68(5), 229-236.

Ganesh, V. K. (2012). NANOTECHNOLOGY IN CIVIL ENGINEERING. European Scientific Journal, ESJ, 8(27). http://eujournal.org/index.php/esj/article/viewFile/592/661.

Gujjari, A. (2017). Interaction of DNA and RNA molecules with nanoclays that have potential for use in gene therapy (Unpublished dissertation). Texas State University, San Marcos, Texas.

Han, S. H. (2007). Influence of diffusion coefficient on chloride ion penetration of concrete structure. *Construction and Building Materials*, *21*(2), 370-378.

Harish, V., Tewari, D., Gaur, M., Yadav, A. B., Swaroop, S., Bechelany, M., & Barhoum, A. (2022). Review on nanoparticles and nanostructured materials: Bioimaging, biosensing, drug delivery, tissue engineering, antimicrobial, and agro-food applications. *Nanomaterials*, 12(3), 457

Haw, T. T., Hart, F., Rashidi, A., & Pasbakhsh, P. (2020). Sustainable cementitious composites reinforced with metakaolin and halloysite nanotubes for construction and building applications. *Applied Clay Science*, 188, 105533.

He, X., & Shi, X. (2008). Chloride permeability and microstructure of Portland cement mortars incorporating nanomaterials. *Transportation Research Record*, *2070*(1), 13-21.

Hearn, N., Hooton, R. D., & Nokken, M. R. (2006). Pore structure, permeability, and penetration resistance characteristics of concrete. In *Significance of tests and properties of concrete and concrete-making materials*. ASTM International.

Hendrik G. Van Oss .2011"Réduire l'empreinte carbone du ciment" U.S Geological Survey 2011. EIA – Emissions of Greenhouse Gases in the U.S. 2006-Carbon Dioxide Emissions Archived 2011-05-23 at the Wayback Machine

Hosseinzadeh Zaribaf, B. (2017). Metakaolin-Portland limestone cements: Evaluating the effects of chemical admixtures on early and late age behavior (Doctoral dissertation). Georgia Institute of Technology.

https://intrans.iastate.edu/app/uploads/2019/12/IMCP_manual.pdf#page=73

Hughes, A. D., & King, M. R. (2010). Use of naturally occurring halloysite nanotubes for enhanced capture of flowing cells. *Langmuir*, *26*(14), 12155-12164.

Jalal, M., Ramezanianpour, A. A., & Pool, M. K. (2013). RETRACTED: Split tensile strength of binary blended self compacting concrete containing low volume fly ash and TiO2 nanoparticles. Composites Part B-engineering, 55, 324–337. https://doi.org/10.1016/j.compositesb.2013.05.050.

Jeevanandam, J., Barhoum, A., Chan, Y. S., Dufresne, A., & Danquah, M. K. (2018). Review on nanoparticles and nanostructured materials: history, sources, toxicity and regulations. *Beilstein journal of nanotechnology*, 9(1), 1050-1074**.**

Jensen, O. M., & Hansen, P. F. (2001). Water-entrained cement-based materials: I. Principles and theoretical background. *Cement and concrete research*, *31*(4), 647-654.

Joussein, E. (2016). Geology and mineralogy of nanosized tubular halloysite. In Developments in clay science (Vol. 7, pp. 12-48). Elsevier.

Joussein, E., Petit, S., Churchman, J., Theng, B., Righi, D., & Delvaux, B. (2005). Halloysite clay minerals—a review. *Clay minerals*, *40*(4), 383-426.

Karthick, S. P., Muralidharan, S., Saraswathy, V., & Kwon, S. J. (2016). Effect of different alkali salt additions on concrete durability property. *Journal of Structural Integrity and Maintenance*, *1*(1), 35-42.

Keeling, J. L., Pasbakhsh, P., & Jock Churchman, G. (2012). Halloysite from the Eucla Basin, South Australia–comparison of physical properties for potential new uses. In Proceedings of the 10th International Congress for Applied Mineralogy (ICAM) (pp. 351-359). Springer, Berlin, Heidelberg.

Kiran, T., Anand, N., Nitish Kumar, S., Andrushia, D., Singh, S. K., & Arulraj, P. (2021). Influence of nano-cementitious materials on improving the corrosion resistance and microstructure characteristics of concrete. Journal of Adhesion Science and Technology, 35(18), 1995–2022.

Koch, G., Varney, J., Thompson, N., Moghissi, O., Gould, M., & Payer, J. (2016). International measures of prevention, application, and economics of corrosion technologies study. *NACE international*, *216*, 2-3.

Kosmatka, S. H., Panarese, W. C., & Kerkhoff, B. (2002). Design and control of concrete mixtures (Vol. 5420, pp. 60077-1083). Skokie, IL: Portland Cement Association.

Kurdowski, W. (2014). ***Ce****ment and concrete chemistry*. Springer Science & Business.

Lázaro, B. B. (2015). Halloysite and kaolinite: two clay minerals with geological and technological importance. *Revista de la Academia de Ciencias Exactas, Físicas, Químicas y Naturales de Zaragoza*, (70), 7-38.

Li, G., & Zhao, X. (2003). Properties of concrete incorporating fly ash and ground granulated blast-furnace slag. *Cement and concrete composites*, 25(3), 293-299.

Lisuzzo, L., Cavallaro, G., Lazzara, G., Milioto, S., Parisi, F., & Stetsyshyn, Y. (2018). Stability of halloysite, imogolite, and boron nitride nanotubes in solvent media. *Applied Sciences*, 8(7), 1068.

Loke, C. K., Lehane, B., Aslani, F., Majhi, S., & Mukherjee, A. (2022). Non-destructive evaluation of mortar with ground granulated blast furnace slag blended cement using ultrasonic pulse velocity. *Materials*, 15(19), Article 6957. https://doi.org/10.3390/ma15196957

Lomborg, B. (2003). *The skeptical environmental list: measuring the real state of the world* (Vol. 1). Cambridge: Cambridge University Press.

Lu, C., Gao, Y., Cui, Z., & Liu, R. (2015). Experimental Analysis of Chloride Penetration into Concrete Subjected to Drying–Wetting Cycles. *Journal of Materials in Civil Engineering*, 27(12). https://doi.org/10.1061/(asce)mt.1943-5533.0001304

Lu, D., Chen, H., Wu, J., & Chan, C. M. (2011). Direct measurements of the Young's modulus of a single halloysite nanotube using a transmission electron microscope with a bending stage. *Journal of nanoscience and nanotechnology*, *11*(9), 7789-7793.

Lutyński, M., Sakiewicz, P., & Lutyńska, S. (2019). Characterization of Diatomaceous Earth and Halloysite Resources of Poland. *Minerals*, *9*(11), 670.

Lvov, Y. M., Shchukin, D. G., Mohwald, H., & Price, R. R. (2008). Halloysite clay nanotubes for controlled release of protective agents. *ACS nano*, *2*(5), 814-820.

Majhi, R., Nayak, A., & Mukharjee, B. (2018). Development of sustainable concrete using recycled coarse aggregate and ground granulated blast furnace slag. *Construction and Building Materials*, 159, 417–430. https://doi.org/10.1016/j.conbuildmat.2017.10.118.

Mir, Z., Bastos, A., Höche, D., & Zheludkevich, M. L. (2020). Recent Advances on the Application of Layered Double Hydroxides in Concrete—A Review. Materials, 13(6), 1426. https://doi.org/10.3390/ma13061426

Morsy, M. S., Alsayed, S. H., & Aqel, M. (2010). Effect of nano-clay on mechanical properties and microstructure of ordinary Portland cement mortar. International Journal of Civil & Environmental Engineering IJCEE-IJENS, 10(01), 23-27.

N T BUILD 492 (1999). Nord Test Method: Concrete, mortar and cement-based repair materials: Chloride migration coefficient from non-steady-state migration experiments, Finland.

Nicoara, Adrian Ionut, Alexandra Elena Stoica, Mirijam Vrabec, Nastja Šmuc Rogan, Saso Sturm, Cleva Ow-Yang, Mehmet Ali Gulgun, Zeynep Basaran Bundur, Ion Ciuca, and Bogdan Stefan Vasile. 2020. "End-of-Life Materials Used as Supplementary Cementitious Materials in the Concrete Industry" Materials 13, no. 8: 1954. **https://doi.org/10.3390/ma13081954**

Niu, X. J., Li, Q. B., Hu, Y., Tan, Y. S., & Liu, C. F. (2021). Properties of cement-based materials incorporating nano-clay and calcined nano-clay: A review. Construction and Building Materials, 284, 122820.

Papanikolaou, I., Arena, N., & Al-Tabbaa, A. (2019). Graphene nano platelet reinforced concrete for self-sensing structures–A lifecycle assessment perspective. *Journal of Cleaner Production*, *240*, 118202.

Papatzani, S. (2016). Effect of nanosilica and montmorillonite nanoclay particles on cement hydration and microstructure. *Materials Science and Technology*, *32*(2), 138–153.

Paw, S. (2022, July 27). *What Temperature Does Salt Melt Ice?* Safe Paw Ice Melter. https://safepaw.com/what-temperature-does-salt-ice-melt-work/

Purnell, P., & Black, L. (2012). Embodied carbon dioxide in concrete: Variation with common mix design parameters. Cement and Concrete Research, 42(6), 874-877.

Rawtani, D., & Agrawal, Y. K. (2012). Multifarious applications of halloysite nanotubes: a review. *Rev. Adv. Mater. Sci*, *30*(3), 282-295.

Razzaghian Ghadikolaee, M., Habibnejad Korayem, A., Ghoroqi, M., & Sharif, A. (2018). Effect of halloysite nanotubes on workability and permeability of cement mortar. *Modares Civil Engineering journal*, *18*(2), 89-100.

Razzaghian Ghadikolaee, M., Habibnejad Korayem, A., Sharif, A., & Ming Liu, Y. (2021b). The halloysite nanotube effects on workability, mechanical properties, permeability and microstructure of cementitious mortar. *Construction and Building Materials*, 267, 120873. https://doi.org/10.1016/j.conbuildmat.2020.120873

Rooj, S., Das, A., & Heinrich, G. (2011). Tube-like natural halloysite/fluoroelastomer nanocomposites with simultaneous enhanced mechanical, dynamic mechanical and thermal properties. *European Polymer Journal*, 47(9), 1746-1755.

Rytwo, G. (2008). Clay Minerals as an Ancient Nanotechnology: Historical Uses of Clay Organic Interactions, and Future Possible Perspectives. Macla: Revista De La Sociedad Española De Mineralogía, 9, 15–17. https://dialnet.unirioja.es/servlet/articulo?codigo=6404401

Santhanam, M., & Otieno, M. (2016). Deterioration of concrete in the marine environment. *Marine concrete structures*, 137-149.

Shafabakhsh, A.G., Janaki, A. M., & Ani, O. J. (2020). Laboratory investigation on durability of nano clay modified concrete pavement. *Engineering Journal*, *24*(3), 35-44.

Shi, C. (2004). Steel slag—its production, processing, characteristics, and cementitious properties. *Journal of materials in civil engineering*, 16(3), 230-236.

Singh, L. P., Bhattacharyya, S. K., Shah, S. P., Mishra, G., Ahalawat, S., & Sharma, U. (2015). Studies on early stage hydration of tricalcium silicate incorporating silica nanoparticles: Part I. *Construction and Building Materials*, 74, 278-286.

Skutnik, Z., Sobolewski, M., & Koda, E. (2020). An Experimental Assessment of the Water Permeability of Concrete with a Superplasticizer and Admixtures. Materials, 13(24), 5624. https://doi.org/10.3390/ma13245624

Soni, Y., & Gupta, N.(2016) Experimental Investigation on Workability of Concrete with Partial Replacement of Cement by Ground Granulated Blast Furnace and Sand by Quarry Dust.

Statista, "Cement production global 2021," Statista, 2022. [Online]. Available: https://www.statista.com/statistics/1087115/global-cement-production-volume/#:~:text=The%20total%20volume%20of%20cement,4.4%20billion%20tons%20in%202021.

Statista. (2022, April). Global cement production 1995-2021. https://www.statista.com/statistics/1087115/global-cement-production-volume/

Suh, Y. J., Kil, D. S., Chung, K. S., Abdullayev, E., Lvov, Y. M., & Mongayt, D. (2011). Natural nanocontainer for the controlled delivery of glycerol as a moisturizing agent. *Journal of nanoscience and nanotechnology*, *11*(1), 661-665

Suresh, D., & Nagaraju, K. (2015). Ground granulated blast slag (GGBS) in concrete–a review. *IOSR journal of mechanical and civil engineering*, 12(4), 76-82.

Taghiyari, H. R. (2011). Effects of nano-silver on gas and liquid permeability of particleboard. Digest Journal of Nanomaterials and Bioresources, 6(4), 1509-1517.

Torres-Luque, M., Bastidas-Arteaga, E., Schoefs, F., Sánchez-Silva, M., & Osma, J. F. (2014). Non-destructive methods for measuring chloride ingress into concrete: State-of-the-art and future challenges. Construction and building materials, 68, 68-81.

U.S. National Park Service (2023). Mohs Hardness Scale (https://www.nps.gov/articles/mohs-hardness-scale.htm)

Ukpata, J. O., Ogirigbo, O. R., & Black, L. (2022). Resistance of concretes to external chlorides in the presence and absence of sulphates: a review. Applied Sciences, 13(1), 182. https://doi.org/10.3390/app13010182

Vandhiyan, R., & Pillai, E. B. (2018). Influence of nano silica addition on the behavior of concrete and its impact on corrosion resistance. *Journal of Computational and Theoretical Nanoscience*, 15(2), 530-536.

White, G. N., & Dixon, J. B. (2002). Kaolin–serpentine minerals. *Soil mineralogy with environmental applications*, *7*, 389-414.

Yuan, P., Tan, D., & Annabi-Bergaya, F. (2015). Properties and applications of halloysite nanotubes: recent research advances and future prospects. *Applied Clay Science*, 112, 75-93.

Yuan, Q., Shi, C., De Schutter, G., Audenaert, K., & Deng, D.(2015) Chloride binding of cement-based materials subjected to.

Zhuang, S., Wang, Q., & Zhang, M. (2022). Water absorption behaviour of concrete: Novel experimental findings and model characterization. Journal of Building Engineering, 53, 104602. https://doi.org/10.1016/j.jobe.2022.104602

Zych, T. (2015). Test methods of concrete resistance to chloride ingress**.** *Czasopismo Techniczne*

Appendix – B

Material Datasheet

B-1 : Datasheet of Halloysite from Manfance manufactured

TEST REPORT

NO.（2021）:SJZIT035KC-1224 INSPECTION NO.

PRODUCTNAME： ____HALLOYSITE POWDER _____

INSPECTIONCATEGORY： REGULAR INSPECTION

SHIJIAZHUANGQUALITYANDTECHNICAL SUPERVISIONANDINSPECTIONINSTITUTE

1st

PRODUCT REPORT

NO.（2021）:SJZIT035KC-1224

PRODUCTNAME	HALLOYSITE POWDER		
INSPECTIONCATEGORY	AAA GRADE INSPECTION		
PRODUCTQUANTITY	AAA	**PRODUCTDATE**	2021-08-14
PRODUCTGRADE	AAA	**INSPECTOR**	杨文 张丽
PRODUCTNO	(2021)SJZIT035 KC-1224	**SHELFLIFE**	3 years
PRODUCTSTANDARD	JC/T 2012-2010		
STORAGE	Storing with room temperature, placing in the dry, ventilated place, prohibiting sun exposure.		
CONCLUSION	The product was inspected according to JC / T 2012-2010, the conclusion is qualified （TEST STAMPED **DATEOF ISSUE** 20 21-08-.		
RESULT	ALLOWED TO DELIVERY		

2nd

TESTREPORT

NO.（2021）:SJZIT035KC-1224

Test Item	Standard	Test Result
SiO2	**40-50%**	**45.8%**

AL2O3	**30-40%**	**37.3%**
K2O	**5-10%**	**6%**
Na2O	**0.6-1.8%**	**1.2%**
MgO	**0.32-2%**	**1.2%**
Fe2O3	**2-6%**	**2.5%**
TiO2	**0.7-1.2%**	**0.7%**
CaO	**0.02-0.77%**	**0.2%**

Figure(B-1):Partical size distrbuted for halloysite from manufactured

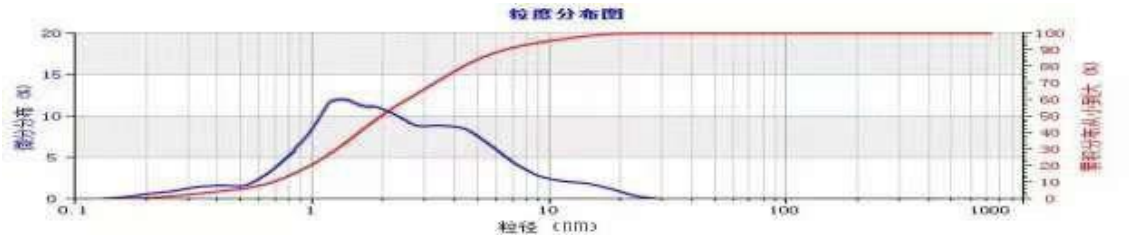

B-2: Datasheet for GGBS from manufactured

Hanson HEIDELBERGCEMENT Group

Chemical Analysis Results

REGEN

Regen Ground Granulated Blastfurnace Slag Produced at	Purfleet
Sample Period	April 2021

The sample was tested following the methods given in BS EN 196-2.
Additions and modifications have been mande in accordance with the Hanson Cement Testing Manual.

Chemical Composition %	
SiO2	35.59

Al2O3	14.32
Fe2O3	0.35
CaO	41.95
MgO	7.41
MnO	0.18
Mn2O3 Calc	0.20
TiO2	0.55
St	0.94
S2-	0.90
SO3	0.09
L.O.I.	0.66
I.R.	0.18
C	0.08
Cl	0.01
Glass content - XRD	
Relative Density g/cm2	2.90

The majority of the feed is manufactured by granulation, though on occasion a proportion of it may be by pelletisation.

The Regen GGBS contained no additional materials other than those permitted. The above results and other tests demonstrate the conformity of the material sold during the month to the requirements of EN 15167-1.

N. Cardinal Signed:

UK CA

Dr Nina Cardinal, Dipl.Ing., CEng, MiMMM National Technical Manager 1333-CPR-00133

B-3: Datasheet of Superplasticizer from Manufactured

MASTER® BUILDERS SOLUTIONS

MasterGlenium® 54

DOSAGE

The normal dosage for **MasterGlenium 54** is between 0.50 and 1.75 litres per 100kg of cement (cementitious material). Dosages outside this range are permissible subject to trial mixes.

COMPATIBILITY

MasterGlenium 54 is not compatible with **MasterRheobuild** superplasticizers.
MasterGlenium 54 is suitable for mixes containing all types of Portland cement and cementious materials as follows:

- microsilica
- fly ash (PFA)
- ground granulated blast furnace slag GGBS

EFFECT ON HARDENED CONCRETE

- increased early and ultimate compressive strengths
- increased flexural strength
- better resistance to carbonation
- lower permeability
- better resistance to aggressive atmospheric conditions
- reduced shrinkage and creep
- increased durability

STORAGE AND SHELF LIFE

MasterGlenium 54 should be stored above 5°C In closed containers or storage tanks to protect from evaporation and extreme temperatures.
The shelf life is 12 months when stored as above.

The occurrence of a surface layer with **MasterGlenium 54** is normal and will have no effect on the performance of the product.

HEALTH AND SAFETY

MasterGlenium 54 contains no hazardous substances requiring labelling. For further information refer to the Material Safety Data Sheet.

QUALITY AND CARE

All products originating from Master Builders Solutions Dubai, UAE facility are manufactured under a management system independently certified to conform to the requirements of the quality, environmental and occupational health & safety standards ISO 9001 and ISO 14001.

* Properties listed are based on laboratory controlled tests.

® = Registered trademark of the MBCC Group in many countries.

MBS_CC-UAE/GI_54_09_07/v2/03_16

Master Builders Solutions Construction Chemicals LLC
P.O. Box 37127, Dubai, UAE
Tel: +971 4 8090800
www.master-builders-solutions.com/en-ae

MasterGlenium® 54

A high performance concrete superplasticiser based on modified polycarboxylic ether

DESCRIPTION

MasterGlenium 54 has been developed for applications primarily in precast but also readymix concrete industries where the highest durability and performance is required.

MECHANISM OF ACTION

MasterGlenium 54 is differentiated from conventional superplasticisers, such as those based on sulphonated melamine or naphthalene formaldehyde condensate as it is based on a unique carboxylic ether polymer with long lateral chains. This greatly improves cement dispersion. At the start of the mixing process the same electrostatic dispersion occurs but the presence of the lateral chains, linked to the polymer backbone, generate a steric hindrance which stabilises the cement particles capacity to separate and disperse.

This mechanism provides flowable concrete with greatly reduced water demand and enhanced early strength.

TYPICAL APPLICATIONS

The excellent dispersion properties of **MasterGlenium 54** make it the ideal admixture for precast or ready-mix where low water cement ratios are required. This property allows the production of very high early and high ultimate strength concrete with minimal voids and therefore optimum density. Due to the strength development characteristics the elimination or reduction of steam curing in precast works may be considered as an economical option.

- high workability without segregation or bleeding
- less vibration required
- can be placed and compacted in congested reinforcement
- reduced labour requirement
- improved surface finish

MasterGlenium 54 may be used in combination with **MasterMatrix** for producing Smart Dynamic Concrete (SDC). The technology produces advanced self compacting concrete, without the aid of vibration. For economic, ecological and ergonomic ready-mix / precast concrete production.

MasterGlenium 54 can be used to produce very high early strength floor screeds. For screed mix designs consult Master Builders Solutions Technical Services.

PACKAGING

MasterGlenium 54 is available in 208 litre drums and in bulk tanks upon request.

STANDARDS

ASTM C-494 Type F& G
BS EN 934-2

TYPICAL PROPERTIES*

Form	Whitish to straw coloured liquid
Relative density	1.07
pH	5-8

APPLICATION GUIDELINES

MasterGlenium 54 is a ready to use admixture that is added to the concrete at the time of batching.

The maximum effect is achieved when the **MasterGlenium 54** is added after the addition of 70% of the water. **MasterGlenium 54** must not be added to the dry materials.

Thorough mixing is essential and a minimum mixing cycle, after the addition of the **MasterGlenium 54**, of 60 seconds for forced action mixers is recommended.

الخـــــــــــــلاصة

كانت هناك العديد من التحديات التي فرضتها ديمومة وانبعاثات ثاني أكسيد الكربون في إنتاج الخرسانة. وتركز الدراسة التجريبية على استبدال مادة الهالوسايت المكلسنة النانوية وخبث الأفران العالية (GGBS) بالأسمنت ودراسة قدرتها على تعزيز البنية الداخلية للخرسانية مع تقليل التأثير البيئي، مما يوفر بديلاً مستدامًا وصديقًا للبيئة لصناعة البناء والتشييد.

تمت اعداد ثلاث خلطات خرسانية،الاولى (NC) بقوة تصميمية ٤٠ ميكاباسكال (أسمنت ٣٧٠ كغم/م^٣، رمل ٧٠٦ كغم/م^٣، حصى ١٠٨٠ كغم/م^٣، وزن سمنت /ماء ٠,٥، مضاف ٠,٥%) وHS بقوة تصميمية ٥٠ ميكا باسكال (أسمنت ٤٢٠ كغم/م^٣، رمل ٦٧٨,٤ كغم/م^٣، حصى ١٠٨٠ كغم/م^٣، وزن سمنت/ ماء٠,٤٥، مضاف ١%)، وكذلك خليط GG بقوة تصميمية ٤٠ ميكا باسكال، (أسمنت ٢٧٧,٥ كغم/م^٣ ، رمل ٧٠٦ كغم/م^٣، حصى ١٠٨٠ كغم/م^٣، وزن سمنت/ماء ٠,٥، مضاف ٠,٥% مع ٢٥% GGBS تستبدل بكتلة الأسمنت). أيضا ثلاثة خليط مونة، MC، MH مع نسبة الخلط (١:٢,٧٥) وw/c=0.5,0.48 على التوالي و MG مع ١,٢,٧٥ C: S و ٢٥% GGBS تستبدل بكتلة الأسمنت.

تم إجراء فحوصات للخرسانة والمونة الطرية وفحوصات ميكانيكية (قابلية التشغيل، مقاومة الانضغاط، قوة الشد المنفصل، قوة الانثناء، امتصاص الماء، المسامية، الامتصاص السطحي، عمق اختراق الكلوريد، هجرة الكلوريد، تركيز الكلوريد، التاكل المعجل بالتيار الكهربائي ، انكماش الجفاف، قيمة ارتداد المطرقة وسرعة الموجات فوق الصوتية).

أظهرت نتائج هذه الدراسة انخفاض في هبوط الخرسانة عند استبدال CHNC مقارنة بخلطة التحكم بنسبة (٢٥ و ٢٣,٠٧%) لخلط NC3 وGG3 بنسبة استبدال ٣%. أما بالنسبة لقوة الانضغاط فقد بدأت تزداد مع زيادة نسبة الإحلال لعمر ٧ و ٢٨ و ٩٠ يوما (١٧,١٤ و ١٢,٨٦ و ١٤,٢٦%) لمخاليط GG4.5، لتحل محل ٤,٥% CHNC بسبب فعالية الهالوسايت في تحسين الترابط وتعزيز المنطقة الانتقالية بين العجينة الأسمنتية والركام. أيضاً بالنسبة لكل من اختبار الشد الانثناء والانشطاري كانت هناك زيادة مع زيادة في نسبة استبدال CHNC للخلائط الثلاثة عند ٧ و ٢٨ و ٩٠ يوماً. أما بالنسبة لديمومة الخرسانة فقد كان هناك تحسن واضح في جميع الاختبارات عند استخدام الهالوسايت، كما أظهر انخفاض في امتصاص الماء والمسامية وامتصاص السطح عند استبدال الهالوسايت للخلطات الثلاثة. ويرجع ذلك إلى أن مادة الهالوسايت تملأ المسام وتكثف الخرسانة. بالإضافة إلى ذلك، كان لاستخدام خبث الفرن العالي المحبب (GGBS) تأثير جيد في

تحسين البنية الدقيقة للخرسانة. أما تأثير CHNC على اختراق الكلوريدات، فقد أدى إلى تقليل اختراق الكلوريدات في الخرسانة، سواء بنسبة ١,٥ بالمائة بكمية صغيرة، وبكمية أكبر عند ٣ و٤,٥ بالمائة من CHNC، كما انخفض معامل الهجرة لـ ٤,٥ % من 21.21%) CHNC، ٤٥,٣٠%، و٥٤,١٨%) NC4.5، HS4.5 وGG4.5. كما أن افحص التاكل باستخدام التيار الكهربائي قلل من اختراق الكلوريدات بنسبة (٢٣,٣٨، ٣٤,٥٩، ٣٦,٦٩%) للخلطات NC3، HS3 وGG3 مقارنة بالخرسانة المرجعية.

خفضت مادة CHNC بالخرسانة المتعرضة للانكماش الجفاف مقارنة بخلطة المرجعية حيث كانت نسبة ٣% أفضل في تقليل انكماش الجفاف للخرسانة. وفي الوقت نفسه أظهرت سلوكاً جيداً عند فحص الخرسانة بالاختبارات غير الإتلافية، إذ أنه بزيادة معدل الإستبدال زادت صلابة السطح وسرعة نبض الموجات فوق الصوتية.

جمـــــــهورية العـــــــــــراق
وزارة التعليم العـــــالي والبحث العلمـــي
جامـــــــعة بابل
كـــليـــة الهنـــدســـة
قســـم الهنـــدســة المـــدنيـــة

أداء طين الهالوسايت النانوي على الخواص الهندسية للخرسانة

رسالة مقدم لكلية الهندسة /جامعة بابل وهي جزء من متطلبات الحصول على شهادة الماجستير في الهندسة / الهندسة المدنية / مواد انشائية

مقدمة من قبل :

نور الهدى حاكم عبد الأمير عيسى

بأشراف :

أ.د عباس سالم الاميري

د. سهيلة غازي مطر

هـ - ١٤٤٤ م - ٢٠٢٣